

DIFFUSION-CONTROLLED COPOLYMERIZATION
KINETICS

By

DHRUBO BHATTACHARYA, B.E., M. TECH.

A THESIS

SUBMITTED TO THE SCHOOL OF GRADUATE STUDIES
IN PARTIAL FULFILMENT OF THE REQUIREMENTS

FOR THE DEGREE

DOCTOR OF PHILOSOPHY

McMASTER UNIVERSITY

(SEPTEMBER) 1985 ©

DIFFUSION-CONTROLLED COPOLYMERIZATION KINETICS

DOCTOR OF PHILOSOPHY (1985)

McMASTER UNIVERSITY

(Chemical Engineering)

Hamilton, Ontario

TITLE: Diffusion-Controlled Copolymerization Kinetics

AUTHOR: Dhrubo Bhattacharya, B.E. (Govt. College of Eng. &
Tech., Raipur)

M.Tech. (Indian Institute of
Tech., Kanpur)

SUPERVISOR: Dr. A.E. Hamielec

NUMBER OF PAGES: (xvii), 210

ABSTRACT

A general kinetic model which accounts for diffusion-controlled termination and propagation in free-radical copolymerization up to high conversions was developed. This model was tested on batch kinetic data for styrene/p-methyl styrene thermal copolymerization and data on the chemically-initiated bulk copolymerization of methyl methacrylate/p-methyl styrene. The model gave reasonable predictions of conversion, copolymer composition and molecular weights for these copolymer systems and thus should find use in the design, optimization and control of copolymer reactors.

U

ACKNOWLEDGEMENTS

The author wishes to thank his research supervisor Dr. A.E. Hamielec for his enthusiasm, advice and guidance throughout the course of this study and his fellow graduate students for their encouragement and moral support.

Thanks are also due to the Chemical Engineering Department, McMaster University for providing the necessary financial assistance to accomplish this research.

TABLE OF CONTENTS

	PAGE
CHAPTER 1 INTRODUCTION	1
CHAPTER 2 LITERATURE REVIEW	5
2.1 Homopolymerization Kinetics	5
2.1.1 Introduction	5
2.1.2 Low conversion kinetics	5
2.1.3 Moderate to high conversion kinetics	9
2.1.4 High to very high conversion kinetics	25
2.2 Thermal Homo- and Copolymerization of Styrene	32
2.2.1 Introduction	32
2.2.2 Chemical and diffusion-controlled thermal home- and copolymerization of styrene	33
2.3 Copolymerization Kinetics	39
2.3.1 Introduction	39
2.3.2 Propagation reactions	39
2.3.3 Termination reactions	42
CHAPTER 3 EXPERIMENTAL	45
3.1 Chemicals Used	45
3.2 Experimental Conditions	46
3.3 Apparatus and Experimental Procedure	46

CHAPTER 4	MODEL DEVELOPMENT	50
4.1	Introduction	50
4.2	Kinetic Scheme for Copolymerization	50
4.3.1	Rate of thermal initiation	54
4.3.2	Rate of chemical initiation	55
4.4	Rate of Monomer Consumption	56
4.5	Copolymer Composition	58
4.6	Molecular Weight Development	59
4.6.1	Linear copolymer	59
4.6.2	Copolymer with long chain branching	61
4.7	Diffusion-Controlled Reactions	62
4.7.1	Empirical approach	63
4.7.2	Application of the free-volume theory	63
CHAPTER 5	DATA INTERPRETATION	66
5.1	Introduction	66
5.2	Parameter Estimation	66
5.2.1	Styrene/p-methyl styrene copolymerization	66
5.2.2	Methyl methacrylate/p-methyl styrene copolymerization	77
CHAPTER 6	RESULTS AND DISCUSSION	88
6.1	Model for Styrene/PMS Copolymerization using Empirical Approach to Model Diffusion-controlled Propagation and Termination	88

6.2	Model for Styrene/PMS Copolymerization using Free-volume Theory to Model Diffusion-controlled Propagation and Termination	105
6.3	Model for MMA/PMS Copolymerization using Free-volume Theory to Model Diffusion-controlled Propagation and Termination	127
CHAPTER 7	CONCLUSIONS AND RECOMMENDATIONS	146
APPENDIX		151
1	Reactivity Ratio Estimation	151
2	Modelling Bulk Polymerization of Vinyl Acetate	156
2.1	Introduction	156
2.2	Model development	157
2.2.1	Rate of monomer consumption	159
2.2.2	Molecular weight development	160
2.3	Results and Discussion	162
2.3.1	Parameter estimation	162
2.3.2	Comparison of model predictions with experimental data	165
3	Semi-Batch Copolymerization of Vinyl Chloride/Vinyl Acetate	175
3.1	Introduction	175
3.2	Policy 1	176
3.3	Policy 2	180
3.4	Policy 3	185

4	Experimental Techniques	189
4.1	Gas chromatography	189
4.2	Light scattering	191
4.3	Size exclusion chromatography	193
4.4	Differential scanning calorimetry	195
5	Derivation of equations (45) and (46) in text	197
6	Effect of changing r_1 and r_2 on copolymer composition drift	199
7	Parameter list for methyl methacrylate/p-methyl styrene copolymerization	201
	REFERENCES	203

LIST OF FIGURES

	<u>Page</u>
Fig. 1: Measured (● :120, ■:160°C) and predicted conversion vs. time, $f_{10} = 0.2$	89
Fig. 2: Measured (● :140, ■:180°C) and predicted conversion vs. time, $f_{10} = 0.2$	90
Fig. 3: Measured (● :120, ■:140°C) and predicted conversion vs. time, $f_{10} = 0.75$	91
Fig. 4: Measured (● :160, ■:180°C) and predicted conversion vs. time, $f_{10} = 0.75$	92
Fig. 5: Measured (■ :SFC, ●:LALLSP) and predicted \bar{M}_W (1:CP = 0, 2:CP = .00011) vs. conversion at 120°C; $f_{10} = 0.2$	95
Fig. 6: Measured (■ :SEC at 140, 160, 180°C; ●:LALLSP) and predicted \bar{M}_W (1,3,4:CP = 0; 2:CP = .00011) vs. conversion at 140, 160 and 180°C, $f_{10} = 0.2$	94
Fig. 7: Measured (■ :SEC at 120, 140, 160, 180°C) and predicted \bar{M}_N vs. conversion, $f_{10} = 0.2$	95
Fig. 8: Measured (■ :SFC; ●:LALLSP at 120, 140, 160°C) and predicted \bar{M}_W (1,3,5:CP = 0; 2,4:CP = .00011) vs. conversion at 120, 140, 160°C, $f_{10} = 0.75$	96
Fig. 9: Measured (●■▲:SEC at 120, 140, 160°C) and predicted \bar{M}_N vs. conversion, $f_{10} = 0.75$	97
Fig.10: Predicted \bar{B}_N vs. conversion at 120°C, $f_{10} = 0.2$	100
Fig.11: Measured (1:SEC) and predicted MWD at 120°C, $f_{10} = 0.2$, $x = 0.06$, $\bar{M}_W(\text{meas.}) = 3.8E5$, $\bar{M}_N(\text{meas.}) = 2.4E5$, $\bar{M}_W(\text{pred.}) = 3.9E5$, $\bar{M}_N(\text{pred.}) = 2.4E5$	101
Fig.12: Measured (1:SEC) and predicted MWD at 160°C, $f_{10} = 0.2$, $x = 0.89$, $\bar{M}_W(\text{meas.}) = 2.3E5$, $\bar{M}_N(\text{meas.}) = 1.2E5$, $\bar{M}_W(\text{pred.}) = 2.2E5$, $\bar{M}_N(\text{pred.}) = 1.2E5$	102
Fig.13: Diffusion controlled termination: measured change in ϕ_x with conversion (1:120, 2:140, 3:160, 4:180°C) $f_{10} = 0.2$	103
Fig.14: Diffusion controlled termination: measured change in ϕ_x with conversion (1:120, 2:140, 3:160, 4:180°C) $f_{10} = 0.75$	104
Fig.15: Measured (● :120, ○:140, ■:170°C) and predicted conversion vs. time, $f_{10} = 1$	106
Fig.16: Measured (● :120, ○:140, ■:160°C) and predicted conversion vs. time, $f_{10} = 0$	107
Fig.17: Measured (● :120, ○:140°C) and predicted conversion vs. time, $f_{10} = 0.2$	108
Fig.18: Measured (● :160, ○:180°C) and predicted conversion vs. time, $f_{10} = 0.2$	109
Fig.19: Measured (● :120, ○:140°C) and predicted conversion vs. time, $f_{10} = 0.75$	110

	<u>Page</u>
Fig.20: Measured (●:160, ○:180°C) and predicted conversion vs. time, $f_{10} = 0.75$	111
Fig.21: Measured (●:SEC, ○:LALLSP) and predicted M_W vs. conversion at 120°C, $f_{10} = 0.2$	113
Fig.22: Measured (○:SEC at 140,180°C, ● at 160°C, ◻:LALLSP at 140,160,180°C) and predicted M_W vs. conversion, $f_{10} = 0.2$	114
Fig.23: Measured (◻:LALLSP at 120,140,160°C, ○:SEC at 120,160°C, ●:140°C) and predicted M_W vs. conversion, $f_{10} = 0.75$	115
Fig.24: Measured (●:SEC at 120,160°C, ○:SEC at 140,180°C) and predicted M_W vs. conversion, $f_{10} = 0.2$	116
Fig.25: Measured (●:SLC at 120,160°C, ○:SEC at 140°C) and predicted M_W vs. conversion, $f_{10} = 0.75$	117
Fig.26: Measured (f_{10} : ●:0, Δ:0.2, ◻:0.75, ◻:1) and predicted k_3 vs. $(1/T)(^{\circ}K^{-1})$, $A = 0.85$	118
Fig.27: Measured (f_{10} : ●:0, Δ:0.2, ◻:0.75, ◻:1) V_{FCR2} vs. $T(^{\circ}K)$ $B = 0.5$	119
Fig.28: Predicted ($f_{10} = 0.2$, $T = 140^{\circ}C$) change in k_{tc} and k_{trd} (1/mole,min.) with conversion.	120
Fig.29: Measured (○:DSC) and predicted T_{gp} vs. limiting conversion.	122
Fig.30: Measured (○:120°C, $f_{10} = 0$) and predicted conversion vs. time, $\alpha_m = 0.00193$, $\alpha_p = 0.00057$	123
Fig.31: Predicted ($T = 120^{\circ}C$, $f_{10} = 0.2, 0.75$) f_1 vs. conversion.	125
Fig.32: Chemically-controlled k_t as a function of f_{10} (styrene/PMS).	126
Fig.33: Measured (○:80, ●:60°C, $[I]_0 = .0157$; ▼:80, ◻:60°C, $[I]_0 = .0057$ mol/l) and predicted conversion vs. time, $f_{10} = 0.54$	128
Fig.34: Measured (○:80, ●:60°C) and predicted conversion vs. time $[I]_0 = .0157$ mol/l, $f_{10} = 0.83$	129
Fig.35: Measured ($[I]_0$:○:0.0252, ●:0.0157, ◻:0.0057 mol/l) and predicted conversion vs. time, $T = 80^{\circ}C$, $f_{10} = 0.21$	130
Fig.36: Measured ($[I]_0$:○:0.0252, ●:0.0157, ◻:0.0057 mol/l) and predicted conversion vs. time, $T = 60^{\circ}C$, $f_{10} = 0.21$	131
Fig.37: Measured (▼:50, ▼:70, ○:90°C) and predicted conversion vs. time, $[I]_0 = 0.0252$ mol/l, $f_{10} = 1$	132
Fig.38: Measured (f_1 : ○:0.83, ●:0.54, ◻:0.21) and predicted f_1 vs. conversion, $T = 60^{\circ}C$, $[I]_0 = .0157$ mol/l	133
Fig.39: Measured (f_{10} : ○:0.83, ●:0.54, ◻:0.21) and predicted f_1 vs. conversion, $T = 80^{\circ}C$, $[I]_0 = .0157$ mol/l	134

	<u>Page</u>
Fig.40 Predicted f_1 vs. conversion; $f_{10} = .83$, $f_{10} = .54$, $f_{10} = .2$ with r_1, r_2 dependent on conversion at high conversions	136
Fig.41: Measured (○:60, ●:80°C) and predicted \bar{M}_w vs. conversion, $[I]_0 = .0157$ mol/l, $f_{10} = .54$	137
Fig.42: Measured (○:60, ●:80°C) and predicted \bar{M}_w vs. conversion, $[I]_0 = .0057$ mol/l, $f_{10} = .54$	138
Fig.43 Measured (○: \bar{M}_w , ●: \bar{M}_n) and predicted \bar{M}_n and \bar{M}_w vs. conversion, $[I]_0 = .0252$ mol/l, $T = 50^\circ\text{C}$, $f_{10} = 1$	139
Fig.44: Measured (○: \bar{M}_w , ●: \bar{M}_n) and predicted \bar{M}_n and \bar{M}_w vs. conversion, $[I]_0 = .0252$ mol/l, $T = 70^\circ\text{C}$, $f_{10} = 1$	140
Fig.45: Measured (○: \bar{M}_w , ●: \bar{M}_n) and predicted \bar{M}_n and \bar{M}_w vs. conversion, $[I]_0 = .0252$ mol/l, $T = 90^\circ\text{C}$, $f_{10} = 1$	141
Fig.46: Predicted k_t vs. conversion, $[I]_0 = .0157$ mol/l, $T = 80^\circ\text{C}$, $f_{10} = .59$	143
Fig.47: Chemically-controlled k_t as a function of f_{10} (MMA/PMS)	144
Fig.48: 95% Joint Confidence Region for r_1, r_2 (styrene/PMS)	155
Fig.49: Measured (●:50°C, [I] ₀ = .004, X:60°C, [I] ₀ = .004; ○:70°C, [I] ₀ = .001 mol/l) and predicted conversion vs. time.	166
Fig. 50: Measured (○:80°C, [I] ₀ = .0002 mol/l) and predicted conversion vs. time.	167
Fig.51: Measured (○:60°C, [I] ₀ = .004 mol/l) and predicted \bar{M}_w vs. conversion	168
Fig.52: Measured (○:.002, ■:.00002 mol/l) and predicted \bar{M}_w vs. conversion, $T = 60^\circ\text{C}$.	169
Fig.53: Measured (○:.001, ■:.00002 mol/l) and predicted \bar{M}_w vs. conversion, $T = 70^\circ\text{C}$.	170
Fig.54: Measured (○:.0001, ■:.0002 mol/l) and predicted \bar{M}_w vs. conversion, $T = 80^\circ\text{C}$.	171
Fig.55: Predicted \bar{B}_N vs. conversion; $T = 60, 70, 80^\circ\text{C}$, $[I]_0 = .004$ mol/l.	173
Fig.56: Arrhenius temperature dependence of $r(k_p/k_t^{.5})$ for vinyl acetate polymerization.	174

LIST OF TABLES

Table No.	Title	Page
3-1	List of Solvents	45
5-1	Time Conversion Data	80
5-2	Conversion Molecular Weight Data	83
5-3	Reproducibility Studies	85
5-4	Variation of K_3 and V_{Fcr2} with temperature	87
7-1	Data for r_1, r_2 estimation	154
7-2	Semi-batch copolymerization Policy 1	180
7-3	Semi-batch copolymerization Policy 2	183
7-4	Effect of monomer concentration on rate of heat generation Policy 2	184
7-5	Semi-batch copolymerization Policy 3	185

NOMENCLATURE

A	diffusion-coefficient parameter for macroradicals
B	diffusion-coefficient parameter for monomer molecules
A,B,C	diffusion-control parameters, empirical model
A_2	second virial coefficient in the M_w equation
\bar{B}_N	branching frequency
B_i	K_{fiy}/K_p ; $i=1,2$
c	polymer concentration
C_M	K_{fm}/K_p
C_p	K_{fp}/K_p
CMOM	mean molecular weight of the comonomer phase
C_w	conversion on a weight basis
d	proportionality constant in equation for K_{tseg}
D_s	self-diffusion coefficient
D_p	self-diffusion coefficient of macroradicals
D_R	reaction-diffusion coefficient
dn/dc	specific refractive index
f	initiator efficiency
F(v)	SEC detector response
F_1	instantaneous mole fraction of monomer 1 in copolymer
\bar{F}_1	cumulative mole fraction of monomer 1 in copolymer
f_1	mole fraction of monomer 1 in residual monomer
K_3	diffusion-control onset parameter

K_p	propagation rate constant
K_T	diffusion-controlled K_t
K_{tseg}	segmental diffusion-controlled K_t
K_t	termination rate constant
K_{fij}	reaction rate constant for transfer to monomers
K_{fiy}	reaction rate constant for transfer to oligomers
K_{fpij}	reaction rate constant for transfer to polymer
K_d	initiator decomposition constant
K_{td}	termination by disproportionation rate constant
K_{tc}	termination by combination rate constant
K_{tcr1}	value of K_t at onset of diffusion-control
K_{trd}	reaction-diffusion rate constant
K_{Ii}	Z_i formation rate constant
K_{ij}	rate constant for propagation
K_{tij}	chemically-controlled termination rate constant
K_{sij}	rate constant for formation of monoradicals (thermal)
k_i	rate constant for formation of monoradicals (chemical)
K	K_p^*/K_p
K_p^*	rate constant for terminal double-bond polymerization
l_0	length of monomeric unit
$[M]$	monomer concentration
\bar{M}_N	number average molecular weight of the accumulated polymer
\bar{M}_W	weight average molecular weight of the accumulated polymer
\bar{M}_{Wcr1}	value of \bar{M}_W at onset of diffusion-control

N_I moles of initiator
 N_{AV} Avagadro's number
 N_r moles of polymer of chain length r
 n_s number of monomer molecules in a polymer segment
 N_m number of moles of monomers 1 and 2
 n_0 refractive index of solvent
 P_s polymer molecule with s monomer units
 P'_s polymer molecule with terminal double bond
 $[P]$ polymer concentration
 Q_i, \bar{Q}_i i^{th} moments of polymer size distribution
 Q heat generation rate
 R_p rate of polymerization
 $[R]$ total radical concentration
 $[R_i]$ total concentration of radicals having M_i as their terminal monomer unit
 r_1, r_2 binary reactivity ratios
 R_t total termination rate
 R_r^* polymer radical with r monomer units
 R_r' polymer radical with r monomer units and with double bond
 R_0 Rayleigh ratio
 r_N instantaneous number average chain length
 r_W instantaneous weight average chain length
 R_I radical generation rate
 r_T characteristic temperature ratio in Fedor's relation

t time
 T temperature
 T_{gp} glass transition temperature of polymer
 T_{gm} glass transition temperature of monomer
 T_m, T_b melting and boiling points of monomer
 V_F fractional free-volume
 V_{Fcr1} value of V_F at onset of diffusion-control
 V_{Fcr2} value of V_F at onset of diffusion-controlled propagation
 V_M, V_P, V_T volume of monomer, polymer and total volume
 v reactor volume
 V_M molar volume
 $W(r, x)$ instantaneous differential chain length distribution of polymer
 $\bar{W}(r, x)$ differential chain length distribution of accumulated polymer
 W_1, W_2 weight fraction of monomers
 x fractional conversion
 x_{crit2} value of x at onset of diffusion controlled propagation
 Y_n, Y'_n n^{th} moments of polymer radical size distribution
 Z_i reactive Diels Alder adduct
 ϕ_M volume fraction of monomer
 $(-\Delta H_i)$ heat of polymerization of monomer i
 ρ_{Mi} moles of monomer i /volume
 ϕ_0 jump frequency of polymer segment
 Δ jump distance

ϵ volume contraction factor
[ϕ_i] fraction of radical of type i
 ϕ_x, ϕ_0 diffusion control parameters
 τ, β molecular weight parameters

INTRODUCTION

The expanded industrial use of copolymers, has motivated research, both theoretical and experimental, in the field of free-radical copolymerization reactor modelling (1). Classical copolymerization kinetics with all reactions chemically-controlled are reasonably well understood. This, however, cannot be said for commercially important copolymerizations which are done at high conversions (high polymer concentrations).

The study of high conversion kinetics is most important for polymer reactor modelling, as most of the characteristics of these processes such as 1) the rate of polymerization 2) the molecular weight averages and others, show a marked departure from classical kinetic behavior at high polymer concentrations. Although substantial work has been done on diffusion-controlled termination and propagation reactions in homopolymerization, there is a dearth of literature pertaining to these phenomena in high conversion copolymerization. There thus exists

a need for high conversion copolymerization kinetic data with commercially relevant monomers and predictive kinetic models which account for diffusion-controlled termination and propagation reactions. Such models could accurately predict copolymerization rates, chain microstructure and molecular weight distribution (MWD) development to high conversions in different reactor types and configurations for both isothermal and non-isothermal conditions and generally under conditions far removed from those used in model parameter estimation.

The objective of the research reported herein is to develop a model capable of describing copolymerization kinetics up to high conversions and to test the validity of this model for bulk thermal copolymerization of styrene/p-methyl styrene at high temperatures and conversions. The tests to be used include model predictions of conversion/time and of the development of number and weight average molecular weights versus conversion for an isothermal batch reactor. Thermal bulk polymerization is a cheap and thereby commercially attractive means of producing styrenic polymers and this particular copolymer was chosen for this study because of its

potential for commercial and industrial use (2).

Two approaches found to be equivalent for this system, have been used to account for diffusion-controlled termination and propagation reactions; 1) free-volume theory 2) an empirical approach based on direct fitting of the kinetic data. The free-volume theory has already been applied successfully to model styrene/acrylonitrile copolymerization (3). The present free-volume model also accounts for segmental diffusion-control of termination reactions at low conversions, and has been applied successfully to model the bulk copolymerization of methyl methacrylate/p-methyl styrene(PMS) as well as the styrene/PMS system.

In the latter parts of this thesis a kinetic model has been developed to describe the diffusion-controlled homopolymerization of vinyl acetate, to illustrate the effect of long chain branching reactions and molecular weight development, on diffusion-controlled termination. In the concluding part of this dissertation, some optimal feed policies for semi-batch copolymerization processes to minimize composition drift and maximize production, have been

presented for the copolymerization of vinyl acetate/vinyl chloride.

LITERATURE REVIEW

2.1 Homopolymerization Kinetics

2.1.1 Introduction

The development of a comprehensive kinetic model for any industrial polymerization process requires a phenomenological understanding of polymerization kinetics up to high conversions. The following is a review of the chemical and physical phenomena which lead to the diffusion-controlled termination and propagation reactions at high conversions in free-radical homopolymerization. The same phenomena are largely relevant in free-radical copolymerization.

2.1.2 Low conversion kinetics

In the very early stages of polymerization, at very low polymer concentrations, the rate of

polymerization (R_p) has been found to decrease with increasing polymer concentration (c) (5,6,8). This decrease is greater than can be explained on the basis of monomer or initiator consumption. The initial rate decrease was qualitatively explained by North and Reed (5) for methyl methacrylate (MMA) polymerization. Treating the termination mechanism as a diffusive process which is controlled by segmental diffusional resistance at low monomer conversions, they formulated an empirical relationship between the termination constant (K_t) and c . This relation is based on the consideration that the reactive chain end of a polymer radical diffuses across a segment concentration gradient into a region of very low segment concentration and reacts with another such chain end from a neighboring polymer radical. This process is akin to mutual diffusion of radical chain ends and solvent and hence K_t is proportional to the mutual diffusion coefficient (D_{mut}) of these chain reactive ends. The increasing polymer concentration makes the monomer a thermodynamically poorer solvent for the polymer and causes the macro-radical coils to contract, thereby increasing the chain end concentration gradient across the coils and, thereby increases K_t . K_t was

expanded as a polynomial in c with the intrinsic viscosity (η) and the thermodynamic virial coefficients of the solvent as parameters (5).

Ludwico and Rosen (6) reported an initial decrease in the rate of styrene polymerization with pre-dissolved polybutadiene and polystyrene respectively, and found the rate to decrease with increasing c and polymer molecular weight. Their results indicated no correlation between the rate reduction and the viscosity of the reaction medium. Mahabadi and O'Driscoll (7) have presented a theoretical derivation relating K_t and c with the second virial coefficient of the solvent, (η), the number of monomer units in the polymer molecule (N), the linear expansion factor of the polymer and a flexibility parameter (N_0). At very low c , K_t was found to be linear in c and of the following form

$$K_t = K_{t0}(1 + dc) \tag{1}$$

where

$$d = B (\langle h \rangle_0^2 / M)^{1.5} M^{-0.5} Z$$

K_{t0} is the termination rate constant at c equal to zero, B is a constant, Z is an interaction parameter $\langle h \rangle_0$ is the mean-square end-to-end distance of the unperturbed chain of molecular weight M .

d is increased by any factor that decreases the macro-radical coil size. Thus increasing molecular weight of the polymer formed or decreasing goodness of the solvent results in a higher value of d . The effect of solvent on K_t has been investigated by Mahabadi and Rudin (11) who expressed d as $w\bar{N}$, where \bar{N} is the number average chain length of the dead polymer and w depends on the goodness of the solvent. Matthews and Rosen (12) have proposed an empirical relation of the form

$$K_t = K_{t0} N^n \quad (2)$$

where N is the kinetic chain length. They have reported values of n for some alkyl acrylates polymerized upto less than 1% conversion.

2.1.3 Moderate to high conversion kinetics

The viscosity and related transport properties of the polymer solution increase abruptly at a certain critical concentration (c_{crit}). Some authors have attempted to relate c_{crit} with the observed point of autoacceleration in the rate of polymerization. Turner (13) has proposed that the point of molecular overlap due to the close packing of the discrete macromolecular coils corresponds to the onset of the gel-effect. Treating the polymer molecules like uniform rigid spheres with a radius of gyration calculated from their unperturbed dimensions, he proposed a relation of the following form to hold at the onset of gel-effect

$$\bar{N}^a c_{crit} d_c = \text{constant} \quad (3a)$$

where d_c is the density of the polymer solution at $c=c_{crit}$ and $a = 0.5$. Turner et al (92-95) obtained values for a of 0.4, 0.35, and 0.34 for MMA, styrene and vinyl acetate homopolymerizations respectively. Tulig and Tirrel (9) used a temperature-independent K_{crit} to fit equation (3b) for the MMA/PMMA system in the temperature range of 45-90°C, with $a = 0.24$.

$$K_{\text{crit}} = c_{\text{crit}} \bar{M}_N^a \quad (3b)$$

where \bar{M}_N is the number average molecular weight of the accumulated polymer.

Theories of polymer dynamics and rheology have attributed the abrupt cross-over of transport properties to the onset of entanglements and predict the following equation to hold (10)

$$c_{\text{crit}} \bar{M}_K = \text{constant} \quad (4)$$

where \bar{M}_K is the K^{th} average molecular weight of the accumulated polymer. O'Driscoll et al (14) found $K=N$ for styrene polymerization though the value of the constant was observed to be lower than found in rheological measurements on the same system. On the basis of experimental evidence obtained thus far, the exact form of an equation relating polymer concentration and molecular weight at the onset of gel-effect, cannot be established.

While at low polymer concentrations, polymer-solvent interactions are dominant, polymer-polymer interactions influence K_t at higher conversions.

These interactions may take three forms ; first the intermolecular hydrodynamics screen the intramolecular hydrodynamic interactions which dominate dilute solution behavior, second the polymer chains may impose topological constraints upon the motions of surrounding polymer molecules. In this region the translational diffusional mobility of the macroradicals determines the overall rate of polymerization. At higher polymer concentrations, polymer chains may exert direct friction upon one another.

Under translational diffusion-controlled conditions k_t is expected to depend on the self-diffusion coefficient (D_S) of the macroradicals according to the Smoluchowski equation (15)

$$k_t = 4\pi P(D_A + D_B) \quad (5)$$

where D_A and D_B are the self-diffusion coefficients of the macroradicals and P is the interradical separation at reaction. It should be mentioned that the validity of equation (5) for macromolecular reactions has not been established theoretically or experimentally.

deGennes considered the effect of topological constraints upon the motion of a polymer molecule and proposed that the motion of a given macromolecule is confined within a virtual tube defined by the locus of its intersection with adjacent polymer molecules (16). The molecule is constrained to wriggle, snake-like along its own length by curvilinear propagation of length defects such as kinks or twists along the tube. He called the motion reptation. In the absence of significant polymer-polymer friction, the reptation model leads to the following dependence of D_S on N and c

$$D_S \propto N^{-2} c^{-1.75} \quad (6)$$

However, it should be noted that deGennes' treatment does not account for the growth of the macroradicals by monomer addition via the propagation reaction and the treatment has not been generalized for systems polydispersed in molecular weight.

Klein (17) has conducted experiments using five deuterated linear polyethylene samples of varying weight average molecular weights and polydispersities

as the diffusant in a matrix of linear polyethylene of a very high polydispersity (~ 15). A least-squares fit of the diffusion coefficient (D) measured from the slope of the diffusion-broadened concentration profiles and the weight average molecular weight (\bar{M}_W) of the diffusing species gave the following equation

$$D = 0.2 \bar{M}_W^{-2.0 \pm 0.1} \quad (7)$$

However, the scarce experimental findings for polydisperse systems, do not permit any generalizations.

Tulig and Tirrel (18) have reviewed the recent advances made in polymer diffusion theory in the context of modelling diffusion-controlled termination. They proposed a kinetic model for MMA polymerization by identifying three different conversion regimes. At infinitely low to low polymer concentrations (dilute regime), K_t is assumed to be equal to K_{tseg} (segmental diffusion-controlled K_t) and is given by

$$K_t = K_{t0} (1 + k_1 \bar{N}c) \quad (8)$$

where k_1 is a constant. Equation (8) holds till $K_{tseg} = K_{ttrans}$ where K_{ttrans} is given by

$$K_{ttrans} = K_{t0}(1 - k_2c) \quad (9)$$

where k_2 is another constant.

At higher concentrations an entangled, semi-dilute regime has been defined, which does not incorporate significant polymer-polymer friction. Using reptation theory (16) to predict D_S and Smoluchowski equation to predict K_t , they obtain

$$K_t \propto N^{-2} c^{-1.75} \quad (10)$$

assuming P is a constant independent of molecular weight of the macroradicals. Here N is the number average degree of polymerization of the macroradicals. Using this kinetic model they have successfully predicted conversion upto 70% alongwith the number and weight average molecular weights.

It is postulated that macroradicals with $N < N_c$ (N_c is a critical chain length) terminate with a rate constant proportional to N^{-5} (Einstein and Stoke's relation) and those with $N > N_c$ terminate with a K_t proportional to N^{-2} (reptation theory, 19). He formulated kinetic equations with a chain length dependent K_t and computed \bar{M}_N and the weight average

molecular weight of the accumulated polymer (\bar{M}_w) which were compared with experimental data on MMA bulk polymerization. However, the model did not account for polymer concentration dependence of the diffusion coefficient of the macroradicals and the only effect of c entered through the calculation of N_c , based on the formula proposed by Klein (20)

$$N_c = (18\pi^2)^{.5} / (Ac^{1.25}) \quad (11)$$

where A is a constant depending on the size of the monomer.

Ito's model does not correctly describe the high conversion kinetic behavior because of the inadequacy of the reptation scaling laws in this region. He also ignored diffusional-control of propagation reactions. Boots (21) derived equations for instantaneous average degrees of polymerization, by treating the chain length as a continuous variable and allowing for chain length dependence of K_t . He studied the Ito model in detail and his computation of the instantaneous MWD is not very sensitive to the precise reptation behavior as used in Ito's model.

An empirical approach to model diffusion-controlled polymerization up to high conversions has been used by some authors (22-25). They have used the classical rate expression to fit the experimental conversion data by treating K_t and the propagation rate constant (K_p) as adjustable parameters. Ross and Laurence (22) have expressed K_t and K_p as a function of free-volume to fit rate and molecular weight data for MMA polymerization. Hamielec and others (23-25) have correlated K_t with x for some commercial polymerizations. The general form of these models is as follows

$$K_t = K_{t0} \exp(Ax + Bx^2 + Cx^3) \quad (12)$$

where

$$A = A_1 + A_2T$$

$$B = B_1 + B_2T$$

$$C = C_1 + C_2T$$

The linear dependence of the parameters A, B and C on temperature permits easy interpolation and reliable extrapolation over rather large ranges of temperature. The predictive power of such models in non-isothermal conditions has been tested by Wu et al (26) for styrene polymerization under optimal

temperature conditions to maximize R_p and keep \bar{M}_N and \bar{M}_W within specifications.

However, such models are incapable of handling situations where transfer reactions to an external chain transfer agent controls the molecular weight of the polymer as the empirical approach then does not account for the molecular weight of either the macroradicals or the accumulated polymer.

Horie et al (27) were the first to qualitatively use free-volume theory in order to relate the variation of R_p to the rates of diffusion of monomer molecules and polymer radicals in their study of the bulk polymerization of MMA and styrene upto limiting conversions. Following the rate of isothermal polymerization using differential scanning calorimetry (DSC) thermograms, they constructed plots of the ratio of the product of K_p and the total radical concentration ($[R]$) to the same at zero conversion versus x and concluded that the mechanism of diffusion-controlled polymerization could be explained by relating K_p and K_t to the rates of diffusion of monomer molecules and polymer radicals.

Arai and Saito (28) considered the role of the diffusion process in the encounters of the reactants in each elementary reaction viz; initiation, propagation and termination over the entire range of conversion and the rates of all these reactions were correlated with conversion in terms of the jump frequency of a polymer segment. The model was used to predict x , \bar{M}_N and \bar{M}_W for the chemically-initiated bulk polymerization of MMA and styrene. Soong et al (29) have used the Fujita-Doolittle theory to predict the diffusion coefficients of both the macroradicals and monomer molecules. K_t and K_p were assumed to be a function of the diffusion coefficients and the overall expression for these coefficients was written as a product of two functions ;1) a molecular weight dependent term 2) a concentration dependent term. These authors rejected the use of scaling laws to express the molecular weight dependence in favour of an empirical relation between the molecular weight function and the process variables ; temperature and initiator loading. One important feature of this model was the introduction of mass transfer considerations from the beginning of reaction so that break-points for the imposition of gel-effect etc. were avoided. Bulk

polymerization of MMA over three temperatures and two initiator levels was modelled.

The two most widely discussed semi-mechanistic attempts to model diffusion-controlled polymerization are those of Cardenas and O'Driscoll (COD model)(30) and Marten and Hamielec (MH model)(31).

The COD model is based on entanglement ideas. Here the polymer radical population is divided into two groups, those with chain length 1) greater and 2) less than a critical length N_c . N_c is calculated from the following equation based on Bueche's entanglement theory (32)

$$K_c = \phi_p N_c \quad (13)$$

where ϕ_p is the dead polymer volume fraction and K_c is a constant for the polymer and depends on the thermodynamic quality of the monomer and/or solvent. Radicals A and B are assumed to terminate with a rate constant K_{t0} if $N_A, N_B < N_c$; with K_{te} if $N_A, N_B > N_c$ and with K_t if either N_A or $N_B > N_c$. K_t is assumed to be given by

$$K_t = (K_{t0} K_{te})^{.5}$$

Here K_{t0} is the chemically-controlled rate constant and K_{te} is assumed to be inversely proportional to the entanglement density.

$$K_{te} \propto 1/(\phi_p \bar{N}) \quad (14)$$

The COD model has been tested on the bulk polymerization of MMA (30) and ethyl methacrylate (EMA) and solution polymerization of EMA (33). The assumption of a constant K_{t0} throughout the course of reaction is questionable, especially at high conversions. Also, the COD model is incapable of predicting limiting conversions observed in most polymerizations conducted at temperatures below the glass-transition point of the polymer (T_{gp}).

The MH model uses free-volume theory to predict the diffusion coefficient (D_p) of the macroradicals. K_t is assumed to be proportional to D_p under diffusion-controlled conditions

$$K_t = k_1 D_p \quad (15)$$

where k_1 is a temperature dependent proportionality

constant. D_p is given by (32)

$$D_p = \phi_0 \Delta^2 \exp(-A/V_F) / (k_2 M^\alpha) \quad (16)$$

where ϕ_0 is the jump frequency of a polymer segment, Δ is the jump distance, V_F is the fractional free-volume, M is the molecular weight of the monodispersed polymer, A , k_2 and α are constants. M is replaced by \bar{M}_W in the case of a polydisperse polymer as \bar{M}_W is proportional to viscosity and D_p is assumed to depend on the viscosity of the medium. Combining equations (15) and (16), K_t was written as

$$K_t = k_1 ((\phi_0 \Delta^2) / (k_2 \bar{M}_W^m)) \exp(-A/V_F) \quad (17)$$

m was arbitrarily set at 0.5 and 1.75 for unentangled and entangled conditions for both styrene (34) and MMA (31) polymerizations. A parameter K_3 was defined to signal the onset of diffusion-controlled termination

$$K_3 = k_1 \phi_0 \Delta^2 / (K_{tcr1} k_2) = \bar{M}_{Wcr1}^5 \exp(A/V_{Fcr1}) \quad (18)$$

where $K_t = K_{tcr1}$, $\bar{M}_W = \bar{M}_{Wcr1}$ and $V_F = V_{Fcr1}$ at the onset

of diffusion-control. Finally it was assumed that the onset of diffusion-control corresponds to the onset of entanglements, thereby giving

$$k_t = k_{t0} (\bar{M}_{wcr1} / \bar{M}_w)^{1.75} \exp(-A(1/V_F - 1/V_{Fcr1})) \quad (19)$$

The MH model accounts for diffusion-controlled propagation (discussed later) and therefore could predict limiting conversions. It has been successfully employed to model the bulk and solution polymerization of styrene (34) and MMA (31) over a wide range of initiator levels and temperatures. This model has also been extended to model diffusion-controlled copolymerization kinetics (3,4). The model however, does not account for low-conversion segmental diffusion-controlled kinetics. Further as pointed out by Tulig and Tirrel (18), the use of accumulated polymer molecular weight averages alone in the expression for the diffusion-controlled rate constants may be theoretically incorrect, as the diffusion coefficient of the diffusing radicals should depend on some characteristic size of the diffusant and not just the matrix it diffuses in. It should also be pointed out that Bueche's theoretical derivation of equation (16) was for the diffusion of dead polymer molecules. He proposed a value of $\alpha = 1$ for

unentangled polymer, and $\alpha=1,3.5$ for entangled small and large polymer molecules respectively.

Soh and Sundberg (35) used free-volume theory and concepts of chain entanglement to arrive at the following chain length dependent model for K_t

$$K_t = K_{tvf}(f(i) + f(j))/2 \quad (20)$$

where $f(i) = 1 \quad i < N_c$
and $f(i) = (i/N_c)^{-2.4} \quad i > N_c$

$$K_{tvf} = K_{t0} \exp(-A/V_F) \quad (21)$$

and $\phi_p N_c = \text{constant}$

These authors have rightly noted that the total termination rate (R_t) may be related to a mean termination rate constant K_t as follows

$$R_t = [R]^2 \sum K_t(n,n) X_n = K_t [R]^2 \quad (22)$$

where $X_n = N_n / [R]$

and therefore all chain length independent models would be capable of fitting the rate and \bar{M}_N data. However, the accurate prediction of higher molecular weight averages might require a chain length

dependent K_t . Soh and Sundberg, were able to predict successfully \bar{M}_w , \bar{M}_z and \bar{M}_{z+1} for the bulk polymerization of MMA over the entire range of conversion (36). They also modelled the bulk polymerization of EMA, ethyl acrylate, propyl acrylate, styrene and vinyl acetate (36). Low conversion segmental diffusion-control was not accounted for in their work.

The chain length dependence used in the above model is based on the entanglement coupling factor determined experimentally (37). Though the model does not have a sound theoretical basis it is evident that a semi-mechanistic model incorporating ideas from both entanglement and free-volume theories serves as an adequate engineering model for predictive purposes.

2.1.4 High to very high conversion kinetics

The translational mobility of macroradicals reduces greatly at high polymer concentrations. At these concentrations the overall rate of termination can be visualized as a sum of two components viz; 1) the very low rate of translational diffusion of the macroradicals 2) the rate of motion of the chain end of the polymer radical growing via propagation. Gradually as the radicals become trapped in the polymer matrix, termination occurs solely when the macroradical chain ends approach each other through propagation.

At these high conversions propagation reactions may also become diffusion-controlled and if the temperature of polymerization is below the T_{gp} , a transition of the polymer-monomer solution from a highly viscous liquid to a glassy solid occurs with the polymerization rate falling to essentially zero in the normal time scale of commercial polymerizations. A limiting conversion is reached when the glass-transition temperature (T_g) of the polymer-monomer mixture equals the polymerization temperature(27).

The growth of nearly immobilized polymer radical chains during vitreous solidification of the reaction was investigated by Schulz (38). He proposed that the only movement of the chain ends of these radicals occurs via "reaction diffusion"- a term proportional to the rate of propagation, and is given by

$$D_R = (n_s l_0^2 / 6) k_p [M] \quad (23)$$

where D_R = reaction diffusion coefficient

n_s = number of monomer molecules in a polymer segment

l_0 = length of the monomeric unit

$[M]$ = monomer concentration

Hayden and Melville (39) followed MMA polymerization up to very high conversions by measuring the heat of polymerization with time as the exothermic propagation reactions proceeded under adiabatic conditions. At the last stages of reaction they noted that the termination reaction resembled a unimolecular process with the extreme reduction of the mobility of the macroradicals. With each addition of a monomeric unit the chance of effective physical termination process becomes dependent on the

propagation process, which is what equation (23) suggests.

Soh and Sundberg (40) considered the excess chain end mobility of a frozen radical which is incapable of translational motion but whose chain end moves in a sphere of radius (r) with the node of entanglement at the centre. They obtained the following expression for K_{tp} (residual termination rate constant)

$$K_{tp} = 6 D_{AB} \pi r^2 N_{AV} / (1000 l) \quad (24)$$

where D_{AB} is the mutual diffusivity, N_{AV} is Avagadro's number and l is the average jump length.

And finally

$$K_{tp} = f_t \pi r^2 a N_{AV} K_p [M] / (1000 j_c \cdot 5) \quad (25)$$

where f_t is an efficiency factor, a is the average r.m.s. end-to-end distance per square root of the number of monomer units in the chain and j_c is the entanglement spacing.

Stickler (41) used the equation derived by

Schulz for the reaction diffusion coefficient to obtain a mutual diffusion coefficient (D_{AB})

$$D_{AB} = .2 D_R \quad (26)$$

The bimolecular rate constant was then obtained by inserting D_{AB} into Smoluchowski's equation

$$K_t = 4\pi N_{AV} \Delta D_{AB} / 1000 \quad (27)$$

Here Δ is the reaction radius (28) and was obtained from the following approximate equation

$$\Delta = (6 V_M / (\pi N_{AV}))^{1/3} \quad (28)$$

where V_M = molar volume of the monomer. K_t as obtained from equation (27) was used to successfully model the bulk polymerization of MMA at very high conversions ($x > 0.8$).

Hayden and Melville (39) first reported that at 22.5°C the K_p began to decrease at about 50% conversion in the bulk polymerization of MMA. They postulated that at the last stages of polymerization the mobility of the monomer molecules may be severely limited and the polymerization may terminate before 100% monomer conversion. They reported a

limiting conversion of about 80% at 22.5 °C.

Horie et al (27) were the first to mechanistically discuss diffusion-controlled propagation reactions at very high conversions. They used free-volume theory to interpret these reactions in terms of the rate of diffusion of monomer molecules. They followed the rate of bulk polymerization of MMA and found a distinct minimum separating two peaks. This was thought to be due to the simultaneous reduction of k_t and k_p . The limiting polymer volume fraction of the monomer-polymer mixture was calculated using Kelley and Bueche's relation (42) for the T_g of the mixture and the calculated values agreed well with the experimental limiting conversion values.

Under diffusion-controlled propagation conditions k_p is proportional to D_M ; the self-diffusion coefficient of the monomer molecules. A suitable theoretical equation for a small penetrant molecule in a polymer matrix below the T_g of the polymer is not yet available. Fujita et al (43) have derived an equation on the basis of free-volume theory which has been tested on polymer-penetrant systems above the T_{gp} . The experimental data of

Chalykh and Vasenin (44) suggests an experimental dependence of D_M on ϕ_M . A similar dependence has been predicted for the self-diffusion coefficient of monomer molecules in pure monomer by Bueche (32).

Marten and Hamielec (31) proposed a semi-empirical equation for diffusion-controlled k_p based on Bueche's equation. Their model accounted for a glassy-state transition and successfully predicted limiting conversions (31,34). The occurrence of a glassy-state transition has been confirmed for several polymer systems in bulk and emulsion polymerization by Friis and Hamielec (45), Berens (46) and Harris et al (47). The semi-empirical model for k_p has the following form

$$k_p = k_{p0} \exp(-B(1/V_F - 1/V_{Fcr2})) \quad (29)$$

where B is an adjustable parameter and V_{Fcr2} is the value of V_F at which diffusional limitations are assumed to originate. Stickler (41) has used a slightly different form of equation (29) to model MMA polymerizations at very high conversions over a wide range of initiator levels. Using the initial conditions $k_p = k_{p0}$ at $V_F = V_{F0}$ for $x=0$, he obtained

$$K_p = K_{p0} \exp(-V^* (1/V_F - 1/V_{F0})) \quad (30)$$

where V^* is an adjustable parameter.

Arai and Saito (28) and Sundberg et al (49) have also, independently proposed, an equation similar to that proposed by Marten and Hamielec. The former authors used $B = 1$ to model the diffusion-controlled propagation of MMA, as used by Marten and Hamielec and Stickler et al (48) while Sundberg et al used $B = .38$ for styrene and MMA polymerizations. Recently Soh and Sundberg (50) have proposed the following equation

$$K_{pvf} \propto KT/g_m$$

$$\text{where } g_m = (g_s)_{pp} \exp(1/V_F - 1/V_{Fp}) \quad (31)$$

where K is the Boltzmann constant, T is temperature, g_m and g_s are the monomeric and segmental friction factors, respectively.

The above equation was developed by identifying a chain segment of a polymer radical as a monomeric unit and therefore equating g_m to g_s . The limiting conversions obtained with the use of equation (31) are consistently higher than the experimental values.

2.2 Thermal Homo- and Copolymerization of Styrene

2.2.1 Introduction

The study of the thermal homopolymerization of styrene has received considerable attention in the past and work devoted to understanding the thermal initiation process is still continuing. This section includes a review of relevant work done on bulk and solution thermal polymerization of styrene up to high conversions. The review focusses primarily on the main thermal initiation reaction (creation of the primary radicals), however, pertinent literature involving side reactions during thermal initiation has been quoted, wherever appropriate.

2.2.2 Chemical and diffusion-controlled thermal homo- and copolymerization of styrene

Styrene thermal polymerization kinetics were first studied as early as 1936 by Schulz and Husemann (51) who reported that the bulk polymerization rate was first order with respect to styrene concentration up to about 60% conversion. Breitenbach and Rudorfer (52) found that the rate of solution polymerization was second order in monomer concentration. In the same year Flory (53) proposed a thermal initiation scheme based on the formation of a diradical from two styrene molecules which led to subsequent polymerization. This implied a second order dependence of the rate of polymerization on monomer concentration. Suess et al (54) and later Schulz et al (55) also supported a second-order thermal initiation mechanism which was questioned by Mayo (56) who found a third-order initiation of polymer radicals for the thermal polymerization of styrene in bromobenzene. Zimm and Bragg (57) refuted Flory's hypothesis of the thermal initiation based on their statistical calculations on the existing data. Studies conducted on diradical initiators by Russell and

Tobolsky (58) and Overberger and Lapkin (59) and more recently by Kopecky and Evani (60) all indicated that diradicals formed cyclize too rapidly to initiate polymerization. Hiatt and Bartlett (61) confirmed the third-order nature of the reaction proposed by Mayo. Aso et al (62) proposed a similar initiation scheme involving the formation of a Diels-Alder intermediate as the first step in their study of the thermal polymerization of 2-vinyl thiophene and 2-vinyl furan. They concluded that all vinyl monomers undergo self-initiated polymerization by a similar mechanism. Mayo's hypothesis (56,63) indicated the presence of two independent reactions. One being the polymerization reaction by a free-radical chain mechanism involving a Diels-Alder type of intermediate with an apparent order of about 2.5 and the other parallel bimolecular reaction leading to various dimers. Eleven C_{16} hydrocarbons were identified in the dimer fraction (63) with the main products being 1,2-diphenyl cyclobutanes (DCB) and 1-phenyl tetralin (PT). Muller (64) had earlier claimed that PT was the major oligomer formed. Brown (65) refuted his claim, finding cis and trans 1-2 DCB as the principal dimeric products along with some trimeric oligomers. Buchholz and Kirchner (66) have identified the

Diels-Alder (DA) adduct using spectroscopic techniques. Further spectroscopic studies by Kaufmann et al (67,68) indicated the presence of two intermediates DA_1 and DA_2 . Based on the work of Buchholz (66) and Olaj (67,68) Kirchner and Riederle (69) proposed a detailed thermal initiation scheme and investigated the formation of oligomers and intermediates up to very high conversions. They showed that the thermal initiation reactions do not become diffusion-controlled upto 97% conversion. The thermal copolymerization of styrene and acrylonitrile has been investigated by Kirchner and Schlapkohl (70) who found that the initiation step was analogous to that of pure styrene polymerization. Most recently Chong et al (108) have corroborated the Mayo-scheme at 90°C, in their study of the identification of the end groups of thermally-polymerized polystyrene oligomers.

Chain transfer reactions have also been extensively studied. Chain transfer to monomer has been reported to be negligibly small for styrene polymerization (97,98). Pryor and Coco (71) have corroborated the earlier findings of Olaj (98) who had observed that the N at low conversions is

higher than at high conversions in their simulation study. Both attributed this to the chain transfer to DA, the concentration of which rises with conversion to a steady state value. More recently Olaj et al (68) have found that nearly all chain transfer that occurs is due to the DA_1 which is the more reactive intermediate and is also responsible for initiating the polymerization. DA_2 the unreactive intermediate is essentially consumed in copolymerization reactions with the polymer radicals (68).

Termination reactions have been studied by Mayo et al (97) and Matheson et al (72) among others. Both group of workers indicated that termination occurs essentially by combination. Pryor and Coco (71) obtained a similar result at 60°C and also showed that primary radical termination was practically absent. A kinetic model employing the kinetic scheme of Pryor and Lasswell (73) was developed to study the bulk thermal polymerization of styrene in the temperature range of $100\text{-}200^\circ\text{C}$ upto high conversions by Hui and Hamielec (23), and successfully predicted conversions and \bar{M}_N and \bar{M}_W with time. They considered two limiting cases of the

initiation rate expression viz; second and third order in monomer concentration and obtained best results with the third-order model. Chain transfer to monomer and DA was modelled as follows

$$C_M = C_{M0} + B_1 x \quad (32)$$

where $C_{M0} = K_{fm}/K_p$, and K_{fm} is the chain transfer rate constant to monomer.

Modelling high conversion kinetics (up to nearly 100% conversion) required a diffusion-controlled K_{tc} , and an empirical approach referred to earlier (23) was used to express K_t as a function of x . This model has been used by Husain and Hamielec (24) to model the bulk thermal polymerization of styrene at 200-230 °C. They found that at these elevated temperatures dissolved oxygen has negligible effect on the rate and molecular weight development. They also concluded from their experimental investigations that the MWD is strongly influenced by transfer reactions. Chiantore and Hamielec (8) have studied the thermal polymerization of PMS in the temperature range of 120-160 °C in the conversion range of 0-96%. They developed a kinetic model, accounting for

diffusion-controlled termination, based on a kinetic scheme analogous to that of styrene. A third-order thermal initiation rate was used and transfer reactions to polymer were incorporated in the model as the molecular weight data suggested the formation of some long chain branches through the abstraction of p-methyl hydrogen atoms. Transfer to monomer and oligomers was modelled as for styrene. Excellent fits with the experimental kinetic data was observed for all the temperatures. The gel-effect was observed to be weaker than in the case of styrene.

2.3 Copolymerization Kinetics

2.3.1 Introduction

This section reviews the available theoretical and experimental literature in the area of high conversion copolymerization kinetics. Low conversion chemically-controlled copolymerization kinetics of most commercial vinyl monomers are reasonably well understood. High conversion kinetic data are however lacking. The treatment of diffusion controlled copolymerization reactions parallels that of homopolymerization reactions. As copolymerization involves many more kinetic parameters, a purely mechanistic model would have to follow the change in all these parameters with conversion etc. Therefore lumped parameters have been used by most authors wherever justifiable to simplify the kinetic equations and reduce the parameters to be estimated.

2.3.2 Propagation reactions

Wall first proposed a copolymerization composition equation (74) which neglected the chain

structure including the terminal unit in determining the reactivity of the radical towards a monomer molecule. Mayo and Lewis (75) and Alfrey and Goldfinger (76) independently proposed a kinetic scheme which considered the terminal unit of the radical to influence the rate of addition of the monomer to it. This is called the ultimate effect model in copolymerization literature and requires four propagation constants (k_{ij} , $i, j=1,2$). The ultimate effect model has served as appropriate in most free-radical copolymerizations, however, there are instances where penultimate or even units beyond the penultimate substantially affect the propagation reactions (77). In general, these effects have been attributed to polar and steric factors.

The Mayo-Lewis equation (75) was integrated by Meyer and Lowry (96). This equation relates the total monomer conversion to the residual monomer composition with the reactivity ratios (assumed to be constant) serving as parameters. The Mayo-Lewis equation has been used to estimate reactivity ratios (77) as discussed later in the Appendix. deButts (78) integrated the instantaneous rate of polymerization as derived by Walling (79) on the basis of a

constant initiation rate and no gel-effect. O'Driscoll and Knorr (80) have integrated the individual monomer consumption rate equations assuming constant propagation rate constants, but their derivation requires that $r_1 r_2 = 1$.

Johnson et al (81) first reported that the Meyer-Lowry equation was inadequate in explaining their experimentally measured copolymer composition data for the free-radical copolymerization of styrene/MMA at high conversions. These authors have disputed the constancy of the reactivity ratios (r_1, r_2) with conversion and hypothesized that diffusion-controlled propagation caused the changes in r_1 and r_2 . Dionisio and O'Driscoll (82) observed similar differences between the data and theoretical predictions but rejected Johnson's hypothesis on the grounds that the reactivity ratios being ratios of propagation constants should be independent of the diffusional characteristics of the reaction medium. Terramachi et al (83) and O'Driscoll et al (84) have both corroborated the validity of the Meyer-Lowry equation for the styrene/MMA system.

Diffusion-controlled propagation has been

modelled by Lord et al (3) for the bulk copolymerization of styrene/acrylonitrile. The propagation rate constants were assumed to be constant till high conversions, whereafter each of the propagation reactions was modelled as in diffusion-controlled homopolymerization using the MH model. The fastest of these reactions was assumed to become diffusion-controlled first. Next it was asserted that under diffusion-controlled conditions $k_{ij} = k_{ji}$ ($i = j$), so that two critical free-volume parameters had to be estimated. The r_1 and r_2 , consequently, changed with conversion.

2.3.3 Termination reactions

The kinetic model of Mayo and Lewis (75) and Alfrey and Goldfinger (76) assumed that only the terminal unit of the polymer radical influences termination reactions. This necessitates the estimation of three parameters k_{tij} ($i, j = 1, 2$ $k_{tij} = k_{tji}$) to calculate the overall rate of termination (R_t)

$$R_t = \sum_i \sum_j k_{tij} [R_i][R_j] \quad (33)$$

The chemical-control model of Walling (79) and Mellville et al (85) used a parameter ϕ to calculate the cross-termination constant K_{tab} . ϕ is expected to be equal to one, based on purely statistical arguments and any deviation from this value has been ascribed to polar effects.

It has now been generally accepted that termination reactions in free-radical copolymerizations are diffusion-controlled (14,86-88). Atherton and North (86) proposed an empirical expression for the overall termination constant in the form of a weighted average of the individual homopolymerization termination constants. The weighting factors employed were the instantaneous mole fractions of the individual monomers in the copolymer. Russo and Munari (89) interpreted diffusion-control in terms of the segmental rearrangement of the last four carbon atoms in the copolymer radical. Their equation, which requires two adjustable parameters could explain the data on copolymerization of styrene/MMA and styrene/butyl acrylate. O'Driscoll et al (14) considered the terminal dyad concentration in arriving at an equation which required one parameter. Most recently Chiang and Rudin (90) have proposed a variant of

equation (33) where the weighting factors are the instantaneous mole fractions of the monomers in the copolymer and $K_{t12} = \phi(K_{t11}K_{t22})^{.5}$ as in the chemical control model. Prochazka and Kratochvil (91) have reviewed the major models proposed for termination on the basis of experimental data for the dependence of the initial rate on the comonomer composition. They found that none of the models discussed above could fully describe this dependence. However, the models proposed by Atherton and North (86) and Chiang and Rudin (90) were the best among the diffusion-control models, which were better as a rule than the chemically-controlled ones.

Lord et al (3) used the chemical-control model to calculate the overall termination rate constant at zero conversion in their study of the styrene/acrylonitrile system. Under diffusion-controlled conditions free-volume theory was used to model a single K_t as in homopolymerization kinetics. It was asserted that the onset of diffusion-control occurred at zero conversion.

EXPERIMENTAL

3.1 Chemicals Used

Styrene was supplied by Canadian Industries Ltd., Toronto, Ontario. PMS was supplied by Mobil Chemical Co., Edison, N.J. Monomer purification techniques used are discussed later. All the solvents used in the course of various analyses were used directly without further purification. These are listed in Table 3-1.

TABLE 3-1

Solvents	Grade	Used in
1,4 dioxane	Fisher certified	copolymer dissolution
methanol	Fisher certified	copolymer precipitation
toluene	reagent	GPC (solvent) GC (internal standard) LALLSP (solvent)

3.2 Experimental Conditions

Experimental conditions were chosen to generate data that would complement existing data on the homopolymers, in order to provide a copolymerization model which would be valid over the entire composition range. First a set of randomized runs (w.r.t. f_{10}) were planned at 120° C. Further polymerizations were done with a high and low initial styrene composition ($f_{10} = 0.75, 0.2$) respectively at the following temperatures

$$T = 120^\circ, 140^\circ, 160^\circ, 180^\circ \text{ C}$$

3.3 Apparatus and Experimental Procedures

Thermal copolymerizations were carried out in sealed Pyrex glass ampoules. Two sizes of ampoules were used. 5 mm. O.D. ampoules were employed for copolymerizations at 160° and 180° C and 8 mm. O.D. ampoules were used at 120° and 140° C. These two sizes correspond to 3.4 mm. and 6.0 mm. I.D.

respectively.

A test of the validity of isothermal conditions in these ampoules has been previously done (115). The monomers were washed several times with a 10% KOH solution to remove the inhibitor (t-butyl catechol in both styrene and PMS). Stock solutions of these monomers corresponding to $f_{10} = 0.2$ and 0.75 were prepared and stored for no more than a week before polymerization. Oxygen was removed from the contents (about 2-3 mls. of the solution) by vacuum degassing as described below

- 1) The reaction ampoule was connected to the vacuum manifold and immersed in liquid nitrogen.
- 2) Ten minutes later the ampoule contents were evacuated for fifteen minutes.
- 3) Evacuation was stopped. The liquid nitrogen was removed, allowing the frozen ampoule contents to warm upto room temperature.
- 4) Steps 1 and 2 were repeated. The level of vacuum was maintained at $< .001$ mm. Hg.
- 5) With the ampoule contents frozen, the ampoules were sealed using a gas-oxygen torch.

The sealed ampoules were warmed up to room temperature and then immersed in an oil bath set at the temperature of polymerization. Four temperature levels of 120, 140, 160 and 180 °C were used in this study. After polymerization the ampoule was first immersed in cold water and then in a liquid nitrogen flask to ensure that polymerization had stopped. Next the ampoule was broken in an Erlen Meyer flask and dioxane in sufficient quantity to dissolve the polymer was added to the flask contents. Adequate time was allowed - with the ampoule contents being stirred if required, for complete dissolution of the polymer. A small measured amount of toluene was then added to the solution. A few micro-litres of this solution was then injected into the GC for residual monomer analysis and the determination of monomer conversion. Details of GC analysis are reported in the Appendix(4.1). The remaining solution was slowly poured into at least ten times the volume of methanol. The glass pieces were washed repeatedly with dioxane to ensure the removal of any copolymer adhering to them. The precipitated copolymer was filtered and dried under vacuum at 40 °C for at least 24 hours. The amount of dried copolymer, expressed as a fraction of the total

monomers copolymerized gave an independent measure of conversion.

The copolymer was now ready for molecular weight determination. A few milligrams were dissolved in the required amount of toluene and the solution was used with a low angle laser light scattering photometer (LALLSP)(Chromatix-KMX-6) to obtain \bar{M}_w of the sample. Another portion of the copolymer was dissolved in toluene and injected into the size-exclusion chromatograph (SEC-Waters 150 C) for molecular weight distribution and averages determination. Details of LALLSP and SEC analysis are given in the Appendix(4.2,4.3). Some of the copolymer samples synthesized at 120 °C were used to determine the T_{gp} of the copolymer by means of DSC. Details of this measurement are also given in the Appendix(4.4).

MODEL DEVELOPMENT

4.1 Introduction

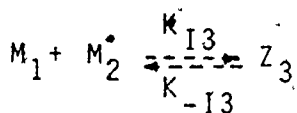
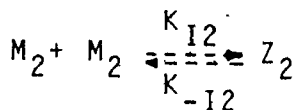
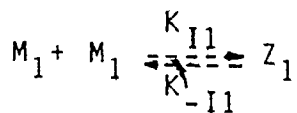
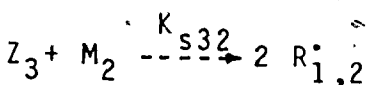
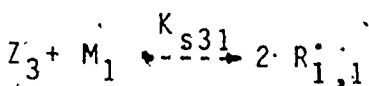
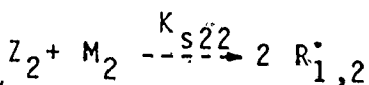
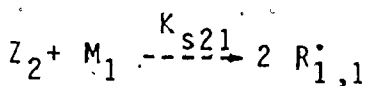
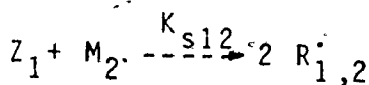
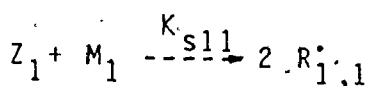
This chapter describes the development of a rather general kinetic model for bulk copolymerization up to high conversions. Equations for the rate of consumption of monomers, copolymer composition drift and molecular weight development have been derived based on a kinetic scheme presented herein. These derivations are presented in this chapter with chapter 5 illustrating the application of this model to two specific copolymerization systems; 1) thermal copolymerization of styrene/PMS 2) chemically-initiated copolymerization of MMA/PMS.

4.2 Kinetic Scheme for Copolymerization

The following system of elementary reactions has been employed to model the bulk thermal copolymerization of styrene/PMS (Monomer 1 is styrene and monomer 2 is PMS) and the bulk copolymerization of MMA/PMS (monomer 1 is MMA and monomer 2 is PMS).

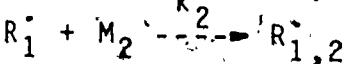
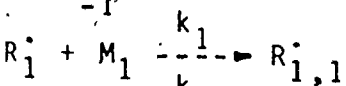
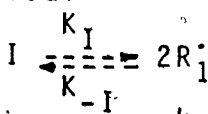
INITIATION

Thermal

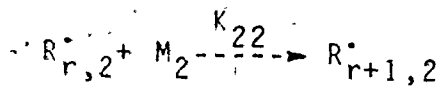
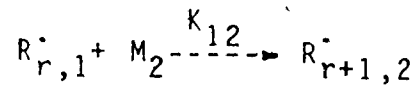
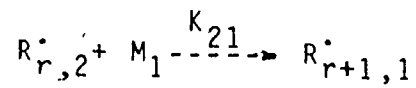
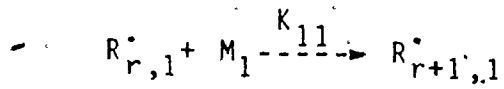
reactive
Diels-Alder
adducts

monoradicals

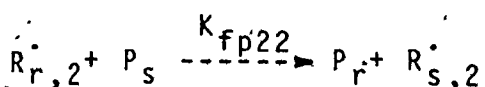
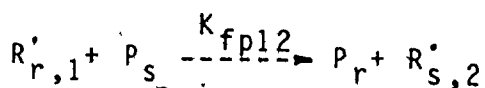
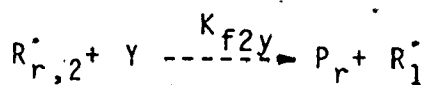
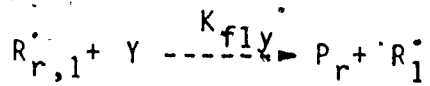
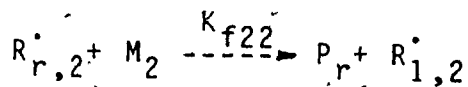
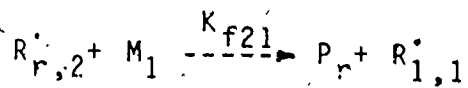
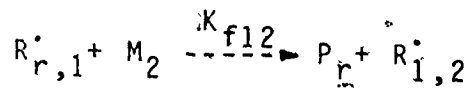
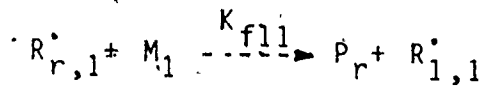
Chemical



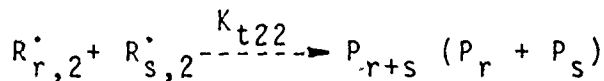
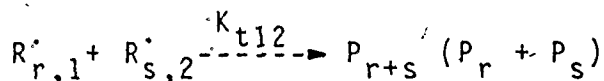
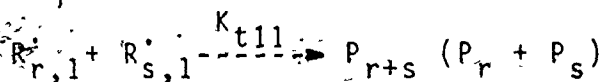
PROPAGATION.



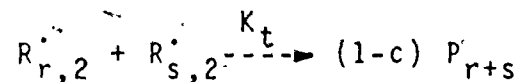
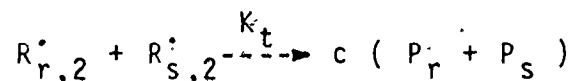
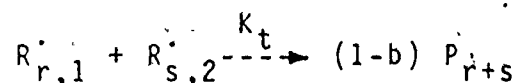
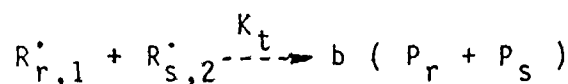
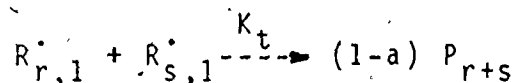
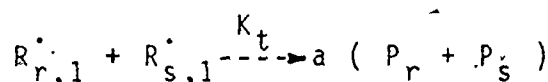
CHAIN TRANSFER



TERMINATION



chemically-
controlled
termination



diffusion-controlled
termination

In the thermal initiation scheme, reactions not affecting the initiation rate of polymer radicals have been excluded. Y represents any unidentified molecule produced via thermal initiation which could act as a chain transfer agent. Termination by disproportionation is considered negligible for styrene/PMS system(24). Transfer to a styrene molecule bound in the copolymer has been neglected with transfer to polymer occurring when a

polymer radical abstracts a hydrogen from the methyl group in the bound PMS. For the MMA/PMS system chain transfer to PMS via abstraction of p-methyl hydrogens is expected to be much greater than chain transfer to MMA. Chain transfer to polymer has been neglected. The I refers to an azobisisobutyronitrile (AIBN) molecule.

4.3.1 Rate of thermal initiation

The radical generation rate (R_i) is given by

$$R_i = 2Z_1(k_{s11}[M_1] + k_{s12}[M_2]) + 2Z_2(k_{s21}[M_1] + k_{s22}[M_2]) + 2Z_3(k_{s31}[M_1] + k_{s32}[M_2]) \quad (34)$$

where $[M_1]$ and $[M_2]$ are concentrations of monomers 1 and 2, and Z_i are the concentrations of the reactive intermediates.

Application of the SSH to Z_i ($i=1,3$) yields

$$Z_i = k_{Ii}[M_j][M_k] / (k_{-Ii} + \sum_j k_{sil}[M_l]) \quad (35)$$

where $j = 1, k = 2$ for $i = 3$

and $j = k = i$ for $i = 1, 2$

Substituting the expression for Z_i in equation (34) and assuming $k_{-Ii} \gg \sum_j k_{sil}[M_l]$ gives

$$R_i = k_{I0}[M]^3 \quad (36)$$

an initiation rate which is third order in total monomer concentration, where

$$K_{I0} = K_1 f_1^3 + K_2 f_2^3 + K_3 f_1^2 f_2 + K_4 f_1 f_2^2$$

$$[M] = [M_1] + [M_2]$$

f_i are the monomer mole fractions

$$K_1 = 2K_{I1}K_{s11}/K_{-I1}$$

$$K_2 = 2K_{I2}K_{s22}/K_{-I2}$$

$$K_3 = 2(K_{I1}K_{s12}/K_{-I1} + K_{I3}K_{s31}/K_{-I3})$$

$$K_4 = 2(K_{I2}K_{s21}/K_{-I2} + K_{I3}K_{s32}/K_{-I3})$$

In the absence of compositional drift during an isothermal batch copolymerization K_{I0} remains constant independent of x till very high conversions (69).

4.3.2 Rate of chemical initiation

R_I for isothermal polymerization is given by

$$R_I = 2fk_d [I]_0 \exp(-K_d t)/(1 - \epsilon x) \quad (37)$$

where f is the initiator efficiency, $[I]$ is the initiator concentration, t is time, x is molar conversion and ϵ is the volume contraction factor as defined below

$$v = v_0(1 - \epsilon x)$$

where v is the reactor volume at any time

4.4 Rate of Monomer Consumption (R_p)

$$R_p = R_{p1} + R_{p2}$$

$$\text{where } R_{p1} = k_{11}[M_1][R_1^\bullet] + k_{21}[M_1][R_2^\bullet]$$

$$\text{and } R_{p2} = k_{12}[M_2][R_1^\bullet] + k_{22}[M_2][R_2^\bullet]$$

where $[R_1^\bullet]$ and $[R_2^\bullet]$ are the concentration of polymer radicals having monomers 1 and 2 as their chain ends respectively. It should be noted that the long chain approximation (LCA) has been used, and penultimate effects have been ignored, hence only four propagation reactions need be considered. Noting that for copolymer chains monomer 1 follows monomer 2 the same number of times that monomer 2 follows monomer 1, it follows that for long copolymer chains

$$k_{21}[M_1][R_2^\bullet] = k_{12}[M_2][R_1^\bullet]$$

$$\text{letting } [R^\bullet] = [R_1^\bullet] + [R_2^\bullet]$$

it can be readily shown that

$$[R_1^\bullet]/[R^\bullet] = [\phi_1^\bullet] = k_{12}f_2/(k_{21}f_1 + k_{12}f_2) \quad (38)$$

$$\text{and } [R_2^\bullet]/[R^\bullet] = [\phi_2^\bullet] = 1 - [\phi_1^\bullet]$$

substituting these definitions in R_{p1} and R_{p2}

$$R_{p1} = (k_{11}[\phi_1^\bullet] + k_{21}[\phi_2^\bullet])[M_1][R^\bullet]$$

$$R_{p2} = (k_{22}[\phi_2^\bullet] + k_{12}[\phi_1^\bullet])[M_2][R^\bullet]$$

Expressing R_p as

$$R_p = k_p[M][R] = R_{p1} + R_{p2} \quad (39)$$

gives

$$k_p = \frac{k_{11}k_{22}(f_1^2k_{11}k_{21} + 2f_1f_2k_{12}k_{21} + f_2^2k_{22}k_{12})}{k_{22}f_1k_{11}k_{21} + k_{11}f_2k_{22}k_{12}} \quad (40)$$

By definition

$$R_p = -(1/v)d(N_m)/dt = ([M]_0/(1-\epsilon x)) dx/dt \quad (41)$$

where N_m , the number of moles of monomers 1 and 2 in the reactor at any time may be expressed in terms of x as

$$N_m = N_{m0}(1-x)$$

$$[M] = N_m/v = [M]_0(1-x)/(1-\epsilon x) \quad (42)$$

Application of the steady state hypothesis (SSH) for polymer radicals gives

$$[R] = (R_i/k_t)^{.5} \quad (43)$$

From equations (39,41-43) one gets

$$dx/dt = k_p(1-x)(R_i/k_t)^{.5} \quad (44)$$

where k_t (diff. controlled) = $k_{tc} + k_{td}$.

$$\text{and } k_{tc} = k_t((1-a)[\phi_1^*]^2 + 2(1-b)[\phi_1^*][\phi_2^*] + (1-c)[\phi_2^*]^2) \quad (45)$$

$$k_{td} = k_t - k_{tc} \quad (46)$$

Under chemically-controlled conditions K_t is obtained as follows

$$\text{rate of termination} = K_{t11}[R_1^*]^2 + K_{t22}[R_2^*]^2 + 2K_{t12}[R_1^*][R_2^*]$$

$$\text{or, } K_t[R]^2 = [R]^2(K_{t11}[\phi_1^*]^2 + K_{t22}[\phi_2^*]^2 + 2K_{t12}[\phi_1^*][\phi_2^*])$$

substituting for $[\phi_1^*]$ and $[\phi_2^*]$

$$K_t = \frac{K_{t11}K_{21}^2f_1^2 + K_{t22}K_{12}^2f_2^2 + 2K_{t12}K_{12}K_{21}f_1f_2}{(K_{12}f_2 + K_{21}f_1)^2} \quad (47)$$

4.5 Copolymer Composition

Defining F_1 as the instantaneous composition of the copolymer formed and then using the definitions of x , f_1 and F_1 one has

$$d[M] = d[M_1]/f_1 - [M_1]df_1/f_1^2 \quad (48)$$

$$\text{thus } f_1 = d[M_1]/d[M] - (df_1/d[M])[M_1]/f_1$$

$$= F_1 - (df_1/d[M])[M_1]/f_1$$

$$\text{or } df_1/(F_1 - f_1) = d \ln(1 - x) \quad (49)$$

$$\text{where } F_1 = \frac{K_{21}[(K_{11} - K_{12})f_1^2 + f_1]}{(K_{11}K_{21} + K_{22}K_{12} - 2K_{12}K_{21})f_1^2 + 2K_{12}(K_{21} - K_{22})f_1 + K_{22}K_{12}} \quad (50)$$

Solution of equations (49) and (50) yields f_1 and F_1 as function of x .

A simple balance on monomer 1 relates \bar{F}_1 , the cumulative copolymer composition, to f_1 and x , to give.

$$\bar{F}_1 = (f_{10} - f_1(1 - x))/x \quad (51)$$

4.6 Molecular Weight Development

4.6.1 Linear copolymer

Considering transfer reactions to monomer and other small molecules (Y) only and neglecting transfer to polymer molecules, one obtains the following expressions for the rate of transfer reactions

$$\begin{aligned} \text{rate of transfer to monomers 1 and 2} &= K_{f12}[M_2][R_1^\bullet] \\ &+ K_{f11}[M_1][R_1^\bullet] + K_{f22}[M_2][R_2^\bullet] + K_{f21}[M_1][R_2^\bullet] \end{aligned} \quad (52)$$

Expressing equation (52) as $= K_{fm}[M][R]$

Substituting for $[R_1^\bullet], [R_2^\bullet]$ one has for K_{fm}

$$K_{fm} = \frac{K_{21} K_{f11} f_1^2 + f_1 f_2 (K_{21} K_{f12} + K_{12} K_{f21}) + K_{12} f_2^2 K_{f22}}{(K_{21} f_1 + K_{12} f_2)} \quad (53)$$

$$\text{rate of transfer to } [Y] = K_{f1y}[R_1^\bullet][Y] + K_{f2y}[R_2^\bullet][Y] \quad (54)$$

Again expressing equation (54) as $= K_{fy}[Y][R]$

one has for K_{fy}

$$K_{fy} = [\phi_1^*] K_{f1y} + [\phi_2^*] K_{f2y} \quad (55)$$

Analogous to homopolymerization kinetics the following equations may be written for r_N and r_W , the number and weight average chain length of the copolymer (instantaneous) and the instantaneous differential chain length distribution ($W(r,x)$) for linear chains

$$r_N = 1/(\tau + \beta/2) \quad (56)$$

$$r_W = 2(\tau + 1.5\beta)/(\tau + \beta)^2 \quad (57)$$

$$W(r,x) = (\tau + \beta)(\tau + \beta/2(\tau + \beta)r) \exp(-(\tau + \beta)r) \quad (58)$$

$$\text{where } \tau = K_{fm}/K_p + K_{fy}[Y]/K_p[M] + K_{td}R_p/(K_p[M])^2 \quad (59)$$

$$\text{and } \beta = K_{tc}R_p/(K_p[M])^2 \quad (60)$$

The cumulative number and weight average molecular weights, \bar{M}_N and \bar{M}_W , and the differential chain length distribution of the accumulated copolymer ($\bar{W}(r,x)$) are given by

$$\bar{M}_N = C_W / \int_0^{C_W} dC_W / M_N \quad (61)$$

$$\bar{M}_W = (1/C_W) \int_0^{C_W} M_W dC_W \quad (62)$$

$$\bar{W}(r,x) = (1/x) \int_0^x W(r,x) dx \quad (63)$$

$$\text{where } M_N = r_N \text{ CMOM}$$

$$M_W = r_W \text{ CMOM}$$

$$\text{CMOM} = F_1 M_{m1} + F_2 M_{m2}$$

M_{m1} and M_{m2} are the molecular weights of the two monomers and C_W is the monomer conversion on a weight basis.

4.6.2 Copolymer with long chain branching

When transfer to polymer becomes significant, the use of $W(r,x)$ is not appropriate. One must then resort to the method of moments to calculate the molecular weight averages. Writing the differential balance equations for polymer radicals and polymer molecules and then applying the SSH to the former, provides the following equations for the leading moments of the MWD (Q_0, Q_1, Q_2) and the average number of long chain branches per polymer molecule (\bar{B}_N).

$$(1/v)d(Q_0 v)/dt = k_p [M][R] (\tau + \beta / 2) \quad (64)$$

$$(1/v)d(Q_1 v)/dt = k_p [M][R] \quad (65)$$

$$(1/v)d(Q_2 v)/dt = \frac{k_p [M][R] (1 + C_p Q_2 / [M]) (2\tau + 3\beta + 2C_p Q_1 / [M] + C_p Q_2 / [M])}{(\tau + \beta + C_p Q_1 / [M])^2} \quad (66)$$

$$(1/v)d(Q_0 \bar{B}_N v) = k_p [M][R] (C_p Q_1 / [M]) \quad (67)$$

where $C_p = K_{fp}/K_p$

and K_{fp} , a pseudo transfer to polymer rate constant for copolymerization is obtained as follows.

rate of transfer to copolymer

$$= K_{fp11}[R_1^*] F_1 Q_1 + K_{fp12}[R_1^*] F_2 Q_1 \\ + K_{fp21}[R_2^*] F_1 Q_1 + K_{fp22}[R_2^*] F_2 Q_1 = K_{fp}[R^*] Q_1$$

whereby $K_{fp} = [\phi_1^*](F_1 K_{fp11} + F_2 K_{fp12}) + [\phi_2^*](F_1 K_{fp21} + F_2 K_{fp22})$ (68)

Here $Q_i = \sum_r r^i P_r$

Unlike the other pseudo rate constants, K_{fp} is defined only for copolymerization without composition drift.

4.7 Diffusion-Controlled Reactions

Under diffusion-controlled conditions K_t and K_{ij} would change with conversion. Two approaches have been used to model these reactions.

4.7.1 Empirical approach

Here the K_{ij} 's were assumed to be constant throughout. K_t was assumed to vary with conversion in the following manner

$$K_t = K_{t0} \exp(-2(Ax + Bx^2 + Cx^3)) \quad (69)$$

$$\text{where } A = A_1 + A_2 T$$

$$B = B_1 + B_2 T$$

$$C = C_1 + C_2 T$$

$$\text{and } K_t = K_{t0} \quad \text{at } x = 0$$

where K_{t0} , the segmentally-controlled rate constant for termination was assumed to be given by equation (47).

4.7.2 Application of the free-volume theory

The initial increase in K_t' with c , due to segmental diffusion-control, was accounted for in the model by using the following equation at the beginning of copolymerization

$$K_t = K_{t0}(1 + dc) \quad (70)$$

Equation (70) was used until the onset of entanglements which was assumed to change the mode of control of termination from segmental to translational diffusion. It should be noted that this represents an approximate attempt to model the real situation since segmental diffusional resistances may

become important before the radical chains get entangled. However, the situation where translational diffusion-control (hereafter referred to simply as diffusion-control) occurs before chain entanglements, has not been accounted for in the present model.

Free-volume theory has been used to predict self-diffusion coefficient of the macroradicals under diffusion-controlled conditions. This model follows the MH model in defining expressions for the D_p of unentangled and entangled polymer radicals. K_3 as defined by the following relation was used to identify the onset of entanglements

$$K_3 = (\bar{M}_{wcr1})^m \exp(A/V_{Fcr1}) \quad (71)$$

Under diffusion-controlled conditions K_t is given by the following equation

$$K_t = K_{tcr1} (\bar{M}_{wcr1}/\bar{M}_w)^n \exp(A(1/V_{Fcr1} - 1/V_F)) \quad (72)$$

where $K_t = K_{tcr1}$ when equation (71) is satisfied.

At very high conversions as the polymer chains become essentially immobilized, the chain ends of the growing macroradicals move only by reaction diffusion. Following Stickler (41) the following expression for K_{trd} was used

$$K_{trd} = (8\pi N_{AV}/6000) n_s 10^2 k_p [M] \quad (73)$$

$$= D k_p [M]$$

Chain propagation is also a diffusion-controlled reaction at high conversions. Following Marten and Hamielec (31) the diffusion-controlled propagation rate constant was defined as follows

$$K_{ij} = K_{ij0} \exp(-B(1/V_F - 1/V_{Fcr2ij})) \quad \text{at } x > x_{crit2ij} \quad (74)$$

DATA INTERPRETATION

5.1 Introduction

This chapter describes the application of the previously derived kinetic models to first, the bulk thermal copolymerization of styrene/PMS and second, the chemically-initiated bulk copolymerization of MMA/PMS.

5.2 Parameter estimation

5.2.1 Styrene/PMS copolymerization

Application of the kinetic models to both comonomer systems requires values for r_1 and r_2 . The following expression relating total conversion to the residual and initial monomer composition was used to calculate r_1 and r_2 .

$$C_W = 1 - (N/N_0) \left(\frac{f_1 M_{m1} + f_2 M_{m2}}{f_{10} M_{m1} + f_{20} M_{m2}} \right) \quad (75)$$

$$\text{where } N/N_0 = (f_1/f_{10})^\alpha (f_2/f_{20})^\beta ((f_{10}-\Omega)/(f_1-\Omega))^\Delta \quad (76)$$

$$\text{and } \alpha = r_2/(1-r_2)$$

$$\beta = r_1/(1-r_1)$$

$$\Omega = (1-r_2)/(2-r_1-r_2)$$

$$\Delta = (1-r_1r_2)/((1-r_1)(1-r_2))$$

The simplified error in variables approach (102) was used and the non-linear estimation routine was fed with the best starting values available on the styrene/PMS system (107) viz; $r_1 = .83$ and $r_2 = .96$. A set of randomized runs scanning the full composition range of f_{10} at 120°C and conversion ranging from 0-90% was used in the estimation. Converged estimates of the reactivity ratios were as follows

$$r_1 = 0.971 \pm 0.007$$

$$r_2 = 0.907 \pm 0.0135$$

$$\text{correlation coefficient} = 0.35$$

As further polymerizations at 140, 160 and 180°C revealed no discernible composition drift within experimental error, it was decided to model this system assuming no composition drift with conversion. As the individual propagation constant K_{22} was not available, and since styrene and PMS have been observed to follow similar conversion-time profiles (2), K_{22} was assumed to be equal to K_{11} (24). In other words $K_{11} = K_{22} = K_{12} = K_{21}$.

The empirical model can account for diffusion-controlled K_t and K_p . In the present application propagation reactions were assumed to be chemically-controlled throughout the course of reaction so that K_p remains constant at K_{p0} for a particular temperature.

Defining ϕ_x and ϕ_0 as follows

$$\phi_x = (K_p^2 K_{I0} [M]_0^3 / K_{tc})^{.5} \quad ; \quad \phi_0 = (K_{p0}^2 K_{I0} [M]_0^3 / K_{tc0})^{.5}$$

one has from equations (36,42,44)

$$dx/dt = \phi_x ((1-x)^5 / (1-\epsilon x)^3)^{.5} \quad (77)$$

$$\text{Also} \quad \phi_x / \phi_0 = (K_{tc0} / K_{tc})^{.5}$$

where K_{tc0} is given by equation (47).

ϕ_x was expressed as

$$\phi_x = \phi_0 \exp(Ax + Bx^2 + Cx^3) \quad (78)$$

Substituting equation (78) into equation (77) one has

$$dx/dt = \phi_0 \exp(Ax + Bx^2 + Cx^3) ((1-x)^5 / (1-\epsilon x)^3)^{.5} \quad (79)$$

ϕ_0 was estimated for each temperature and f_{10} from

the x-time data by integrating equation (79) over a small time interval

$$\phi_0 = 1/\Delta t \int_x^{x_0} ((1-\epsilon x)^3 / (1-x)^5)^{.5} dx \quad (80)$$

where $x=x_u$ at $t=\Delta t$

The parameters A, B, C were estimated by fitting the solution of equation (79) to the experimental data for each temperature and f_{10} . These were regressed on temperature and then on F_1 to obtain a model applicable over the composition levels investigated in the present work ($f_{10}=0.2, 0.75$) and reported earlier ($f_{10}=0, 1$).

$$A = A_1 - 0.00505 T$$

$$B = B_1 - 0.0176 T$$

$$C = C_1 - 0.00785 T$$

$$\text{where } A_1 = 0.405 + 2.11F_1 - 1.51F_1^2 + 1.56F_1^3$$

$$B_1 = 16.65 - 16.17F_1 + 15.97F_1^2 - 6.9F_1^3$$

$$C_1 = 8.98 - 16.48F_1 + 16.627F_1^2 - 6.095F_1^3$$

Parameter estimation was done by using a non-linear least squares routine which uses a combination of Gaussian linearization and the method of steepest descent.

The molecular weight calculations require values of τ and β . It was decided to employ the following relation for τ assuming $[Y]/[M] \propto x$, as has been done earlier for the homopolymers (8,23).

$$\tau = K_{fm}/K_p + [\phi_1]B_1x + [\phi_2]B_2x \quad (81)$$

where $B_i = K_{fis}/K_p \quad i = 1,2$

The value of K_{tc0} was estimated in the following manner; the transfer constants K_{f21} and K_{f12} were assumed to be equal to known values of K_{f11} and K_{f22} (references 24,8) respectively. In other words the rate of hydrogen abstraction from the monomers was assumed to be dependent on the monomer itself and independent of the radical type. This gives a value for K_{fm} . \bar{M}_W obtained by LALLSP at low conversions was then used to calculate K_{tc0} .

at $x \sim 0$

$$\bar{M}_W = \sqrt{(2 \text{ CMOM} (\tau + 1.5\beta) / (\tau + \beta)^2)} \quad (82)$$

$$\tau = K_{fm}/K_p$$

$$\beta = K_{tc0}R_p / (K_p [M]_0)^2$$

$$R_p = [M]_0 \cdot dx/dt$$

R_p at $x \sim 0$, was obtained from the initial slope of x -time profiles and then equation (82) was solved for K_{tc0} .

Values of K_1 , K_2 and K_{t11} were obtained from (8) and (24). Setting K_{22} equal to K_{11} enabled the calculation of K_{t22} from the known value of $K_{22}/K_{t22}^{.5}$ (8). K_{t12} , K_3 and K_4 were then obtained from the K_{tc0} and ϕ_0 values.

$$K_3 = .189E7 \exp(-26070/(RT)) \text{ lit.}^2/\text{mole}^2, \text{min}$$

$$K_4 = .134E7 \exp(-23470/(RT)) \text{ lit.}^2/\text{mole}^2, \text{min}$$

$$K_{t22} = .141E12 \exp(-1976/(RT)) \text{ lit/mole, min}$$

$$K_{t12} = .142E13 \exp(-3974/(RT)) \text{ lit/mole, min}$$

$$K_1 = 2.628E7 \exp(-27440/(RT)) \text{ lit}^2/\text{mole}^2, \text{min}$$

$$K_2 = .136E7 \exp(-24560/(RT)) \text{ lit}^2/\text{mole}^2, \text{min}$$

$$K_{t11} = .753E11 \exp(-1677/(RT)) \text{ lit/mole, min}$$

The cross-initiation constants K_3 and K_4 are found to be comparable in magnitude to K_1 and K_2 . The values of the activation energy and frequency factor found for K_{t12} are higher than those for K_{t11} and K_{t22} . This is clearly due to the high correlation between these two parameters.

The use of the free-volume model required the calculation of the free-volume fraction. The following equation was used to calculate V_F

$$V_F = (.025 + \alpha_{M1}(T - T_{gM1}))V_{M1}/V_T + (.025 + \alpha_{M2}(T - T_{gM2}))V_{M2}/V_T + (.025 + \alpha_p(T - T_{gp}))V_p/V_T \quad (83)$$

where M_1, M_2 and P denote monomers 1, 2 and polymer respectively; T is polymerization temperature; V is volume; V_T total volume; $\alpha = \alpha_l - \alpha_g$; α is expansion coefficient; l, g denote liquid and glassy state respectively. The following equation after Fedors (105) was used to estimate T_{gM1} and T_{gM2}

$$T_g = (T_M + T_b - r_T T_b) / r_T \quad (84)$$

where r_T is a characteristic temperature ratio, T_M and T_b are the melting and boiling points of the monomers.

$T_{M1}, T_{M2}, T_{b1}, T_{b2}$ were obtained from Kaeding et al (116). α_{M1} and α_{M2} were both set at .001 and α_p at .00048 as these values have been used to model styrene polymerization at low temperatures (34):

$$T_{M1} = -31 \text{ }^\circ\text{C}$$

$$T_{M2} = -34 \text{ }^\circ\text{C}$$

$$T_{b1} = 145 \text{ }^\circ\text{C}$$

$$T_{b2} = 170 \text{ }^\circ\text{C}$$

$$T_{gM1} = -117 \text{ }^\circ\text{C}$$

$$T_{gM2} = -123 \text{ }^\circ\text{C}$$

$$r_T = 1.15$$

Three regions of conversion have been identified in the present model. These are :

Interval 1 $t = 0$ to the point where equation (71)

is satisfied, with $m = .5$

$$K_{tc} = K_{tc0} (1 + d c)$$

$$K_{ij} = K_{ij0} \quad i, j = 1, 2$$

$K_{tc} = K_{tcr1}$ when equation (71) is satisfied

$\bar{M}_W = \bar{M}_{Wcr1}$ when equation (71) is satisfied

Interval 2 $K_{tc} = K_{tcr1} \exp(-A(1/V_F - 1/V_{Fcr1})) + DK_p[M]$ (85)

$$K_{ij} = K_{ij0}$$

Interval 3 $x > x_{crit2ij}$

$$K_{ij} = K_{ij0} \exp(-B(1/V_F - 1/V_{Fcr2ij}))$$

$K_{tc} = K_{tc}$ as in interval 2

Equation (85) was used in intervals 2 and 3 as the experimental data showed no evidence of \bar{M}_W increasing with conversion. Such an equation has been used by Soh and Sundberg (36) for low temperature styrene polymerization upto moderate to high conversions.

A rigorous theoretical calculation of d for segmentally-controlled K_t requires parameters that were unavailable in the literature (7). The plots of K_{tc} as a function of conversion obtained by using

equation (69) were used to estimate d . Assuming a linear relation between K_{tc} and c at low conversions ($x < .1$), d was found to be approximately equal to $.001(\text{lit./gm})$. This value for d compares well with that found by Dionisio et al (108) for styrene polymerization at 77°C and was found to be largely independent of temperature and comonomer composition, permitting a single value to be used in the model. The calculation of K_{trd} required the values for n_s and l_0 . Schulz (38) gives $n_s = 10$ and $l_0 = .25 \text{ nm}$. for MMA and these values have been used by Stickler (41) for MMA polymerization. The corresponding values for styrene/PMS system were unavailable, hence the same values were used here. The model predictions are quite insensitive to values used for n_s and l_0 (see section 6.2).

An initial parameter search for styrene thermal homopolymerization, at temperature levels of 140 and 170°C using experimental low to moderate conversion versus time data yielded a value of $A = 0.85$. A sixth-order Runge-Kutta differential equation solver within a Gauss-Marquadt optimization scheme was used to fit the conversion-time profiles. This value for A was also found to fit experimental low

to moderate x-time profiles for PMS thermal homopolymerization at temperatures of 120, 140 and 160 °C as well as all the thermal copolymerization data. A was then fixed at 0.85 and B and x_{crit2} were next estimated by visually fitting all the x-time data available on this system, since the parameter estimation routine proved to be inefficient because of the high correlation between these parameters. A value of 0.5 for B was found to fit adequately all the x-time data. A single value of V_{fcr2} was searched for as $K_{ij} = K_{ji}$ (i,j=1,2).

Other physical and kinetic parameters used in this work are as follows

$$\epsilon = (1/(W_{M1}d_{M2} + W_{M2}d_{M1})) / (d_p(W_{M1}d_{M2} + W_{M2}d_{M1}) - d_{M1}d_{M2}) / d_p$$

where d is density and W is the weight fraction in monomer phase.

$$d_{M1} = 0.924 - .918E-3(T-273.1) \text{ gm/cc} \quad \text{reference (24)}$$

$$d_{M2} = 0.9261 - .918E-3(T-273.1) \text{ gm/cc} \quad \text{assumed}$$

$$d_p = 1.084 - .605E-3(T-273.1) \text{ gm/cc} \quad \text{reference (24)}$$

The composition dependence of d_p has been neglected.

$$K_{11} = 6.306E8 \exp(-7068/(RT)) \text{ lit/mole, min} \quad \text{reference (24)}$$

$$K_{f11} = 1.38E8 \exp(-12670/(RT)) \text{ lit/mole, min.} \quad \text{reference (24)}$$

$$K_{f22} = K_{22}^* .15 \exp(-5630/(RT)) \text{ lit/mole, min} \quad \text{reference (8)}$$

$$B_1 = K_{f1S}/K_p = -1.01E-3 \log_{10} ((473.12-T)/202.5) \text{ reference (23)}$$

$$B_2 = K_{f2S}/K_p = -(.0015 + 2.5E-6(T-393.12)) \log_{10} (473.12-T)/202.5$$

$$K_3 = 3.0 \exp(3423/T) \quad \text{non-linear least squares fit}$$

$$T_{gp}(F_1=0) = 113^\circ\text{C} \quad \text{reference (2)}$$

$$T_{gp}(F_1=0.2) = 108^\circ\text{C} \quad \text{measured}$$

$$T_{gp}(F_1=0.75) = 104^\circ\text{C} \quad \text{measured}$$

$$T_{gp}(F_1=1) = 100^\circ\text{C} \quad \text{reference (2)}$$

The specific refractive index (dn/dc) for the copolymer was found to obey the following relationship for the levels of composition investigated (109)

$$(dn/dc)_{cop} = W_1 (dn/dc)_1 + W_2 (dn/dc)_2$$

$$(dn/dc)_1 = 0.11 \text{ cc/gm}$$

$$(dn/dc)_2 = 0.0913 \text{ cc/gm}$$

Both measured in toluene at 25°C at $\lambda = 632.8 \text{ nm}$. W_1 and W_2 are the weight fractions of each monomer in the copolymer.

5.2.2 MMA/PMS copolymerization

Reactivity ratios were estimated in a manner similar to that discussed earlier in 5.2.1. a was set equal to λ , the fraction of radicals terminating by disproportionation in the homopolymerization of MMA, as obtained by Stickler et al (48) and b was assumed equal to 0.5 with $c=0$ in equation (45).

$$\lambda = \exp(3.55 - 1460/T) \quad (86)$$

K_{p0} could be calculated as K_{11} (reference 31) and K_{22} were known. K_{t0} and d were obtained by fitting the initial x -time data as the R_I could be independently calculated. The values for K_{t0} appear to be independent of temperature and at high MMA concentration, approach the K_{t11} for MMA homopolymerization as reported by Meyerhoff (110). This value for K_{t11} was used to simulate MMA homopolymerizations. d (segmental diffusion-control) was found to be independent of temperature, initiator level and comonomer compositions. The initial value for C_M (C_{M0}) was obtained from \bar{M}_W measured by LALLSP at low conversions. The C_M was set equal to C_{M0} upto $x=x_{crit2}$ since the individual rate constants K_{f12} and K_{f21} were not available. This is felt justifiable because of the small value of the

pseudo rate constant and lack of appreciable composition drift until very high conversions. Equation (71) was used with $m=0.5$ to identify the onset of diffusion-controlled termination. The model divides the copolymerization into the following three intervals

Interval 1 $t = 0$ till equation (71) is satisfied

$$K_{ij} = K_{ij0} \quad i, j=1, 2$$

$$K_t = K_{t0} (1 + dc')$$

$$K_t = K_{tcr1} \quad \text{when equation (71) is satisfied}$$

Interval 2 $K_t = K_{tcr1} (\bar{M}_{wcr1} / \bar{M}_w)^{1.75} \exp(-A(1/V_F - 1/V_{Fcr1}))$
 $+ D K_p [M]$

$$K_{ij} = K_{ij0}$$

Interval 3 $x > x_{crit2ij}$

$$K_t = \text{as in interval 2}$$

$$K_{ij} = K_{ij0} \exp(-B(1/V_F - 1/V_{Fcr2ij}))$$

$$\text{where } V_{Fcr2ij} = V_F \text{ at } x = x_{crit2ij}$$

D was obtained from values given by Stickler (41) for MMA homopolymerization as the appropriate values for the copolymer were not available.

Fitting only the azeotropic runs from low to moderate conversion, a simultaneous search for K_3 and A gave a constant value for A of 1.24 for all conditions. It was then found that this value satisfied the remaining runs as well. With A fixed, a search for V_{Fcr2ij} for all the x-time data was conducted. A single value for V_{fcr2} was found to satisfactorily fit all the data. The significance of this finding is discussed in section 6.3. Experimental details for this system may be found in reference (4). The parameters found for copolymer characterization have been listed therein. The complete list of model parameters appears in the Appendix(7).

TABLE 5-1

$T=120^{\circ}\text{C}$ $f_{10}=0.2$	time (hours)	$C_W(\text{GC})$	$C_W(\text{grav.})$
	0.5	0.058	0.06
	1.0	0.138	0.14
	1.5	0.192	
	2.0	0.231	0.23
	2.0	0.204	0.21
	3.0	0.323	0.28
	4.0	0.378	
	5.0	0.465	0.45
	6.0	0.602	0.60
	8.2	0.715	0.70
	12.0	0.815	0.84
	20.0	0.902	0.90
$T=120^{\circ}\text{C}$ $f'_{10}=0.75$			
	1.0	0.092	0.09
	2.3	0.228	
	3.0	0.291	0.27
	5.0	0.421	0.42
	7.0	0.568	0.57
	12.0	0.754	0.75
	22.0	0.882	

T=140 °C	time	C _W	'C _W
f ₁₀ =0.2		GC	grav.
	0.5	0.203	0.18
	1.0	0.321	
	2.0	0.534	0.51
	3.0	0.618	0.62
	4.0	0.723	
	5.0	0.798	0.77
	7.0	0.881	
	15.0	0.945	0.95

T=140 °C	time	C _W	'C _W
f ₁₀ =0.75			
	0.5	0.138	0.14
	0.8	0.213	0.21
	1.5	0.394	0.36
	3.1	0.621	0.62
	6.0	0.848	
	7.0	0.849	0.83
	15.0	0.948	

T=160 °C	time	C _W	'C _W
f ₁₀ =0.2			
	0.2	0.252	0.25
	0.6	0.348	0.40
	1.0	0.637	0.64
	2.0	0.795	0.81

	time	$C_W(\text{GC})$	$C_W(\text{grav.})$
	3.0	0.893	
	4.0	0.901	0.86
	5.0	0.91	0.92
	5.9	0.91	0.95
T=160 °C			
$f_{10}=0.75$			
	0.2	0.158	0.16
	0.5	0.382	0.405
	2.0	0.794	
	3.1	0.847	0.82
	4.1	0.882	
	6.0	0.902	0.91
T=180 °C			
$f_{10}=0.2$			
	0.2	0.447	0.45
	0.6	0.731	
	1.0	0.828	0.80
	1.9	0.923	0.89
	3.0	0.94	0.92
	4.0	0.96	0.94
T=180 °C			
$f_{10}=0.75$			
	0.1	0.247	0.25
	0.5	0.699	

time	C_W (GC)	C_W (grav.)
1.0	0.795	0.75
1.3	0.883	0.89
4.0	0.94	

TABLE 5-2

$T=120^\circ\text{C}$	C_W	$\bar{M}_N(.1E-4)$	$\bar{M}_W(.1E-4)$	$\bar{M}_W(.1E-4)$
$f_{10}=0.2$			(SEC)	(LALLSP)
	0.06	2.32	3.77	
	0.14	2.3	3.7	
	0.20			3.75
	0.32	2.3	3.9	4.15
	0.38			4.25
	0.47	2.41	4.0	4.20
	0.60			4.37
	0.72			5.13
	0.84	2.6	4.7	5.20
$T=120^\circ\text{C}$				
$f_{10}=0.75$				
	0.09			4.1
	0.27	2.2	4.6	4.5
	0.42	2.27	4.95	4.55
	0.57	2.0	4.9	
	0.88			4.93

$T=140^{\circ}\text{C}$	C_W	$\bar{M}_N (.1E-4)$	$\bar{M}_W (.1E-4)$	$\bar{M}_W (.1E-4)$
$f_{10}=0.2$			(SEC)	(LALLSP)
	0.32	1.65	2.6	3.12
	0.5	1.65	3.03	3.12
	0.62	1.7	3.20	3.28
	0.77	2.01	3.75	3.95
	0.95	1.6	3.18	3.3

$T=140^{\circ}\text{C}$				
$f_{10}=0.75$				
	0.14	1.44	2.9	
	0.21	1.43	3.0	3.2
	0.39			3.0
	0.62	1.32	3.12	3.12
	0.85	1.41	3.4	3.3
	0.85	1.4	3.3	3.7
	0.95	1.43	3.35	3.1

$T=160^{\circ}\text{C}$				
$f_{10}=0.2$				
	0.25	1.15	1.95	
	0.35	1.21	2.0	2.05
	0.64	1.1	2.12	2.0
	0.80	1.15	2.2	2.15
	0.89	1.1	2.23	2.25
	0.91	1.1	2.18	2.3

	C_W	$\bar{M}_N(.1E-4)$	$\bar{M}_W(.1E-4)$	$\bar{M}_W(.1E-4)$
$T=160^\circ C$	0.95	1.1	2.25	2.25
$f_{10}^0=0.75$				
	0.16	0.98		
	0.38		1.9	2.05
	0.67	0.93	2.05	2.05
	0.79	0.92	2.05	
	0.85	0.93	2.05	2.15
	0.88	0.93	2.15	2.25
	0.91	0.96	2.07	
$T=180^\circ C$				
$f_{10}^0=0.2$				
	0.45	0.82	1.42	1.42
	0.73	0.7	1.41	1.5
	0.83	0.7	1.41	1.45
	0.92	0.64	1.43	1.43
	0.94	0.6	1.4	1.4

TABLE 5-3 Reproducibility studies for styrene/PMS copolymerization

1. conversion by gravimetry

$f_{10}^0=0.2$ $T=120^\circ C$

$t=12$ hrs.

1) .827

2) .813

3) .796

4) .823

mean = .815 std.deviation = .014

2. conversion by GC

1) .821

2) .815

3) .823

4) .805

mean = .816 std.deviation = .002

3. residual monomer analysis

 $f_{10} = .2$ $T = 120^\circ\text{C}$ $t = 12$ hrs.

1) .019

2) .017

3) .017

4) .018

mean = .018 std.deviation = .001

4. \bar{M}_W by LALLSP $f_{10} = 0.2$ $T = 120^\circ\text{C}$ $C_W = 0.715$

1) 5.13E5

2) 4.82E5

3) 4.78E5

mean = 4.91E5 std.dev. = .19E5

 \bar{M}_W by SEC $f_{10} = 0.2$ $T = 120^\circ\text{C}$ $C_W = 0.47$

1) 4.0E5

2) 3.8E5

3) 4.5E5

mean = 4.1E5 std.dev. = .36E5

5. \bar{M}_N by SEC

$$f_{10} = .2 \quad T = 120^\circ\text{C}$$

$$C_W = 0.47 \quad 1) \quad 2.52E5$$

$$2) \quad 2.38E5$$

$$3) \quad 2.33E5$$

$$\text{mean} = 2.41E5 \quad \text{std.dev.} = .1E5$$

TABLE 5-4 Variation of K_3 and V_{Fcr2} with temperature

f_{10}	T ($^\circ\text{C}$)	$K_3 (.1E-3)$	V_{Fcr2}
1	120	1.78	0.12
	140	1.14	0.11
	170	0.65	0.126
0.75	120	1.83	0.121
	140	1.26	0.116
	160	0.95	0.127
	180	0.67	0.13
0.20	120	1.9	0.113
	140	1.24	0.116
	160	0.88	0.126
	180	0.65	0.13
0.0	120	1.6	0.12
	140	1.06	0.117
	160	0.74	0.125

RESULTS AND DISCUSSION

6.1 Model for Styrene/PMS Copolymerization Using Empirical Approach to Model Diffusion-controlled Propagation and Termination

The fits of the experimentally measured conversion data with model predictions are shown in figures 1, 2, 3 and 4. The model predictions are seen to overestimate the conversions at the higher temperatures beyond 90% conversion. An explanation for this discrepancy is deferred till section 6.2 where the free-volume model predictions are discussed.

The model predictions are compared with the measured \bar{M}_N and \bar{M}_W data in figures 5-9. No systematic deviation from experimental data is observed in figures 5-8 for any of the experimental conditions. Agreement between model predictions and \bar{M}_N data for copolymer with a styrene content of 75% in figure 9, is rather poor. The model follows the trend in \bar{M}_N data which shows an almost continuous decrease with conversion, suggesting that the rate of

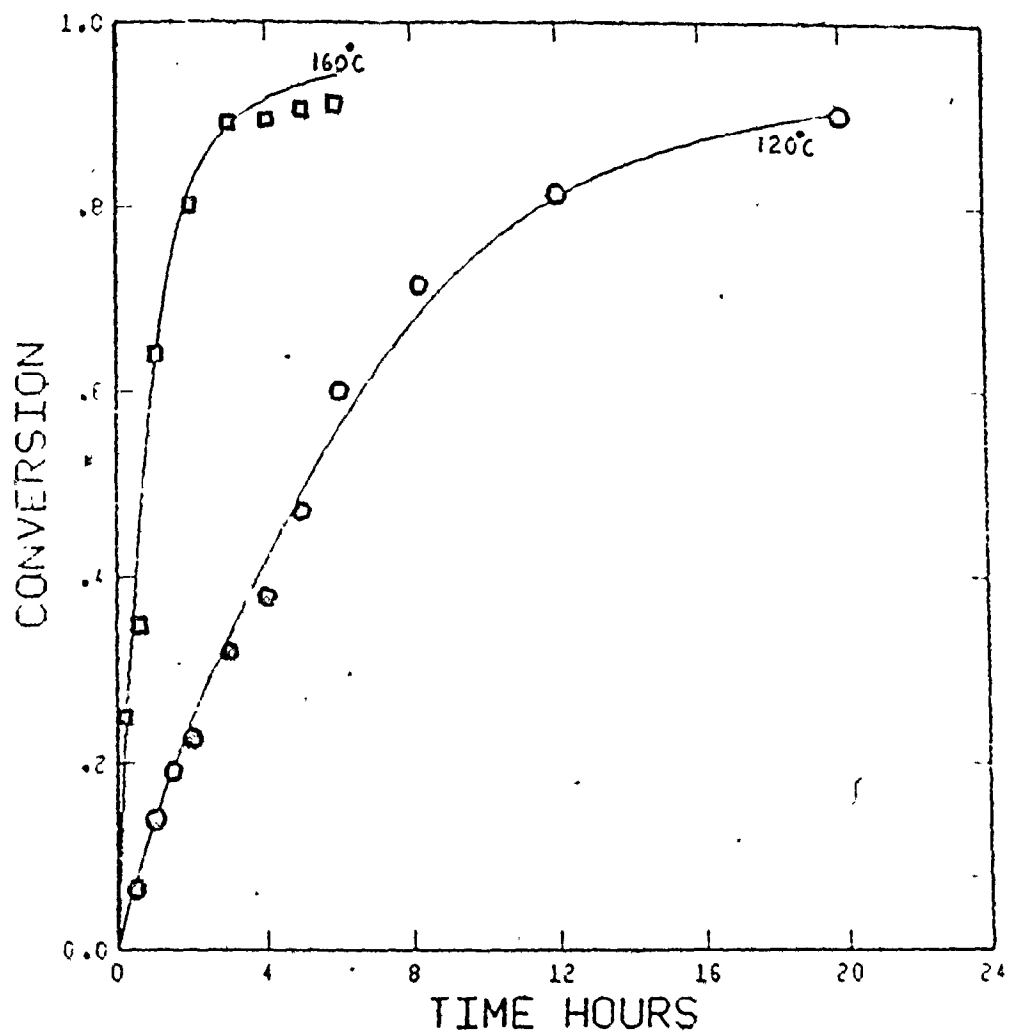


Fig. 1: Measured (\circ :120, \blacksquare :160°C) and predicted conversion vs. time, $f_{10} = 0.2$ (S/PMS)

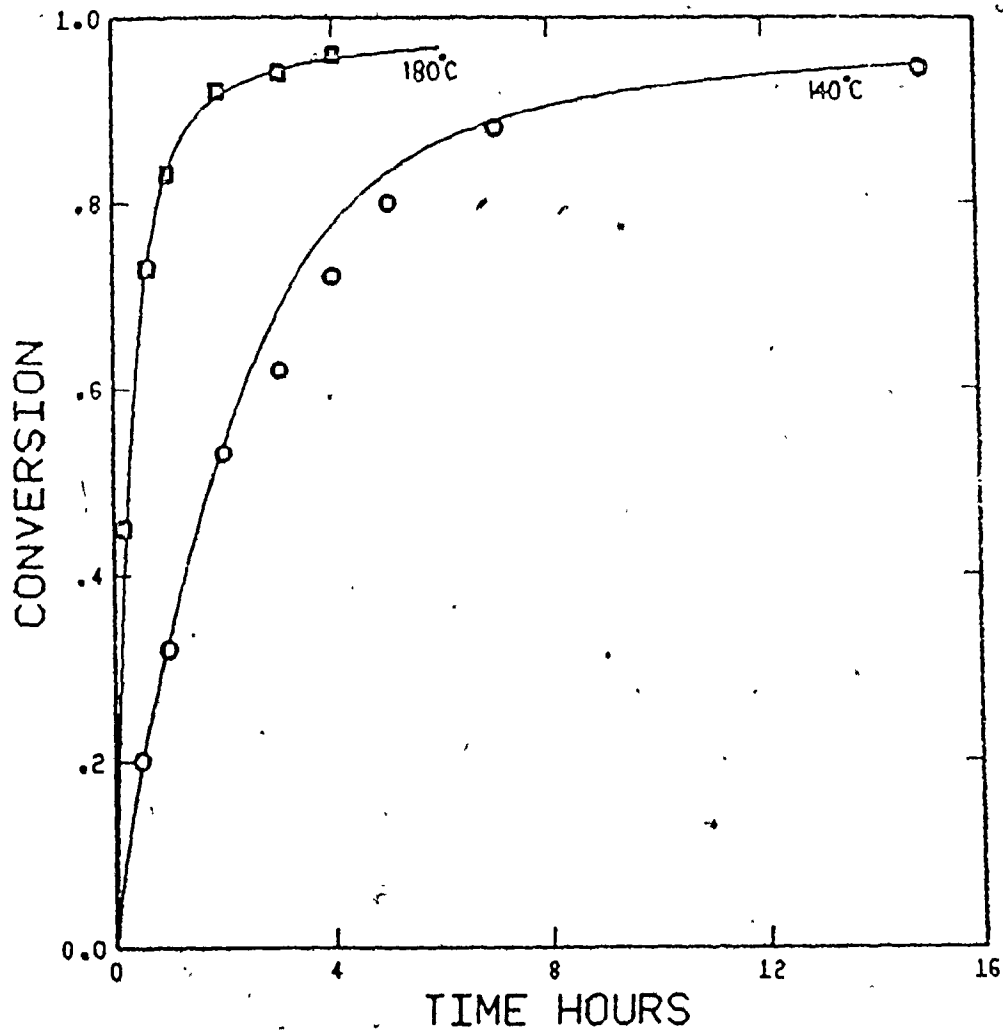


Fig. 2: Measured (○ :140, ■:180°C) and predicted conversion vs. time, $f_{10} = 0.2$ (S/PMS)

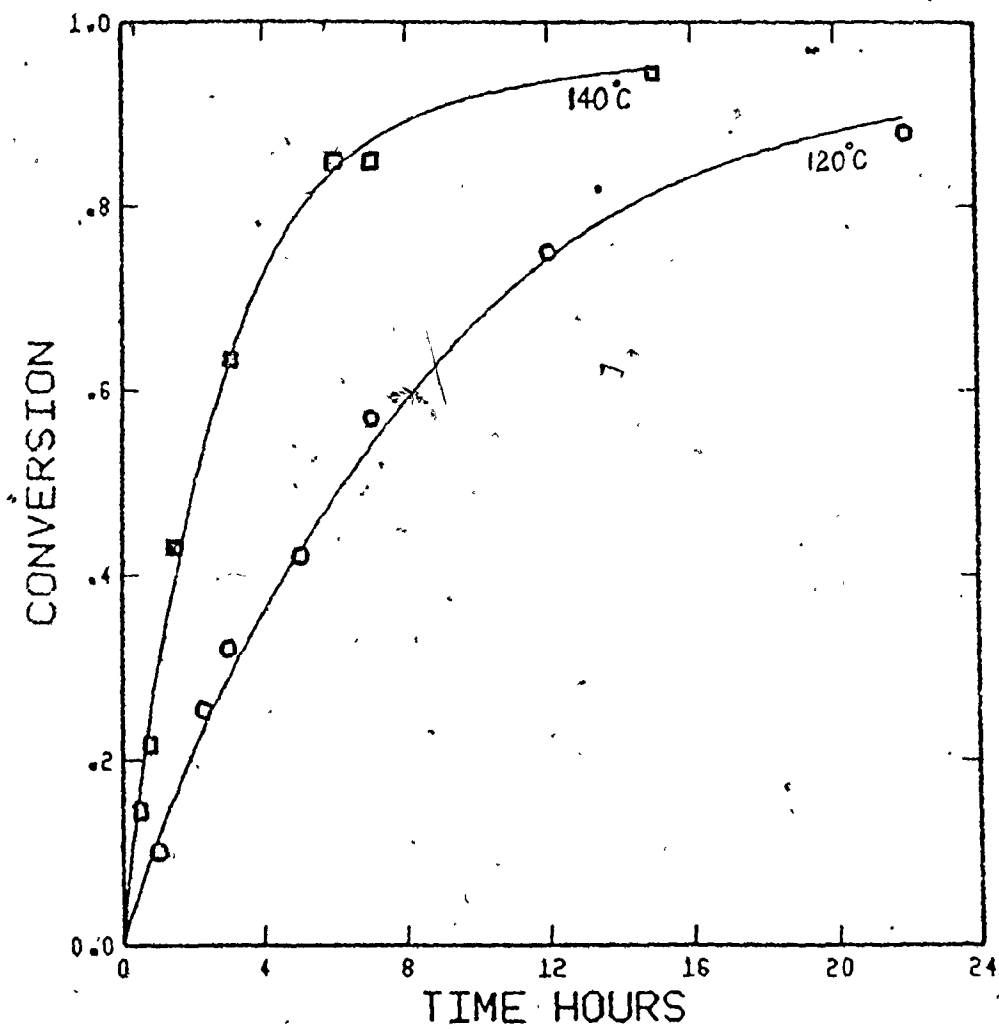


Fig. 3: Measured (\circ :120, \square :140°C) and predicted conversion vs. time, $f_{10} = 0.75$. (S/PMS)

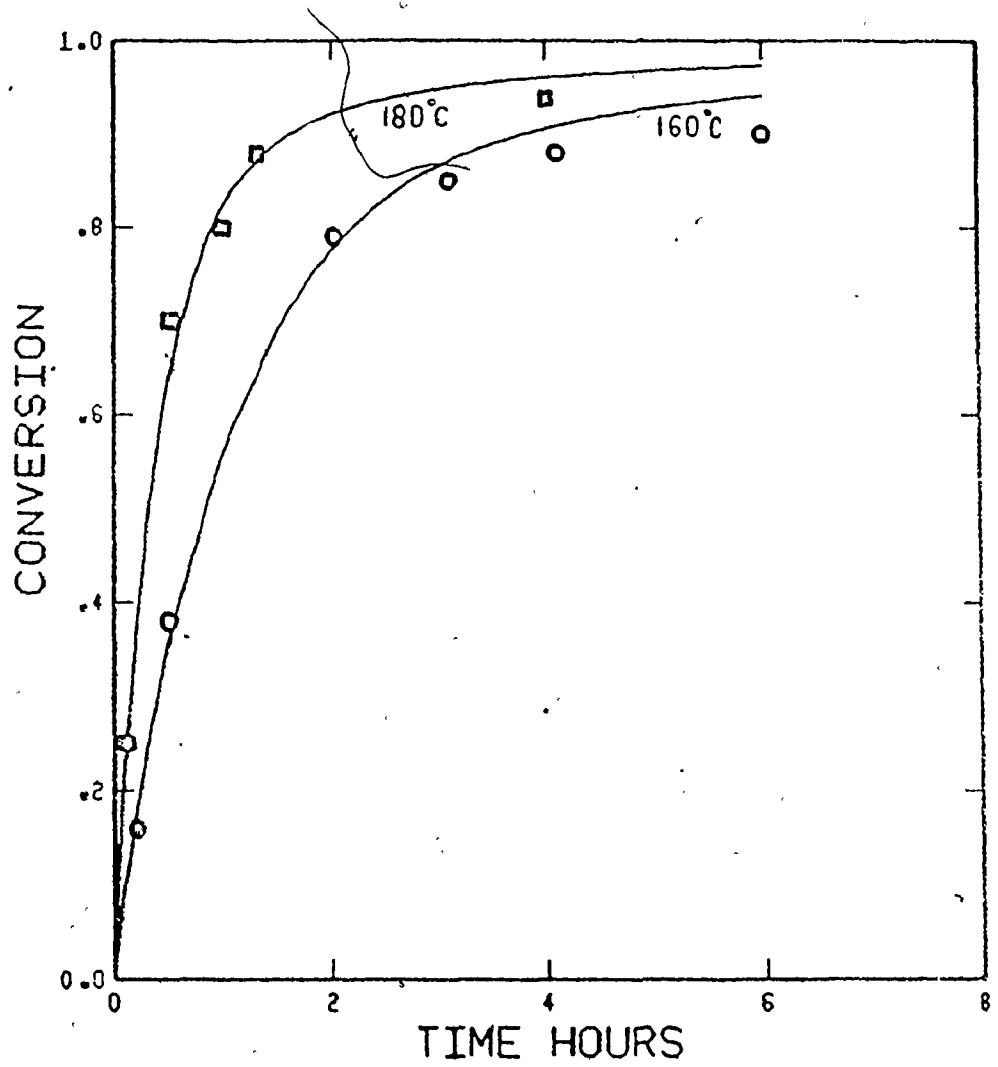


Fig. 4: Measured (○ :160, □ :180°C) and predicted conversion vs. time, $f_{10} = 0.75$ (S/PMS)

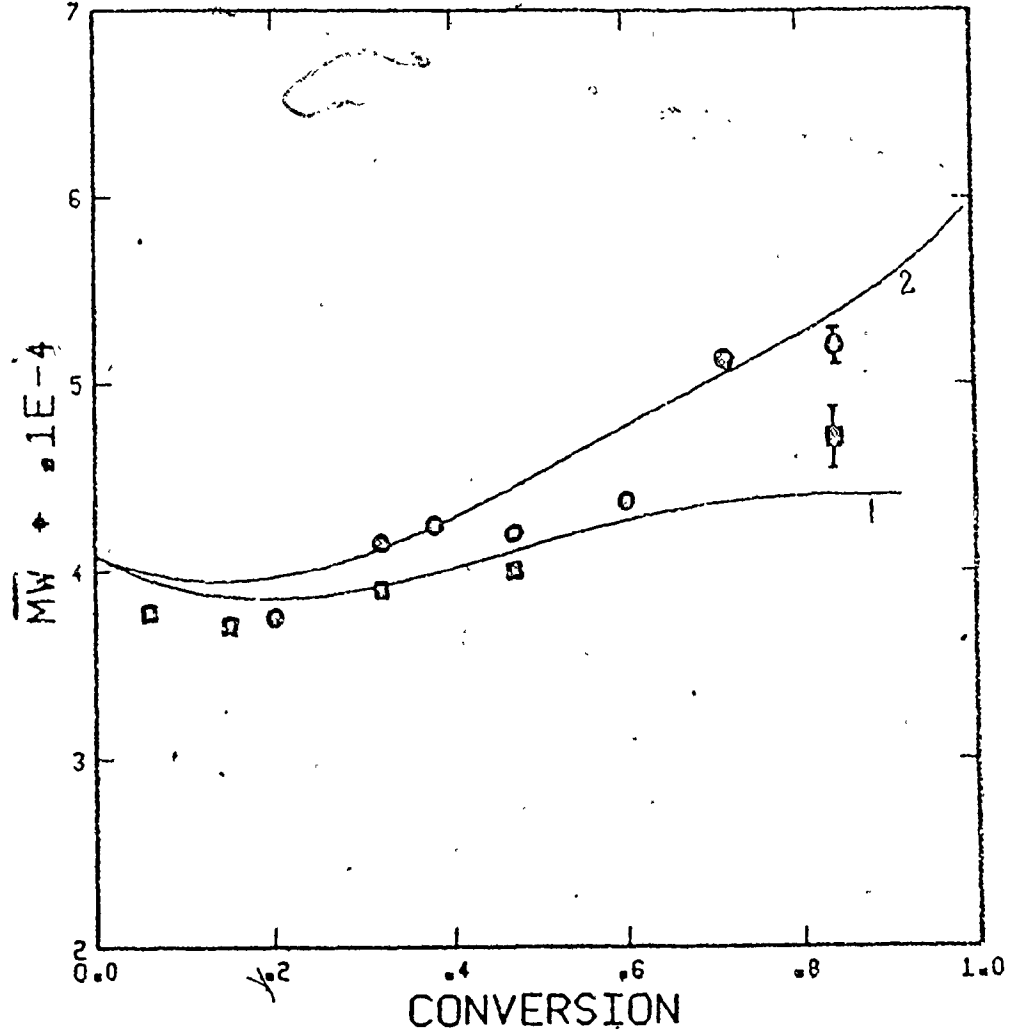


Fig. 5: Measured (\square :SEC, \circ :LALLSP) and predicted \bar{M}_w (1:CP = 0, 2:CP = .00011) vs. conversion at 120°C, $f_{10} = 0.2$ (S/PMS)

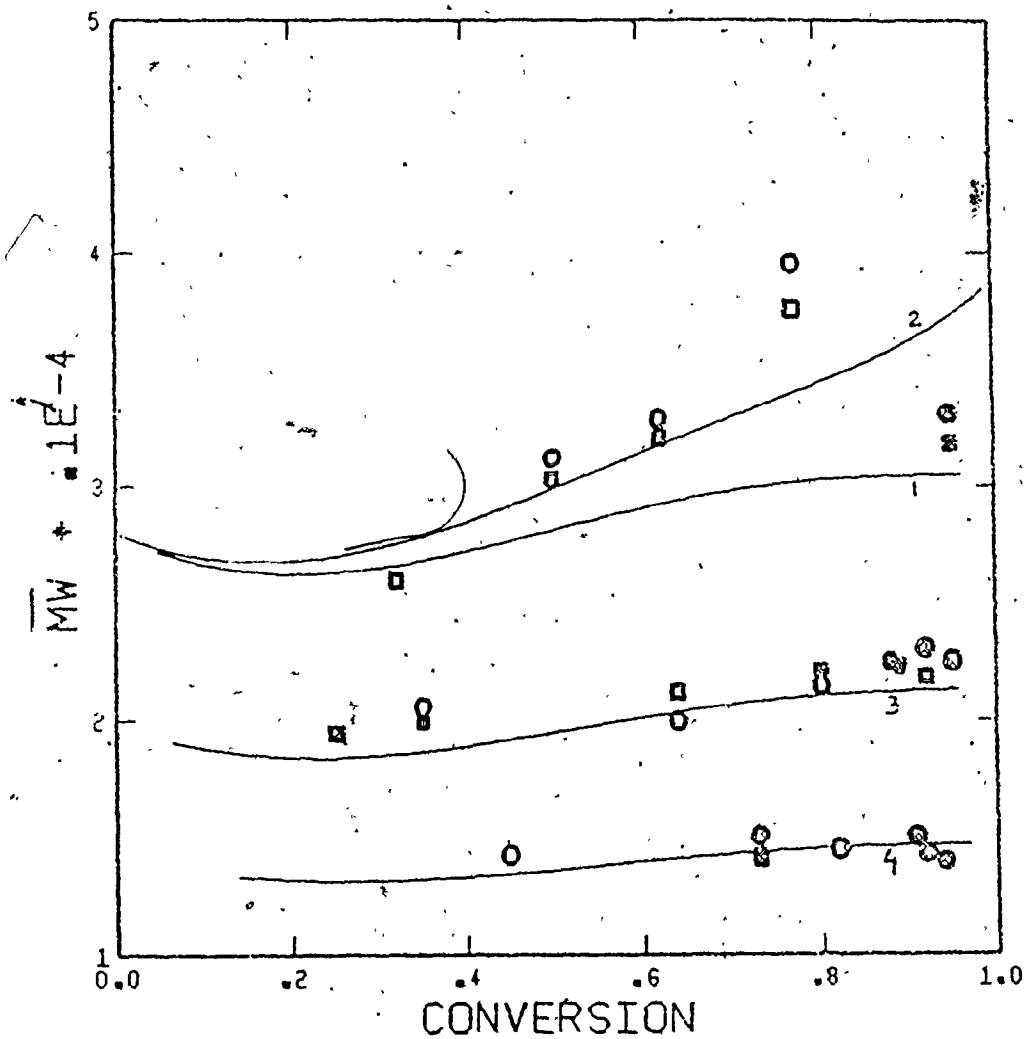


Fig. 6: Measured (\square :SEC at 140, 160, 180°C; \circ :LALLSP) and predicted \bar{M}_w (1,3,4:CP = 0; 2:CP = .00011) vs. conversion at 140, 160 and 180°C, $f_{10} = 0.2$ (S/PMS).

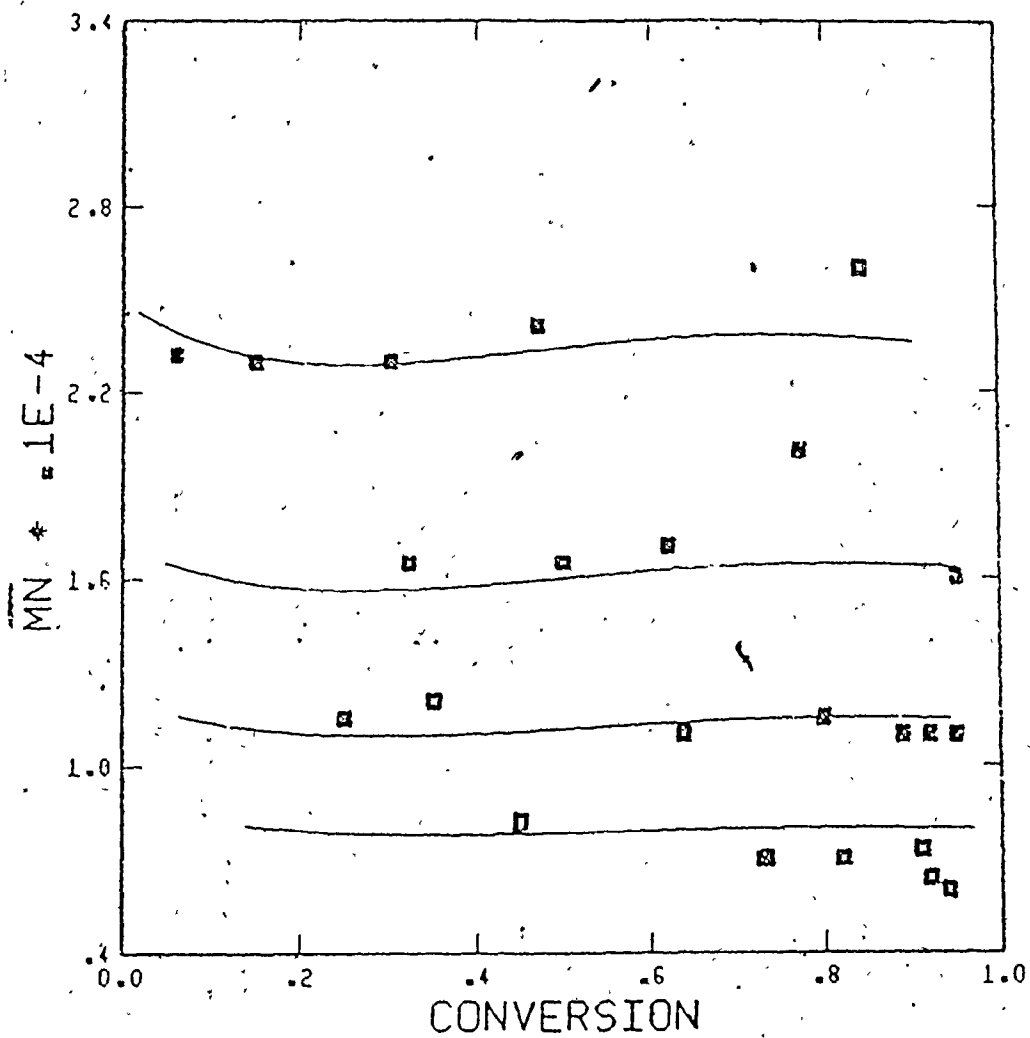


Fig. 7: Measured (\square :SEC at 120, 140, 160, 180°C) and predicted M_n vs. conversion, $f_{10} = 0.2$ (S/PMS).

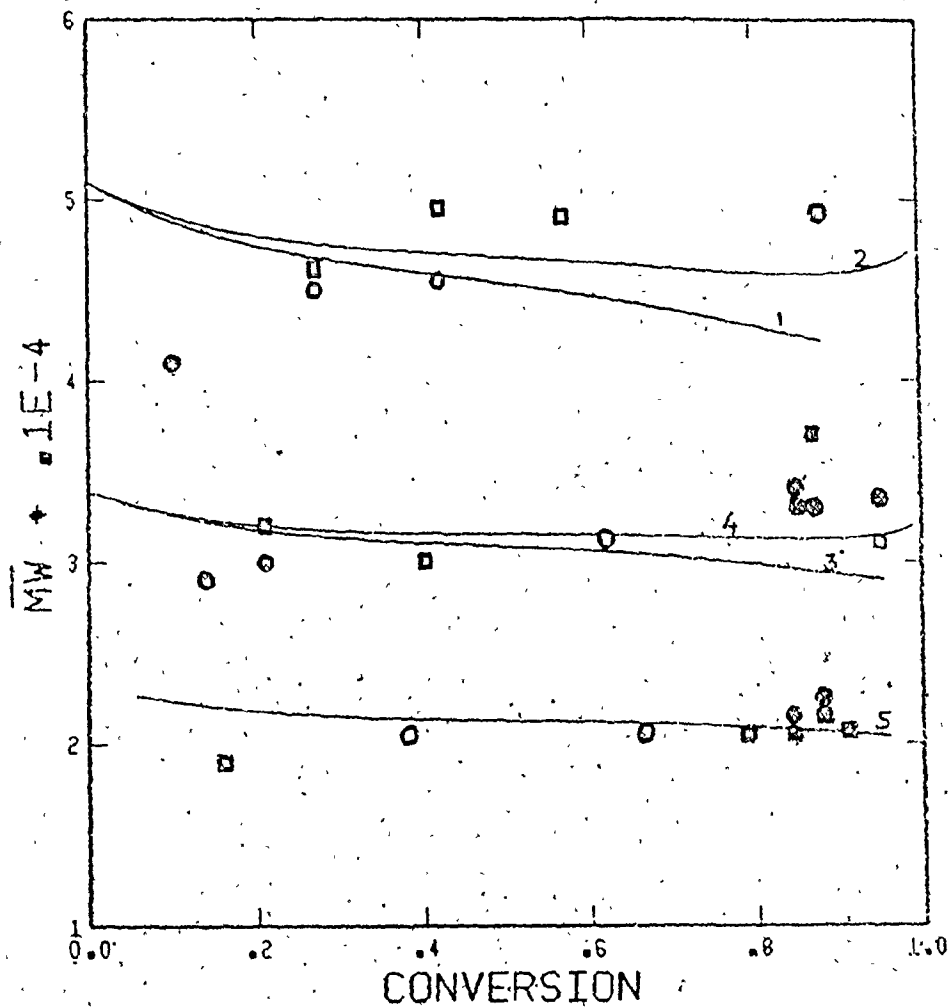


Fig. 8.: Measured (\square :SEC, \circ :LALLSP at 120, 140, 160°C) and predicted \overline{M}_w (1,3,5:CP = 0; 2,4:CP = .00011) vs. conversion at 120, 140, 160°C, $f_{10} = 0.75$ (S/PMS).

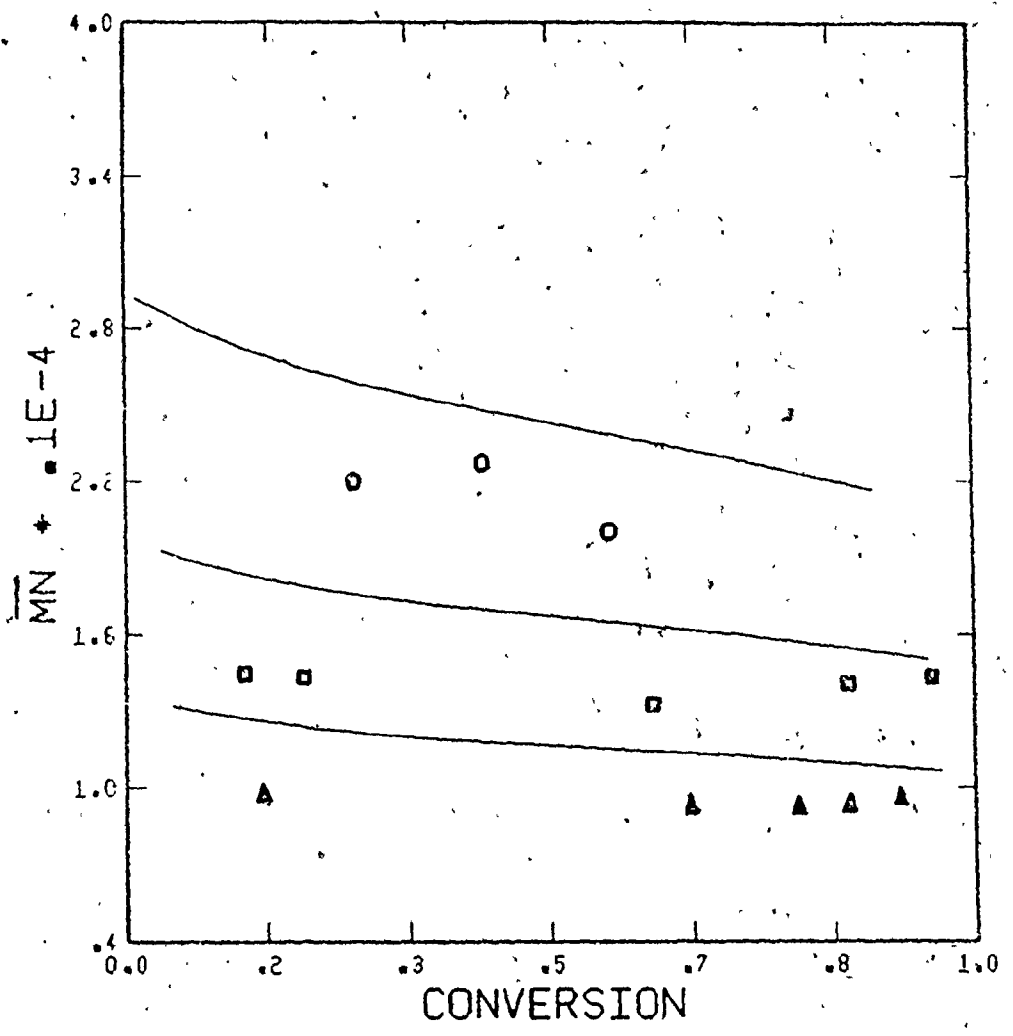


Fig. 9: Measured (O, □, ▲: SEC at 120, 140, 160°C) and predicted \bar{M}_N vs. conversion, $f_{10} = 0.75$ (S/PMS).

chain transfer to the oligomers and intermediates keeps on increasing throughout the course of polymerization as found in earlier work on thermal homopolymerization of styrene (98). The overestimation of the \bar{M}_N data could be due to the inadequacy of equation (81) to model chain transfer to oligomers and other by-products of thermal initiation for styrene rich comonomer. The model predictions for linear copolymer underestimate the \bar{M}_W at the lower temperatures, especially at high conversions. The \bar{M}_W obtained by LALLSP at high conversions for copolymers rich in PMS are generally larger than those measured by SEC and this may be considered evidence for long chain branching. An estimate of C_p equal to $1.1E-4$ was found by fitting the \bar{M}_W values measured by LALLSP using the method of moments. The site for transfer to polymer was assumed to be methyl hydrogens on PMS molecules bound in the copolymer chains as branching appears to be insignificant for copolymers rich in styrene. The level of branching decreases with increasing temperatures as the total number of polymer molecules formed at the higher temperatures increases thereby the number of branches per molecule decreases, which is reflected in the LALLSP

measurements. Figure 10 shows the branching frequency (\bar{B}_N) as a function of conversion at 120 °C and $f_{10}=0.2$, where maximum branching occurs. Clearly much higher levels of branching would be expected for a chemically-initiated polymerization where the radical population would be much higher at comparable levels of conversion. Figures 11 and 12 compare predicted and measured MWD for two samples synthesized at low and high conversion respectively. The theoretical curves are the cumulative MWD. Satisfactory agreement is observed, although the MWD's change little with conversion and are all unimodal.

Figures 13 and 14 show the predicted decrease in K_{tc} with conversion. This is seen to be more rapid for the styrene rich copolymer and is consistent with earlier work (8). Figure 13 shows a small increase in K_{tc} before a gradual and then a steeper fall, as is expected to happen due to the initial segmental diffusion-control followed by translational diffusion-control of termination reactions. This again has been reported earlier for pure PMS (8). Interestingly styrene does not show the initial increase (24) and this again is reflected for $f_{10}=0.75$ in figure 14.

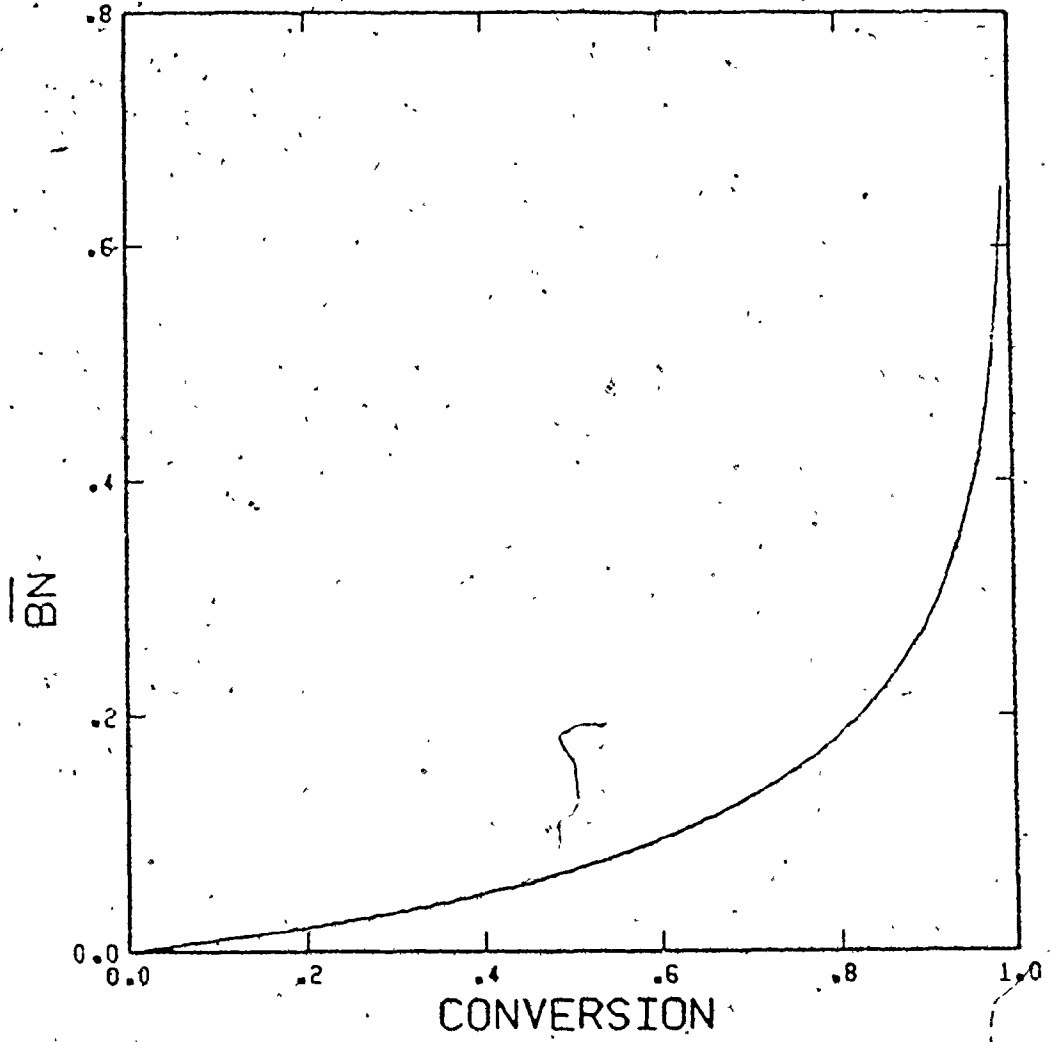


Fig.10: Predicted \bar{B}_N vs. conversion at 120°C, $f_{10} = 0.2$ (S/PMS).

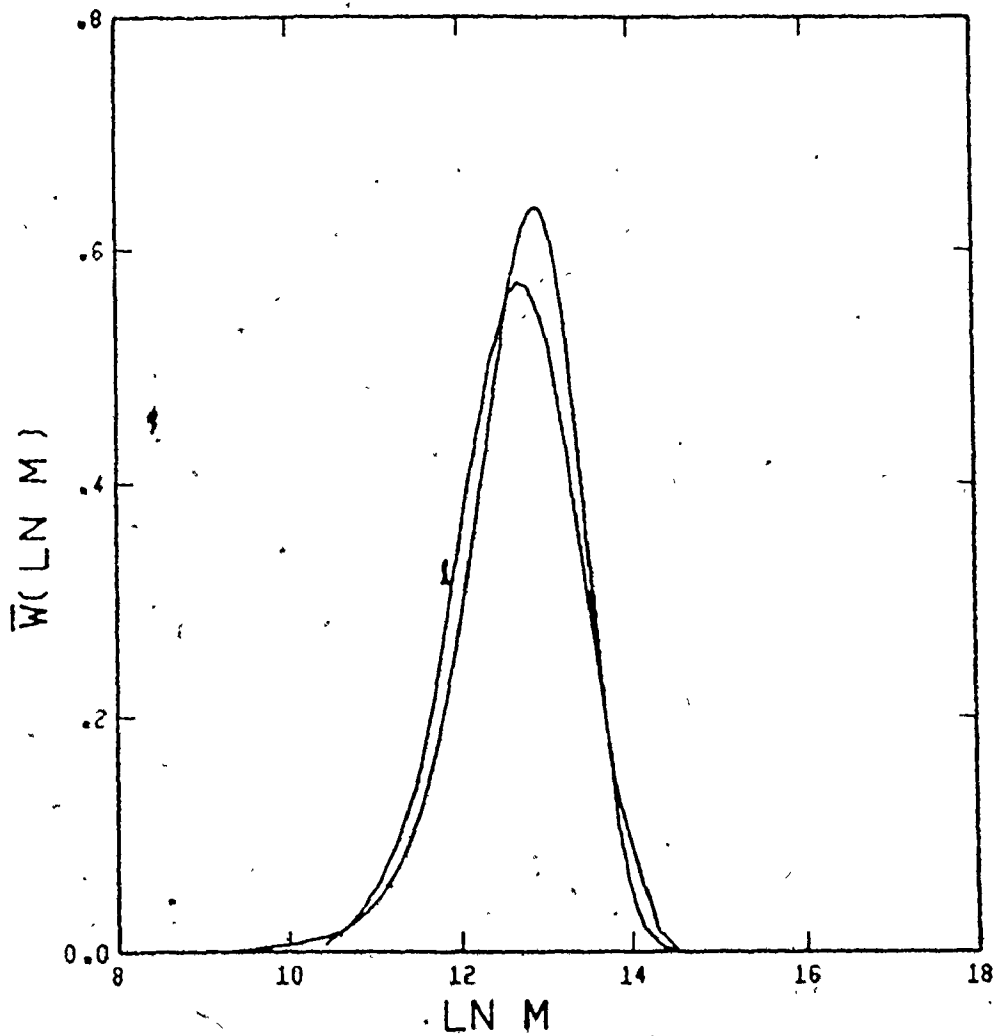


Fig.11: Measured (1:SEC) and predicted MWD at 120°C, $f_{10} = 0.2$,
 $x = 0.06$, $\bar{M}_w(\text{meas.}) = 3.8E5$, $\bar{M}_n(\text{meas.}) = 2.4E5$, $\bar{M}_w(\text{pred.})$
 $= 3.9E5$, $\bar{M}_n(\text{pred.}) = 2.4E5$ (S/PMS).

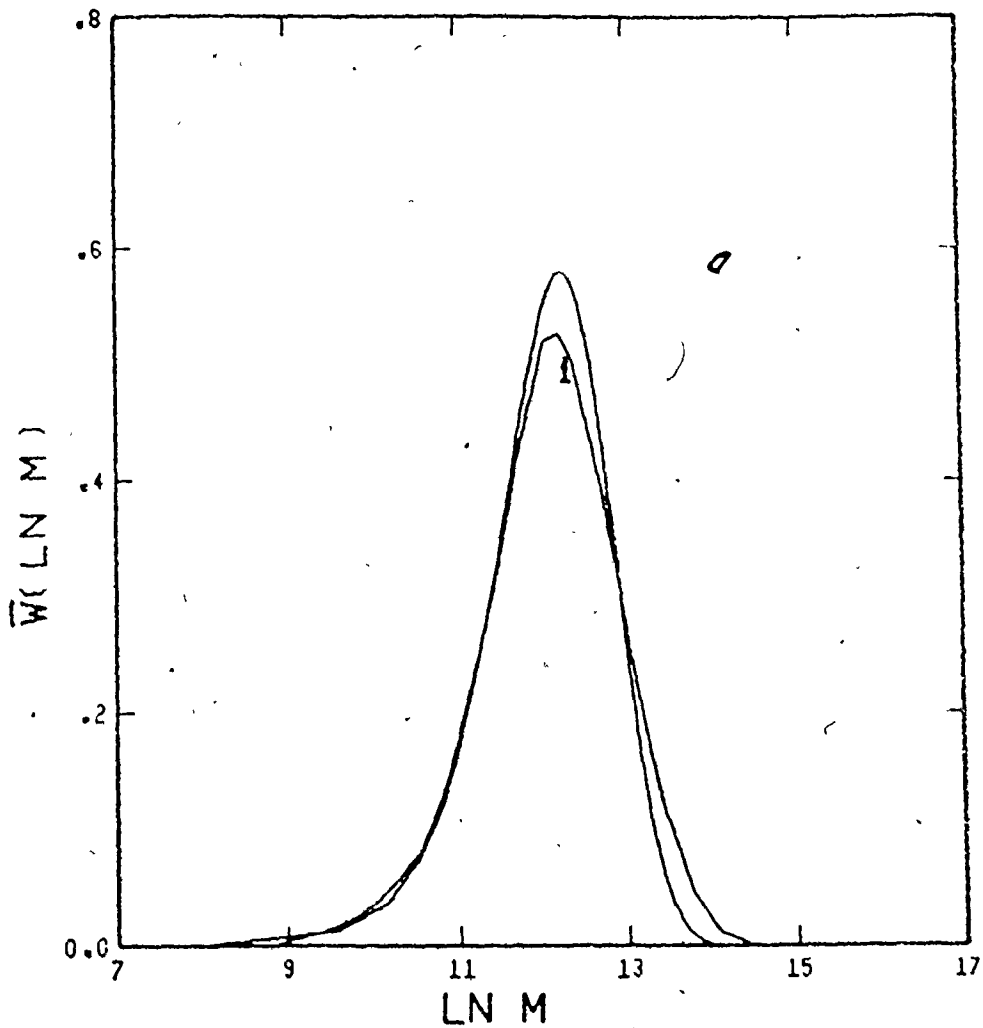


Fig.12: Measured (1:SEC) and predicted MWD at 160°C, $f_{10} = 0.2$,
 $x = 0.89$, $\bar{M}_w(\text{meas.}) = 2.3E5$, $\bar{M}_n(\text{meas.}) = 1.2E5$, $\bar{M}_w(\text{pred.})$
 $= 2.2E5$, $\bar{M}_n(\text{pred.}) = 1.2E5$ (S/PMS).

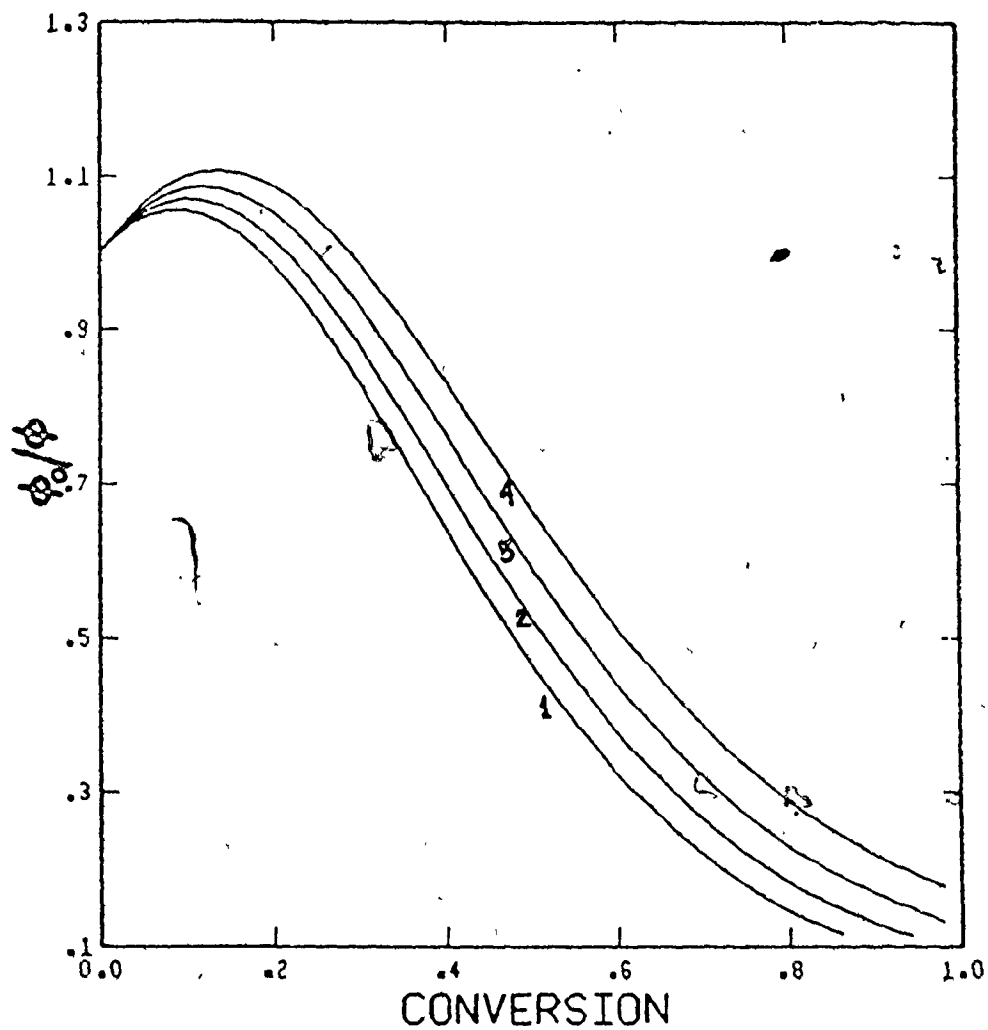


Fig.13: Diffusion controlled termination: measured change in ϕ_x with conversion (1:120, 2:140, 3:160, 4:180°C) $f_{10} = 0.2$ (S/PMS).

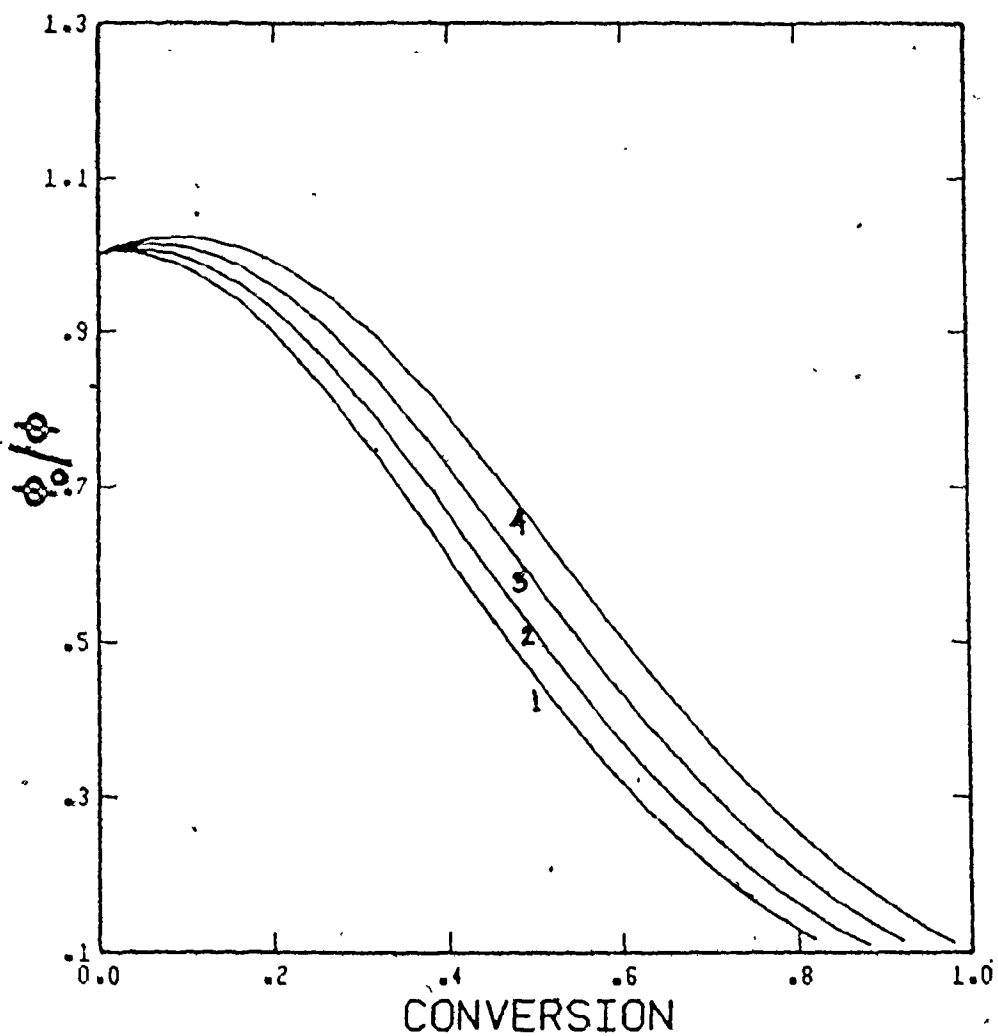


Fig.14: Diffusion controlled termination: measured change in ϕ_s with conversion (1:120, 2:140, 3:160, 4:180°C) $f_{10} = 0.75$ (ϕ_s /PMS).

6.2 Model for Styrene/PMS Copolymerization Using Free-Volume Theory to Model Diffusion-Controlled Propagation and Termination

This model was earlier applied to fit the bulk rate data for the homopolymerization of styrene (24) and PMS (8). Figure 15 compares the model predictions with the rate data for styrene at 120, 140 and 170°C. The agreement is excellent. Good agreement is also observed between model predictions and experimental x data for PMS polymerization in figure 16, at 120, 140 and 160°C. Figures 17-20 compare model predictions with experimental x data on the copolymerization of styrene/PMS for $f_{10} = 0.2$ and 0.75. Reasonable agreement is observed for both the compositions. Better agreement at high conversions is observed than with the predictions of the empirical model because of the inclusion of diffusion-controlled propagation at these conversions. This however may not be valid at the high temperatures employed in this work (above T_{gp}) and serves merely as an artifact to explain the excessive decrease in the rate of polymerization at high to very high conversions. This excessive decrease in rate may

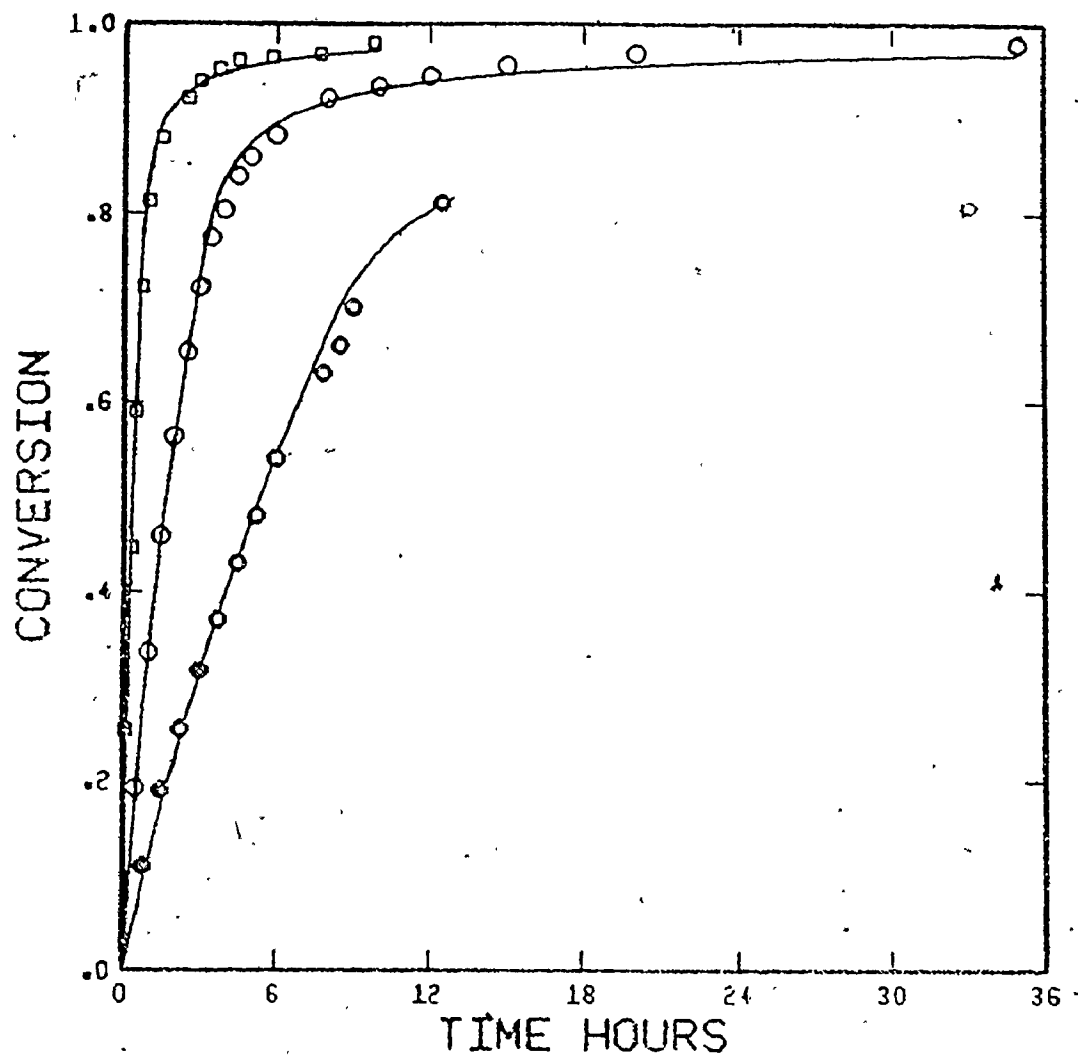


Fig.15: Measured (\bullet :120, \circ :140, \square :170°C) and predicted conversion vs. time, $f_{10} = 1$ (S/PMS).

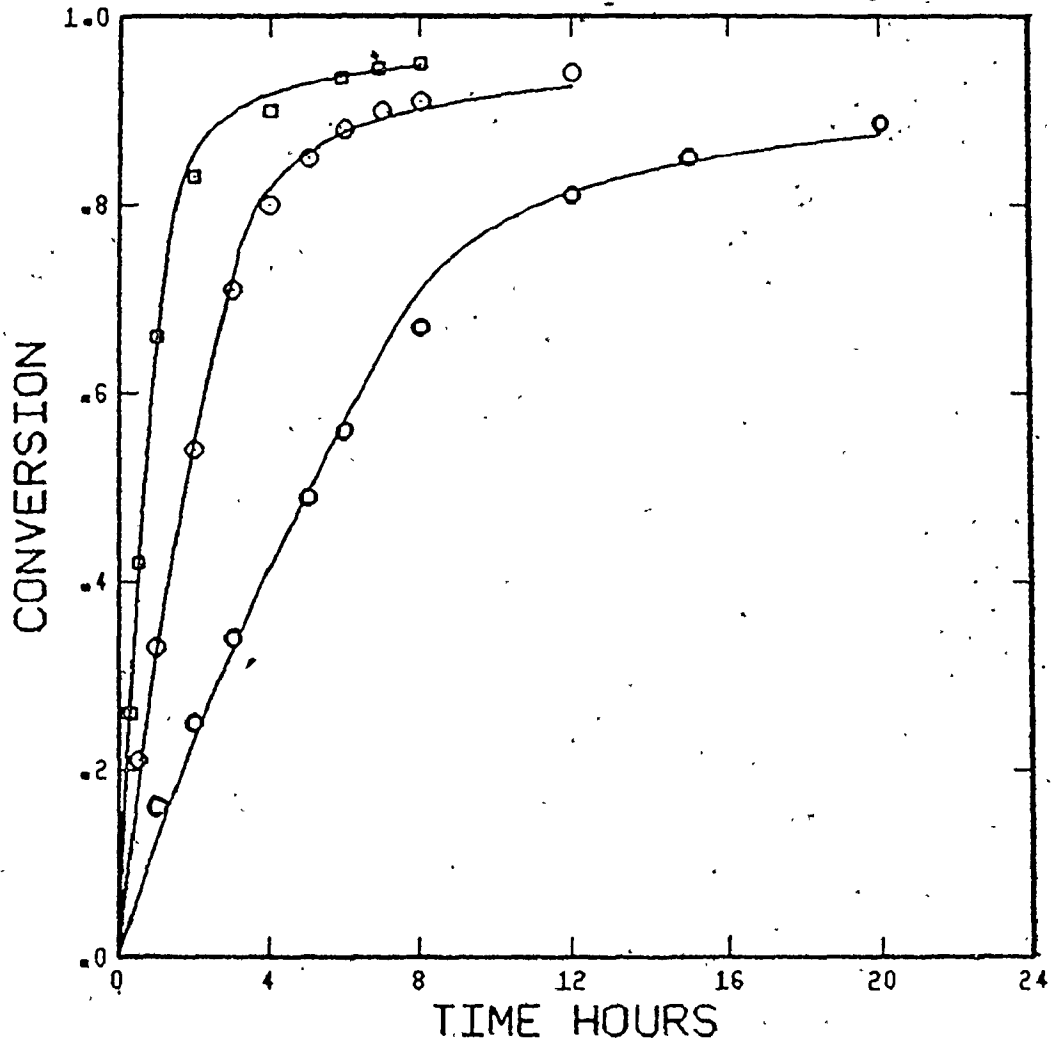


Fig.16: Measured (● :120, ○:140, □:160°C) and predicted conversion vs. time, $f_{10} = 0$ (S/PMS).

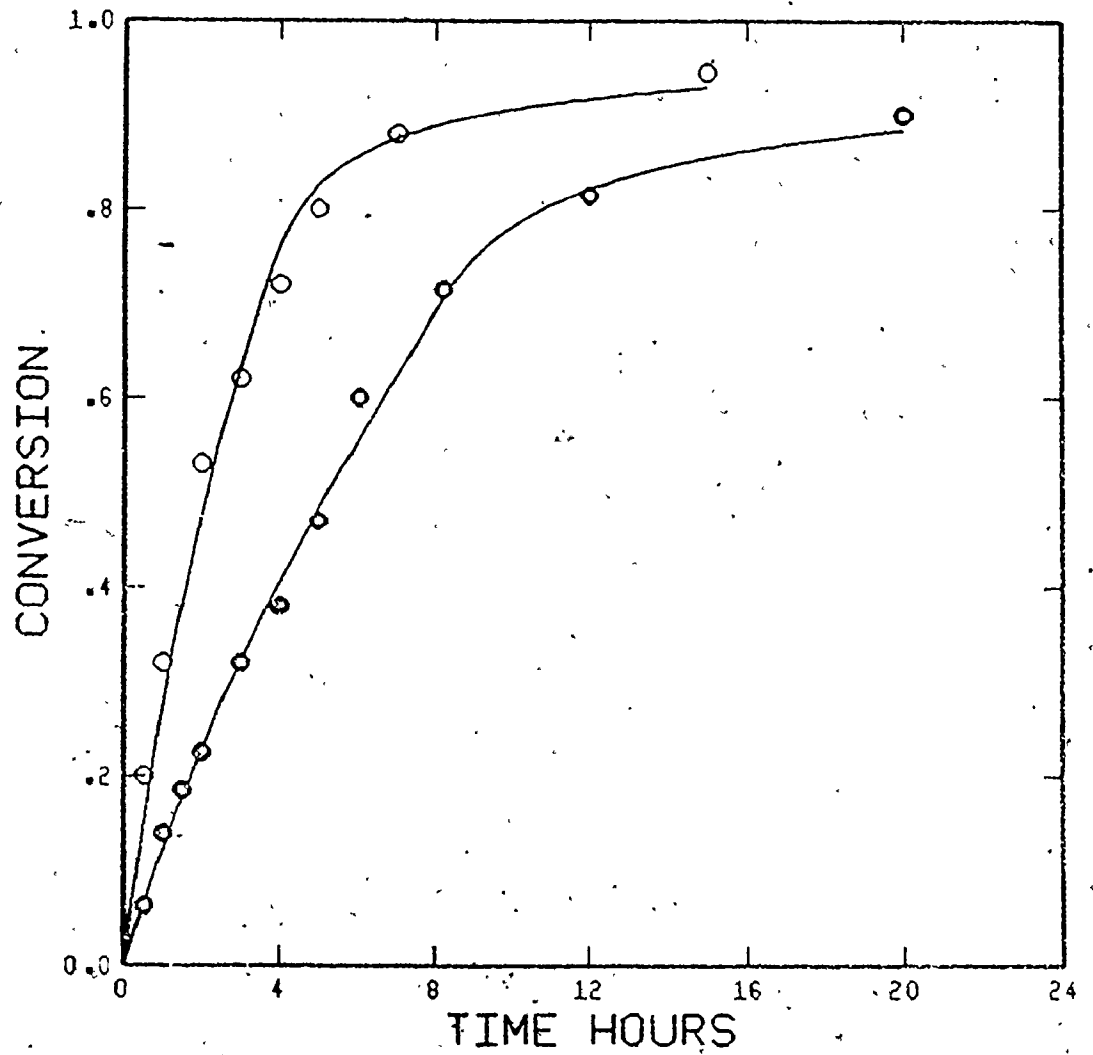


Fig.17: Measured (\bullet :120, \circ :140°C) and predicted conversion vs. time, $f_{10} = 0.2$ (S/PMS).

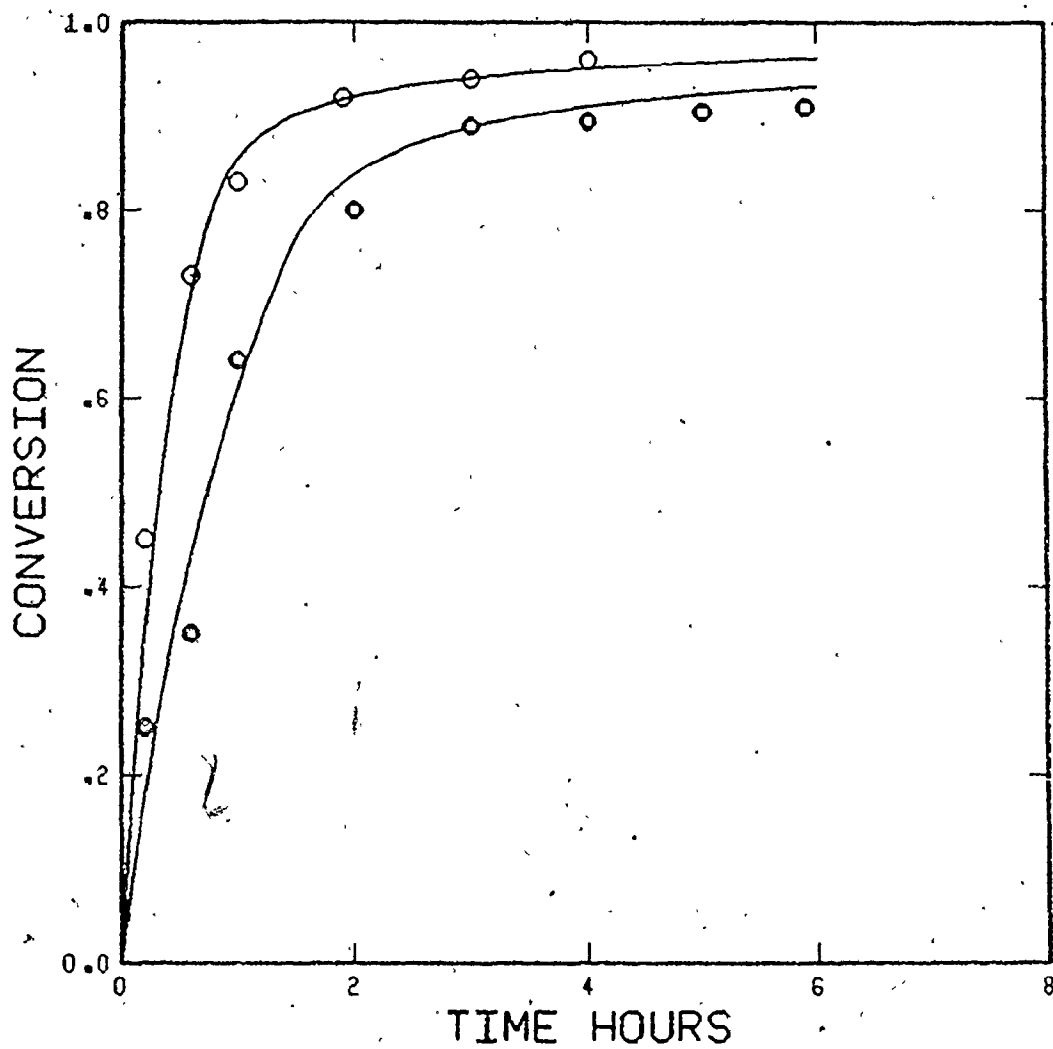


Fig.18: Measured (● :160,○:180°C) and predicted conversion vs. time, $f_{10} = 0.2$ (S/PMS).

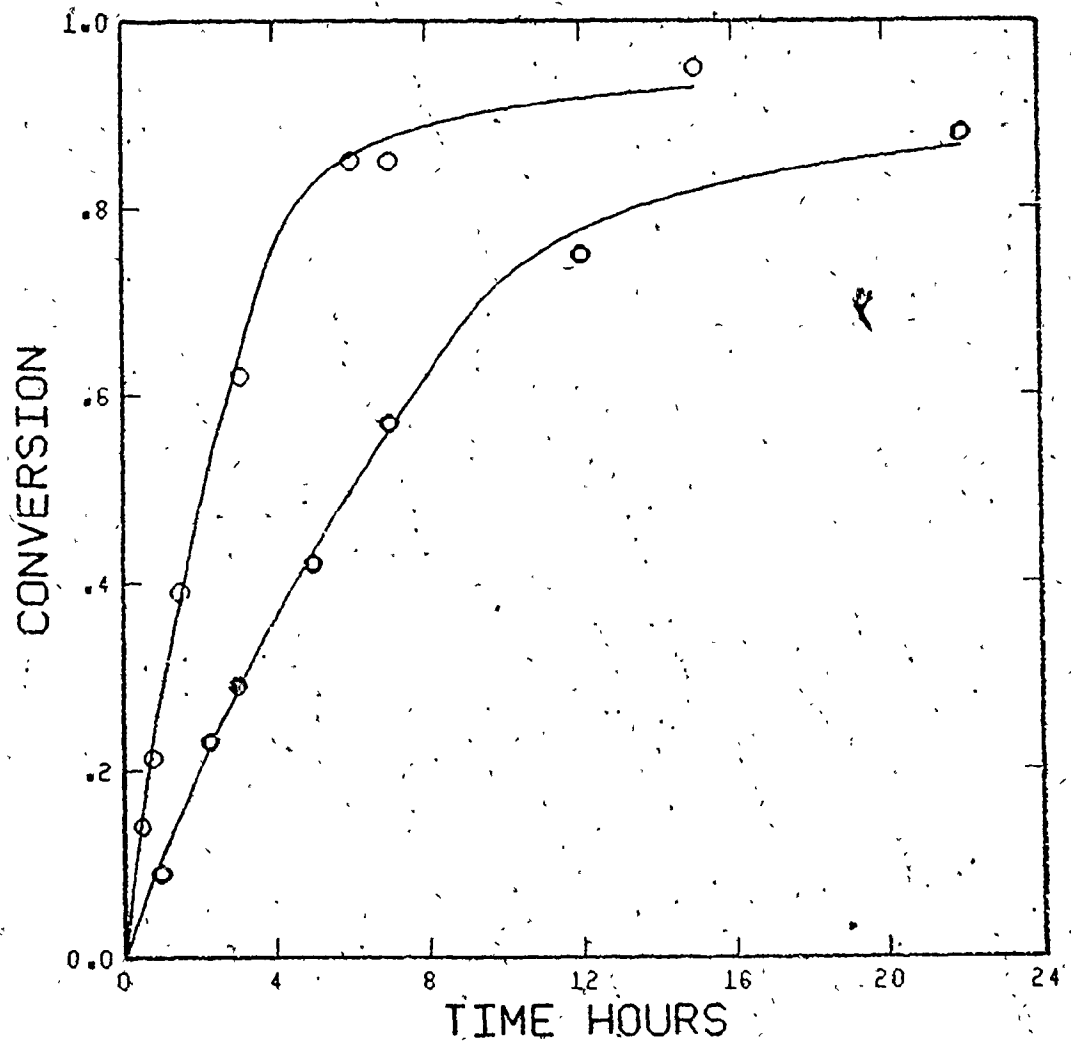


Fig.19: Measured (● :120, ○:140°C) and predicted conversion, vs. time; $f_{10} = 0.75$ (S/PMS).

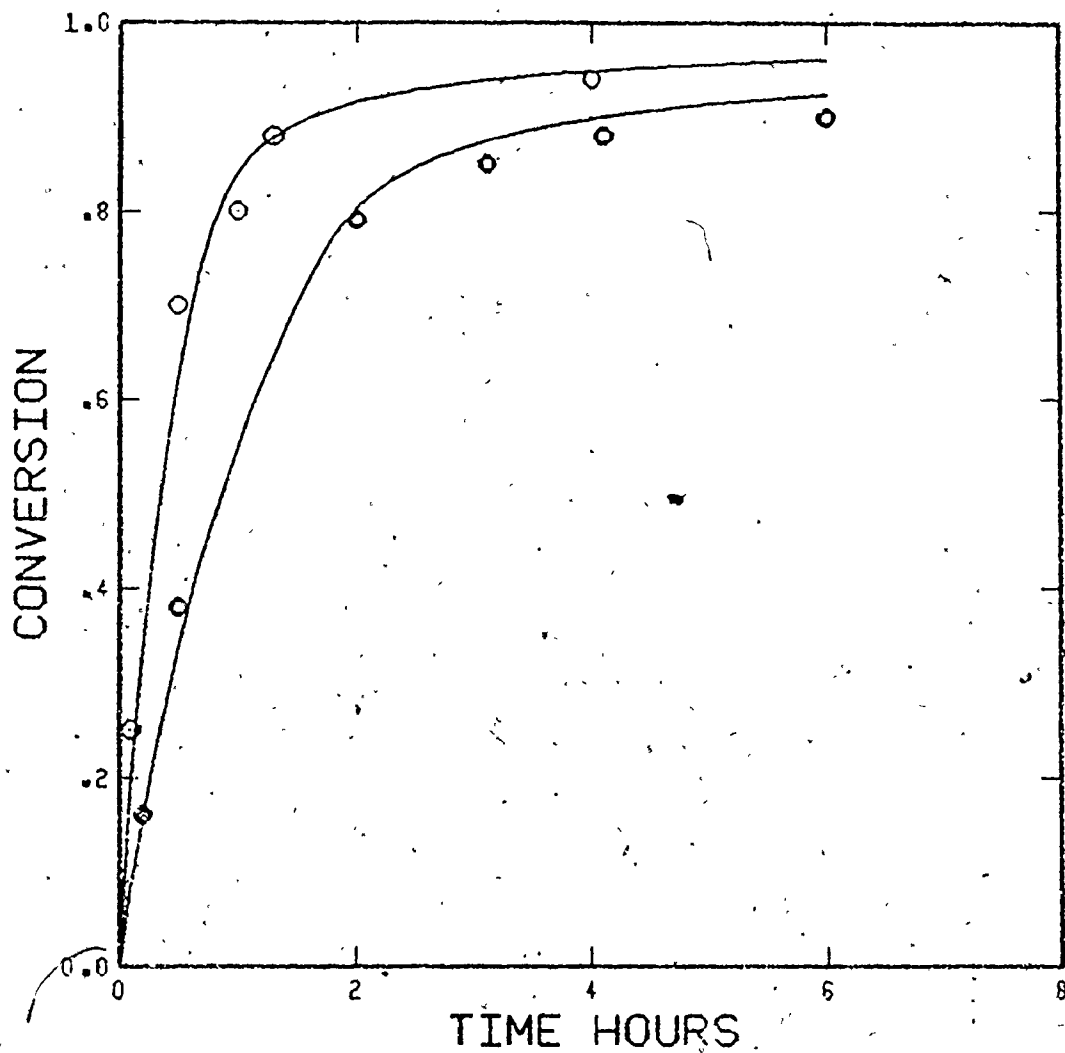


Fig.20: Measured (●:160, ○:180°C) and predicted conversion vs. time, $f_{10} = 0.75$ (S/PMS).

really be due to the retarding influence of one or more of the by-products of thermal initiation, not accounted for in both models. As pointed out earlier chain transfer to these by-products may lead to the creation of transfer radicals of lower reactivity with regard to propagation reactions. Figures 21-23 compare model predictions with experimental \bar{M}_w data for the two compositions of the copolymer. Agreement is seen to be reasonable, considering the fact that the model predictions are for a linear copolymer (some long chain branching may occur). Similar agreement is found in Figure 24 where the experimental \bar{M}_n data are compared with model predictions for $F_1 = 0.2$. The fit of the \bar{M}_n predictions with the data is poor for $F_1 = .75$ (Figure 25) and this may be due to the reasons cited earlier. The temperature dependence of K_3 was determined using all of the reported data (8,23) as well as the data generated in the present work. Figures 26 and 27 show K_3 and V_{Fcr2} plotted as functions of temperature. K_3 is shown to exhibit an Arrhenius dependence on temperature while V_{Fcr2} is nearly independent of temperature. Figure 28 shows a typical variation of K_{tc} and K_{trd} with conversion. The former is observed to fall by about five

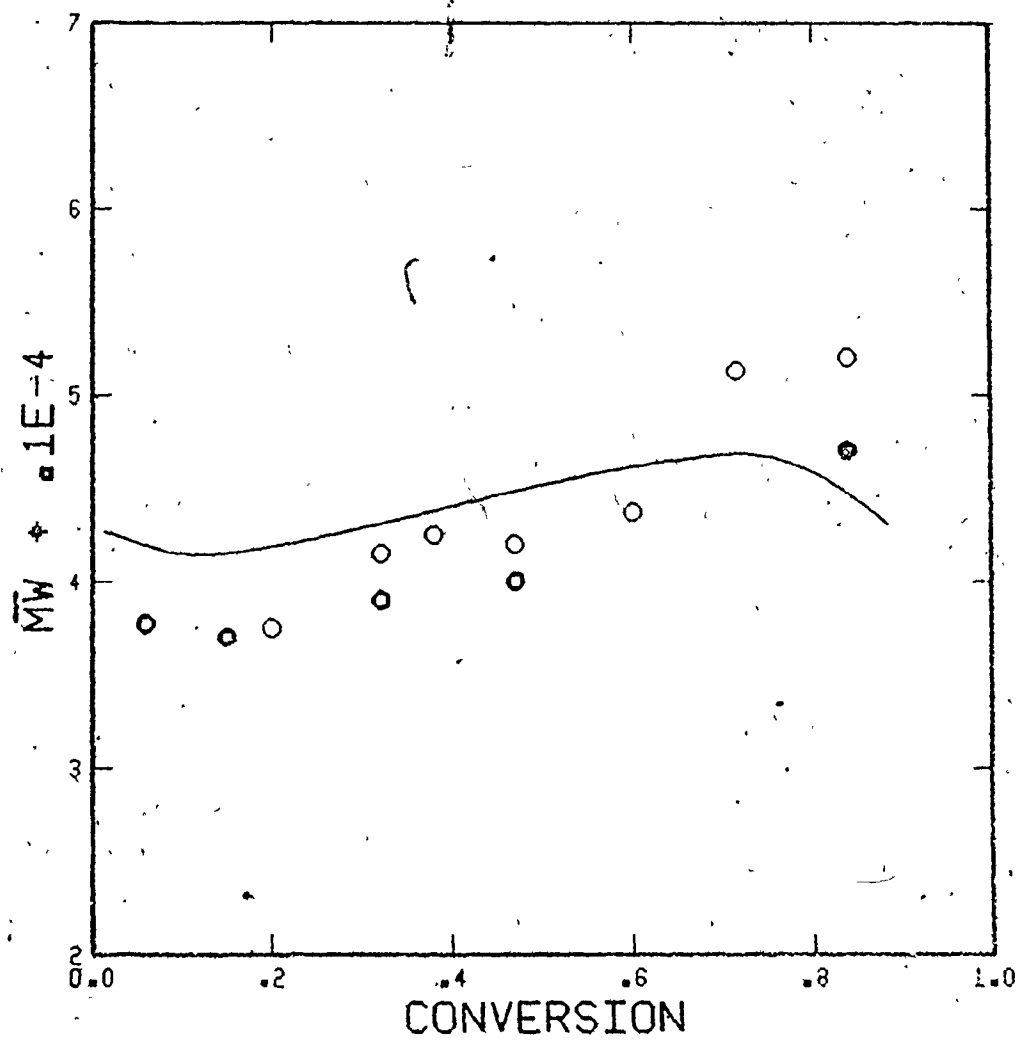


Fig.21: Measured (●:SEC, ○:LALLSP) and predicted \bar{M}_w vs. conversion at 120°C, $f_{10} = 0.2$ (S/PMS).

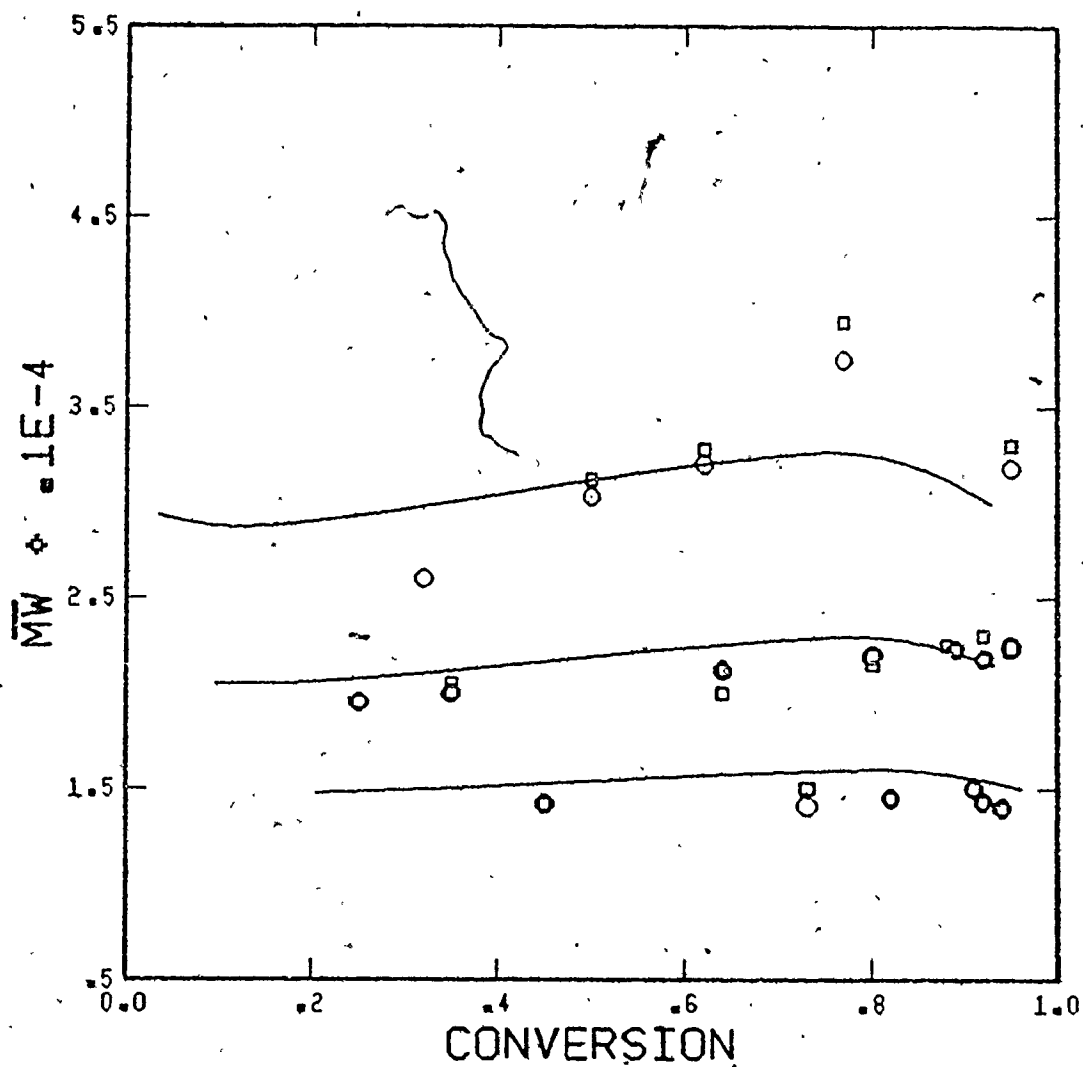


Fig.22: Measured (O:SEC at 140,180°C, ● at 160°C, □:LALLSP at 140,160,180°C) and predicted \overline{M}_w vs. conversion, $f_{10} = 0.2$ (S/PMS).

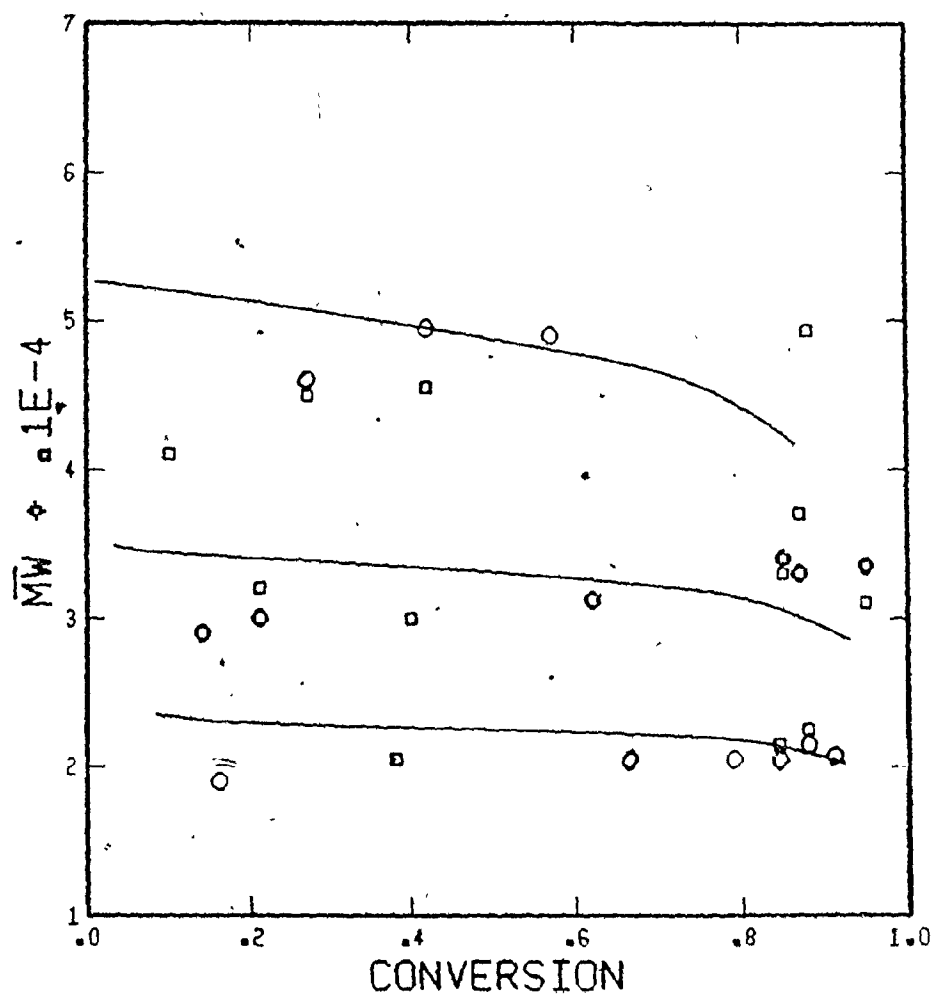


Fig. 23: Measured (\square :LALLSP at 120,140,160°C, \circ :SEC at 120,160°C, \bullet :140°C) and predicted \bar{M}_w vs. conversion, $f_{10} = 0.75$ (S/PMS).

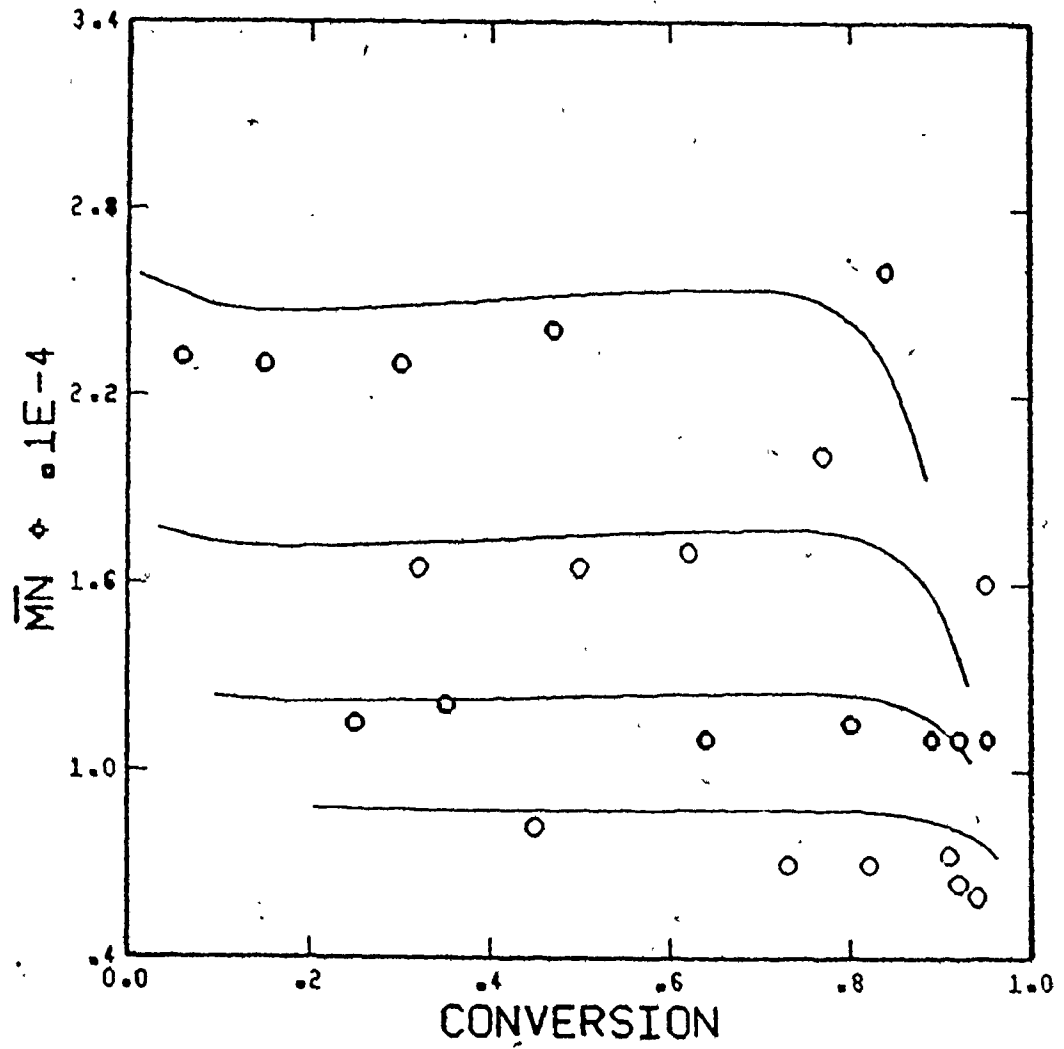


Fig. 24. Measured (\circ : SEC at 120, 160°C, \circ : SEC at 140, 180°C) and predicted \bar{M}_N vs. conversion, $f_{10} = 0.2$ (S/PMS).

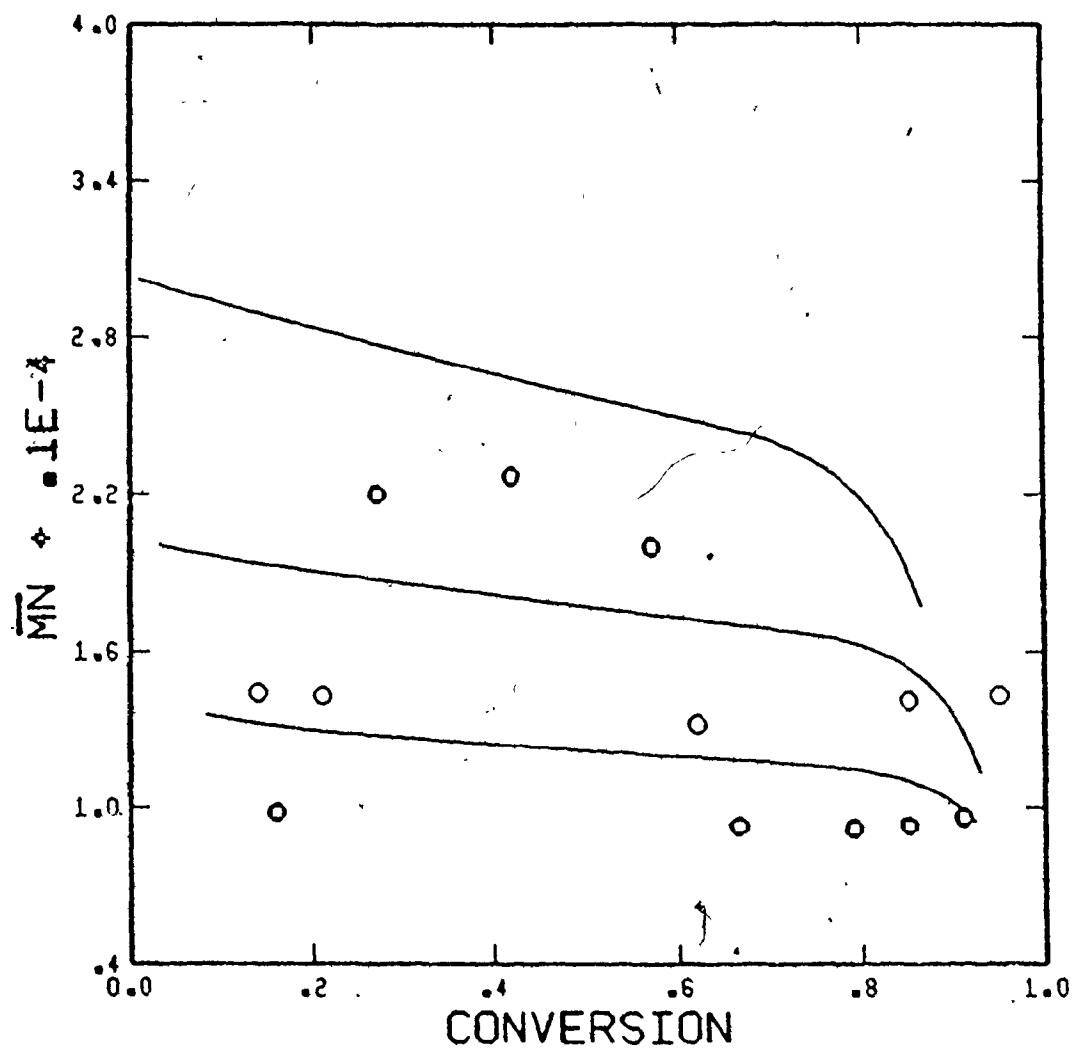


Fig.25: Measured (●:SEC at 120,160°C,○:SEC at 140°C) and predicted \bar{M}_N vs. conversion, $f_{10} = 0.75$ (S/PMS).

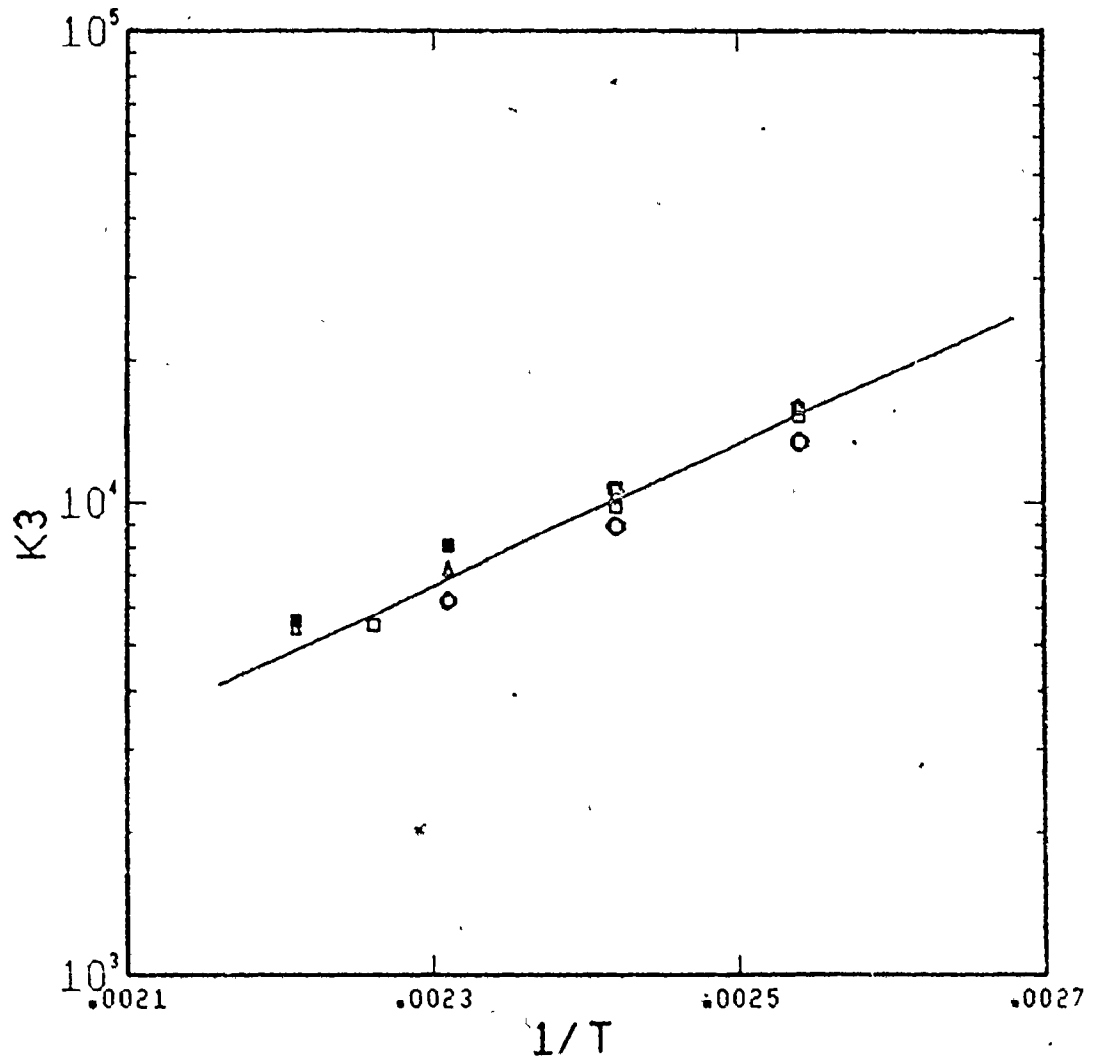


Fig.26: Measured (f_{10} : \circ :0, Δ :0.2, \blacksquare :0.75, \square :1) and predicted K_3 vs. $(1/T)$ ($^{\circ}\text{K}^{-1}$), $A = 0.85$ (S/PMS).

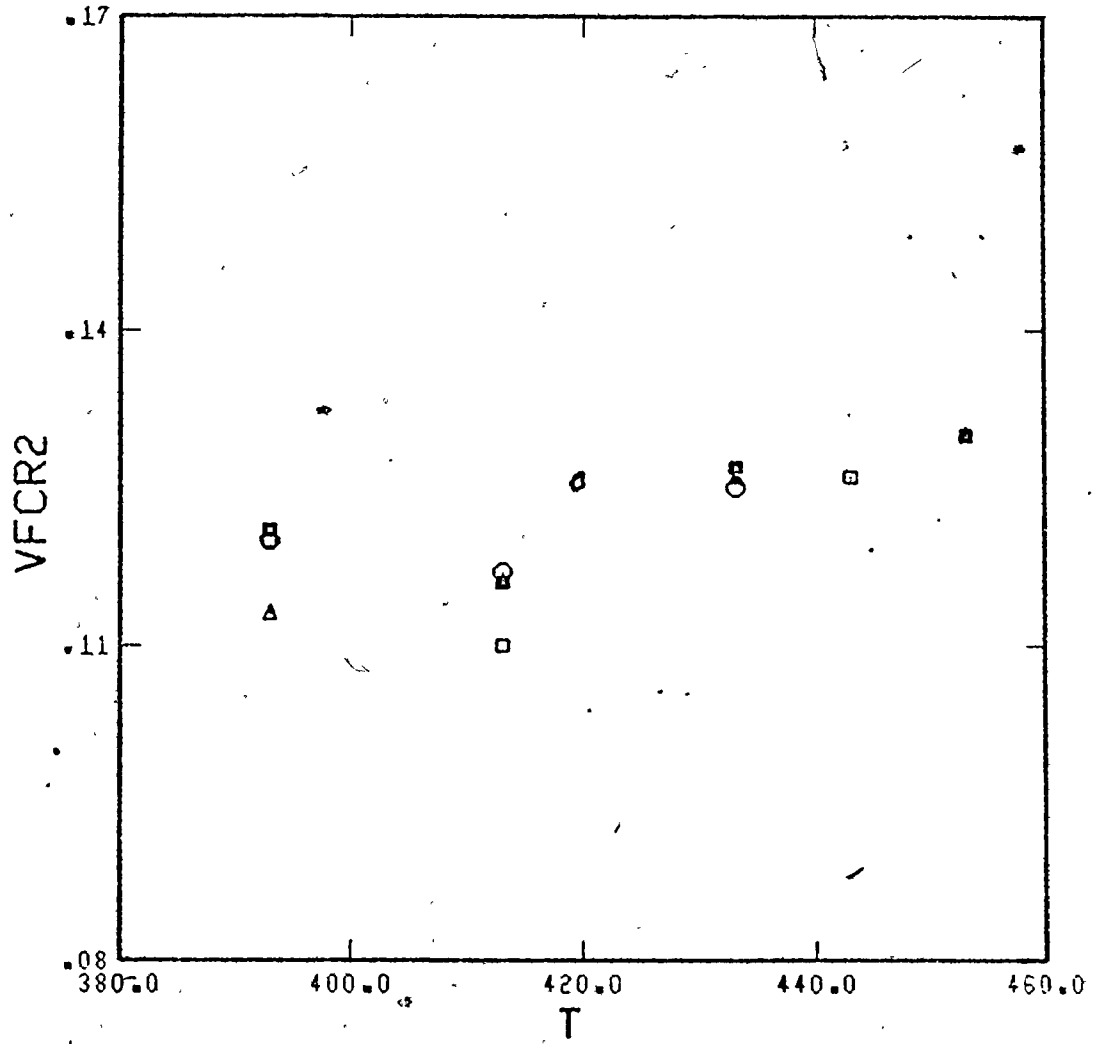


Fig.27: Measured (f_{10} : \circ : 0, Δ :0.2, \square :0.75, \square :1) V_{FCR2} vs. T(°K)
 $B = 0.5$ (S/PMS).

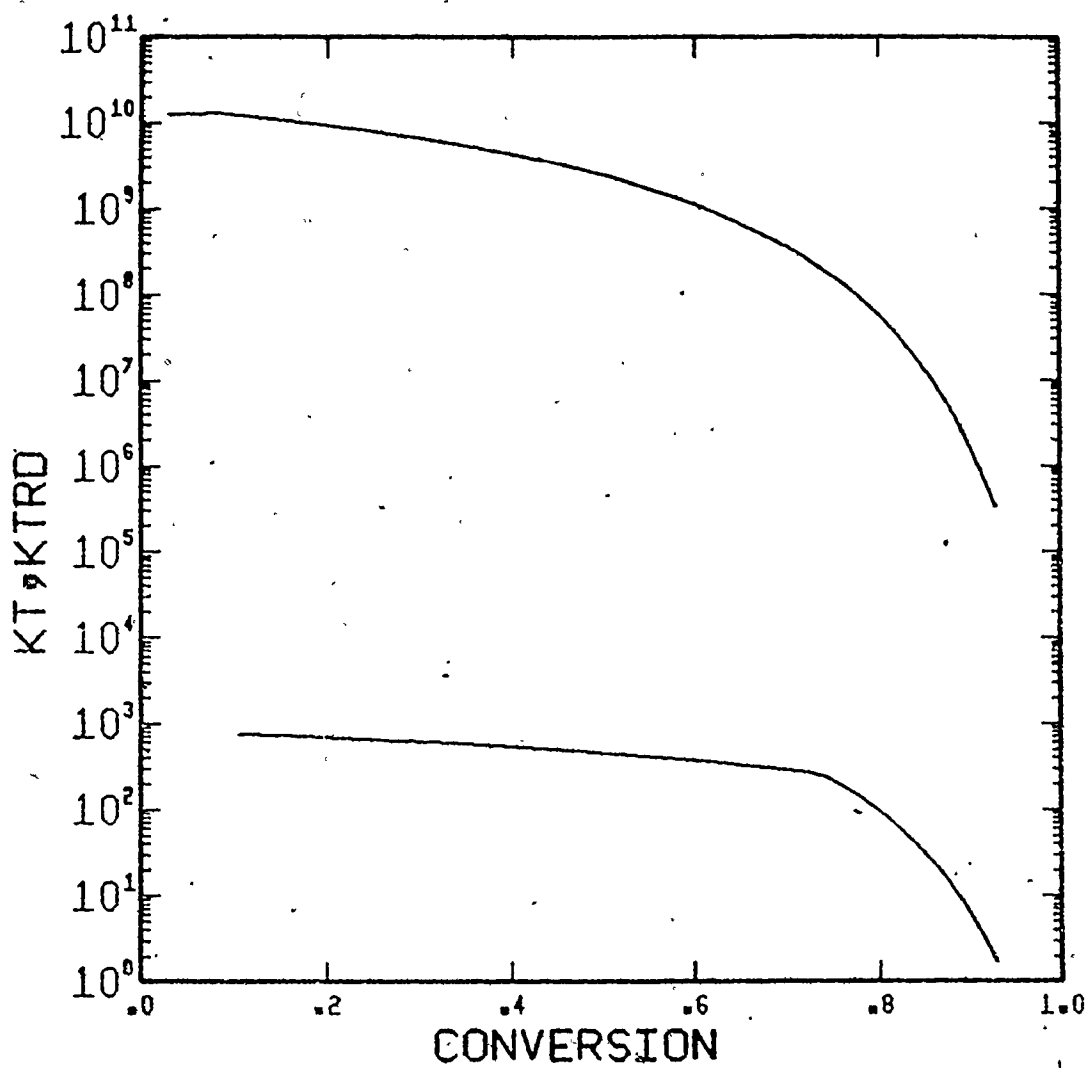


Fig.28: Predicted ($f_{10} = 0.2$, $T = 140^\circ\text{C}$) change in k_{tc} and k_{trd} (l/mole, min.) with conversion (S/PMS).

decades over the entire conversion range. K_{trd} remains negligibly small in comparison throughout, showing the negligibly small effect the values for n_s and l_0 have on the model predictions. Evidently K_{tc} decreases more in this model to offset the falling K_p . However, the empirical model gives the K_t variation only when it is valid to assume that K_p does not become diffusion-controlled.

The following non-linear least squares (NLLS) estimates of α_m and α_p for PMS and polyPMS, respectively, were obtained from the T_g data (measured by DSC) received from Mobil Chemical Co., after the development of the present model

$$\alpha_m = 0.00193 \text{ K}^{-1} \quad \alpha_p = 0.00057 \text{ K}^{-1}$$

Figure 29 compares the experimental data with the limiting conversions predicted using 1) parameters as used in this model 2) NLLS estimates. Figure 30 compares model predictions using NLLS estimates for α_m and α_p with the experimental x data for PMS polymerization at 120°C . The poor fit of the data may be due to 1) the T_{gp} values measured using DSC could be different than those obtained using kinetic

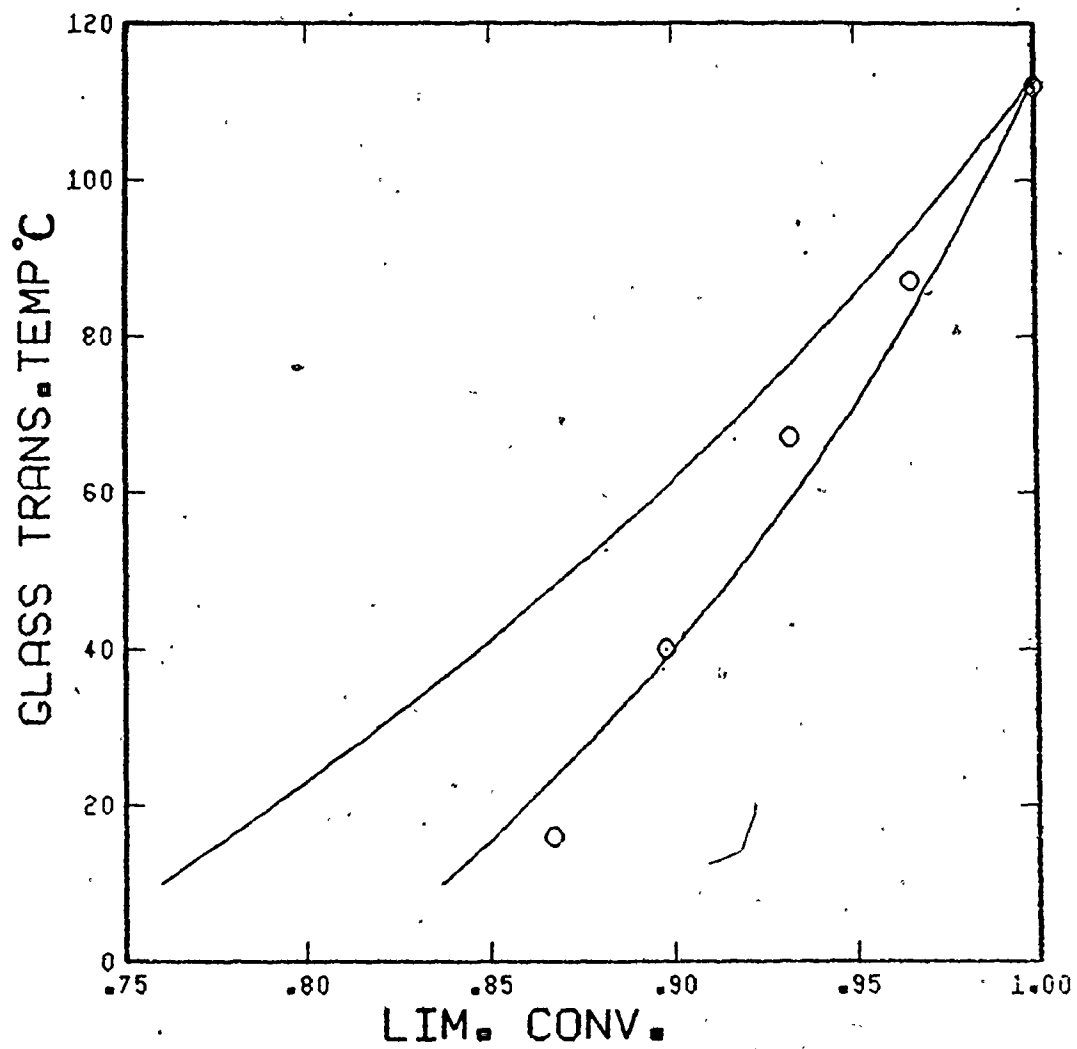


Fig. 29: Measured (O:DSC) and predicted T_{gp} vs. limiting conversion (PMS).

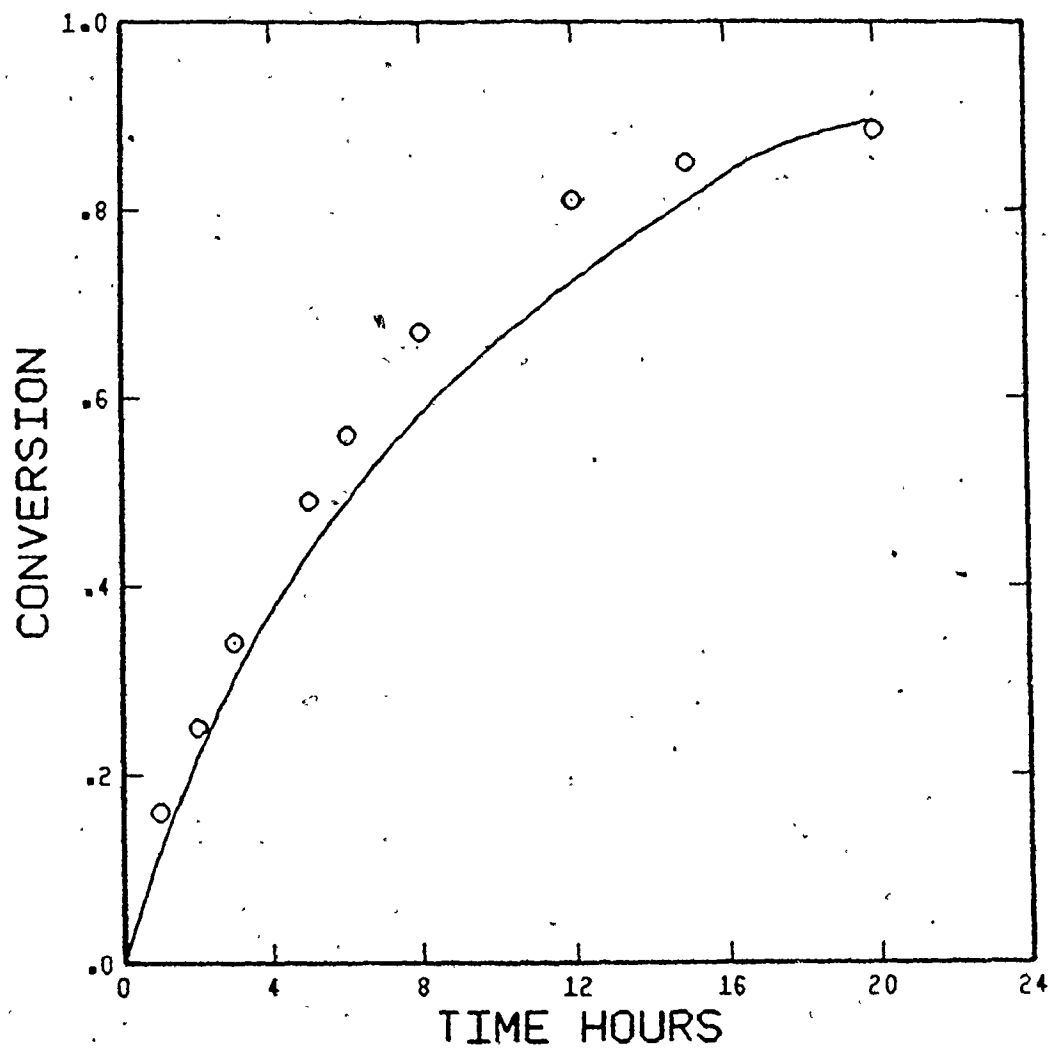


Fig.30: Measured (O; 120°C, $f_{10} = 0$) and predicted conversion vs. time, $\alpha_m = 0.00193$, $\alpha_p = 0.00057 \text{ K}^{-1} (\text{S/PMS})$.

measurements of limiting conversions (measured T_g values differ with measurement technique) and 2) the account for diffusion-controlled propagation may be invalid due to reasons cited earlier.

Equation (44) was also solved using the values for all propagation constants obtained from the estimated reactivity ratios. The effect on x -time histories was negligible. No composition drift was observed for $f_{10} = 0.75$, however, composition drift upto a maximum of 20% was observed for $f_{10} = 0.2$ as shown in Figure 31.

Figure 32 shows the chemically-controlled K_t (equation 47) plotted as a function of f_{10} for the styrene/PMS copolymerization system.

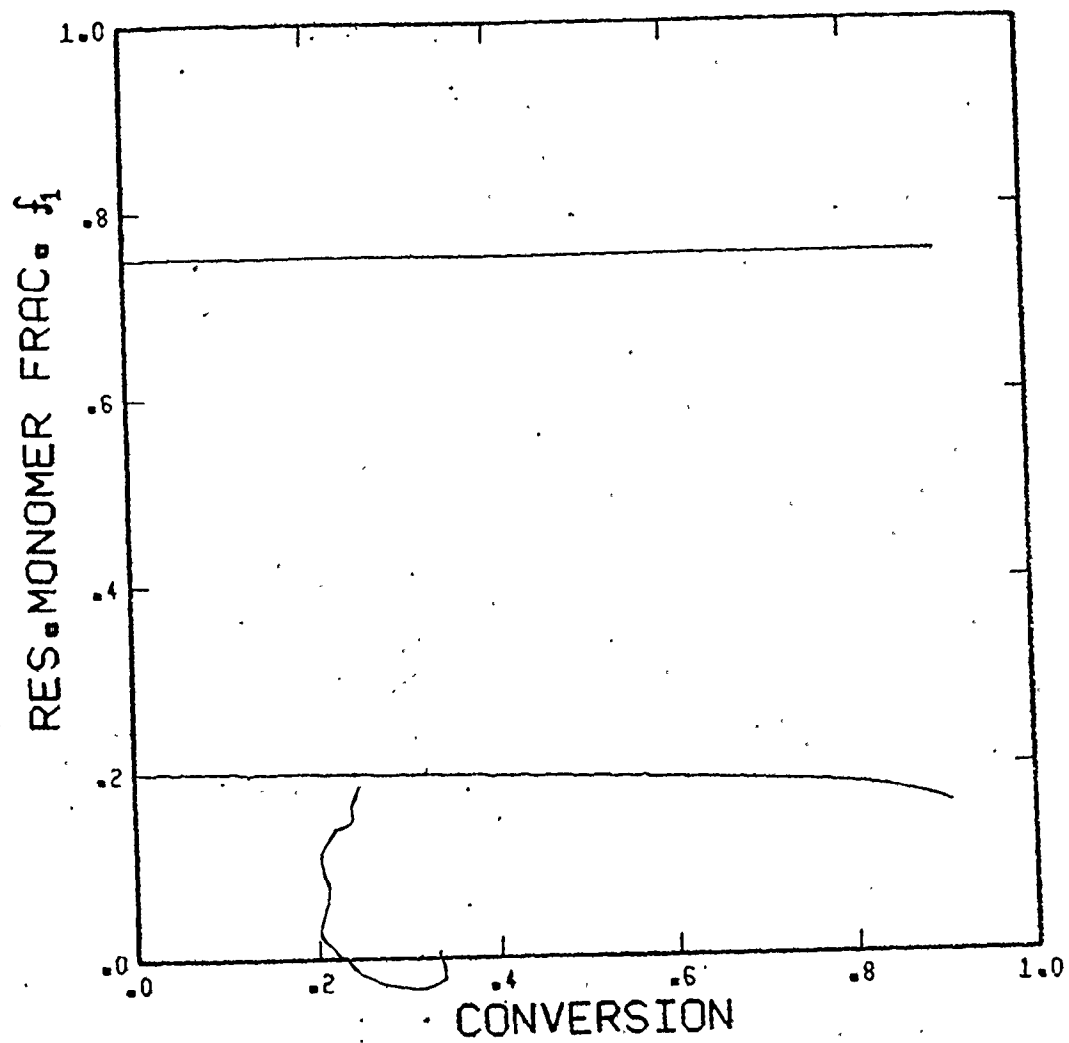


Fig.31: Predicted ($T = 120^\circ\text{C}$, $f_{10} = 0.2, 0.75$) f_1 vs. conversion (S/PMS).

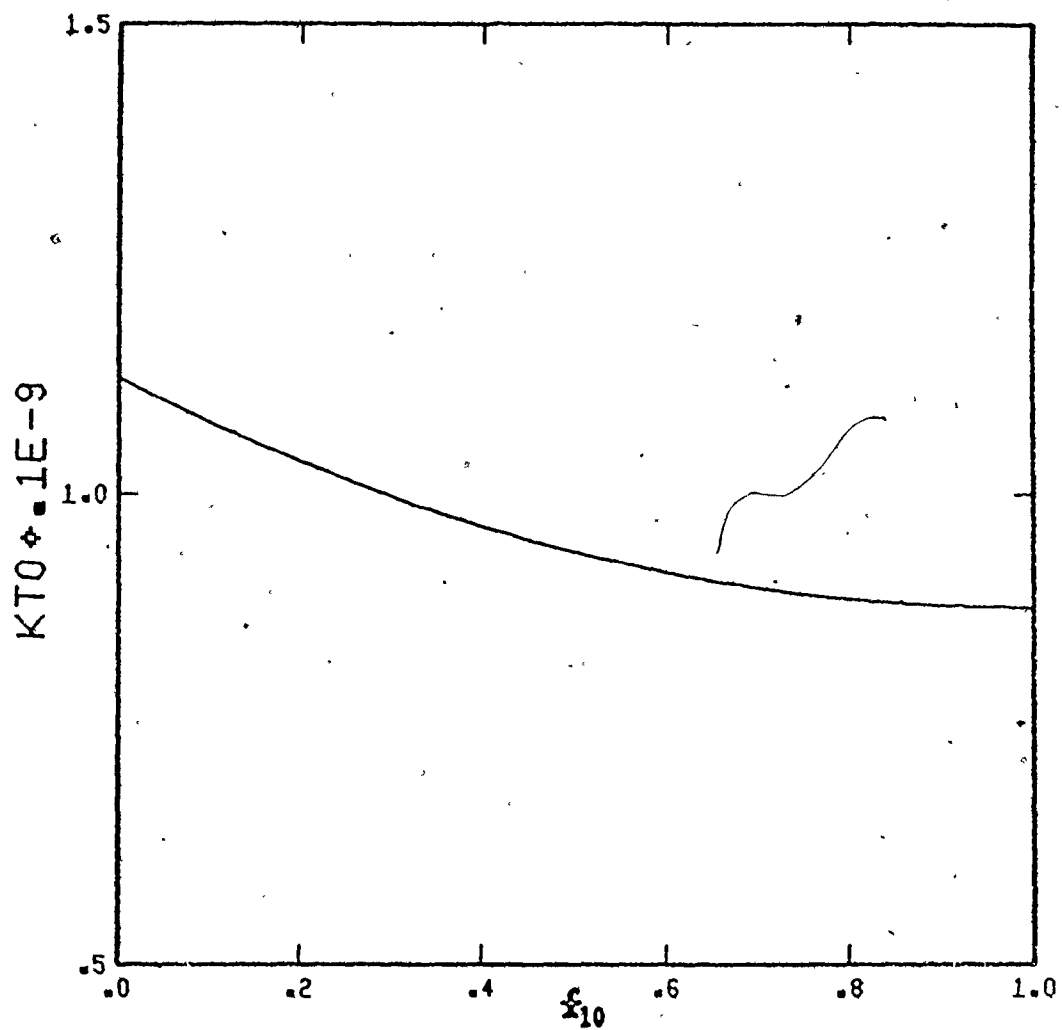


Fig.32: Chemically-controlled k_t as a function of f_{10} (styrene/PMS, l/mole.min)

6.3 Model for MMA/PMS Copolymerization Using Free-Volume Theory to Model Diffusion-Controlled Propagation and Termination

Figures 33-36 show the fits of the experimentally measured conversion data (4) with model predictions. The model reasonably predicts data at various temperatures, initiator levels and initial comonomer compositions upto limiting conversions. Figure 37 compares the data of Balke and Hamielec (111) for $f_{10} = 1$ at various temperatures with model predictions. The model predictions are fair at 90°C but quite inadequate at low temperatures. Figures 38 and 39 show the change in residual monomer composition with x at 60 and 80°C. Reasonable fits upto limiting conversions indicates that the assumption used to impose diffusional limitation on the individual propagation constants at the same V_F is consistent with the data. A corollary of this approach is that the reactivity ratios are independent of conversion. However, under diffusion-controlled conditions, it is expected that the propagation rate constants, are dependent on the

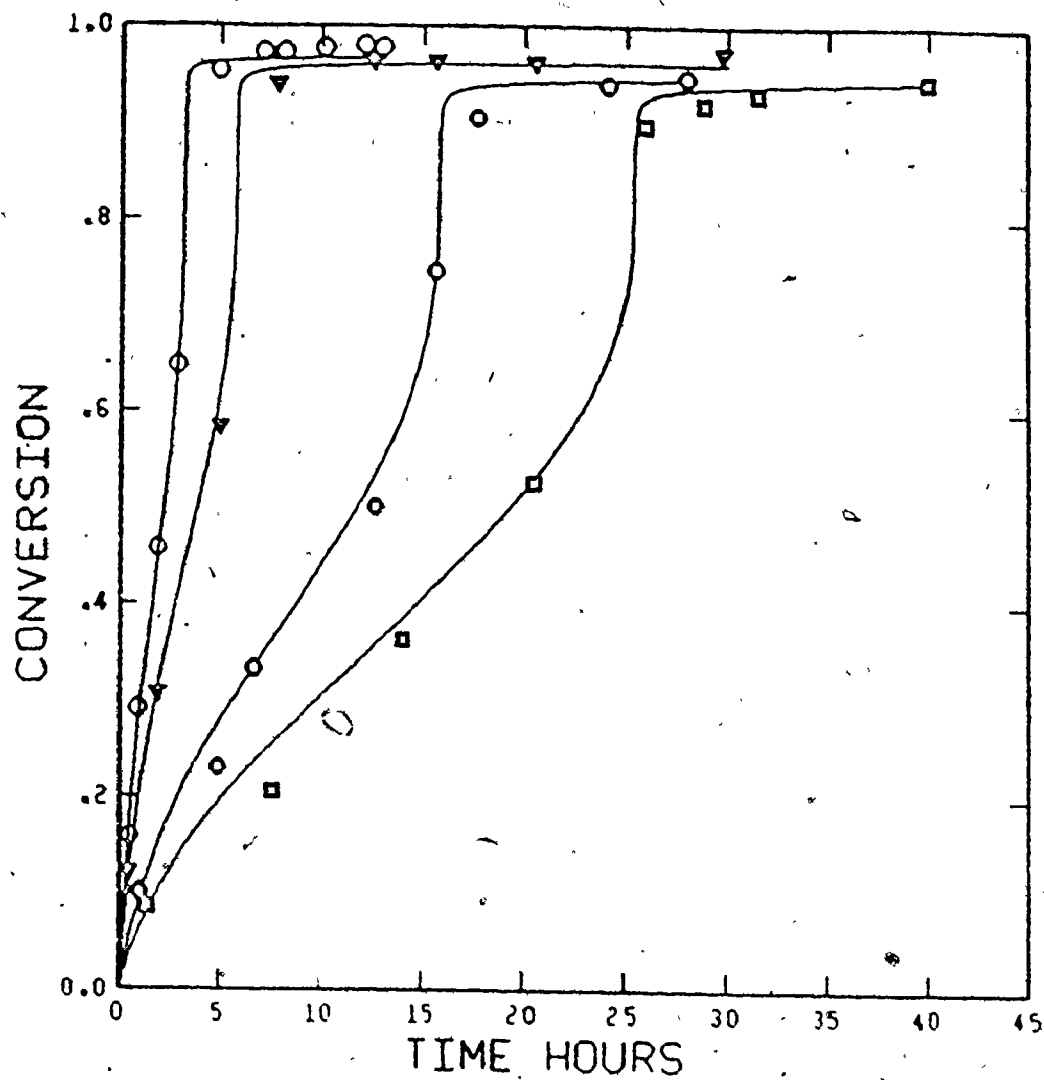


Fig.33 Measured (○:80, ◯:60°C, $[I]_0 = .0157$; ▽:80, ◻ = 60°C, $[I]_0 = .0057$ mol/l) and predicted conversion vs. time, $f_{10} = 0.54$ (MMA/PMS).

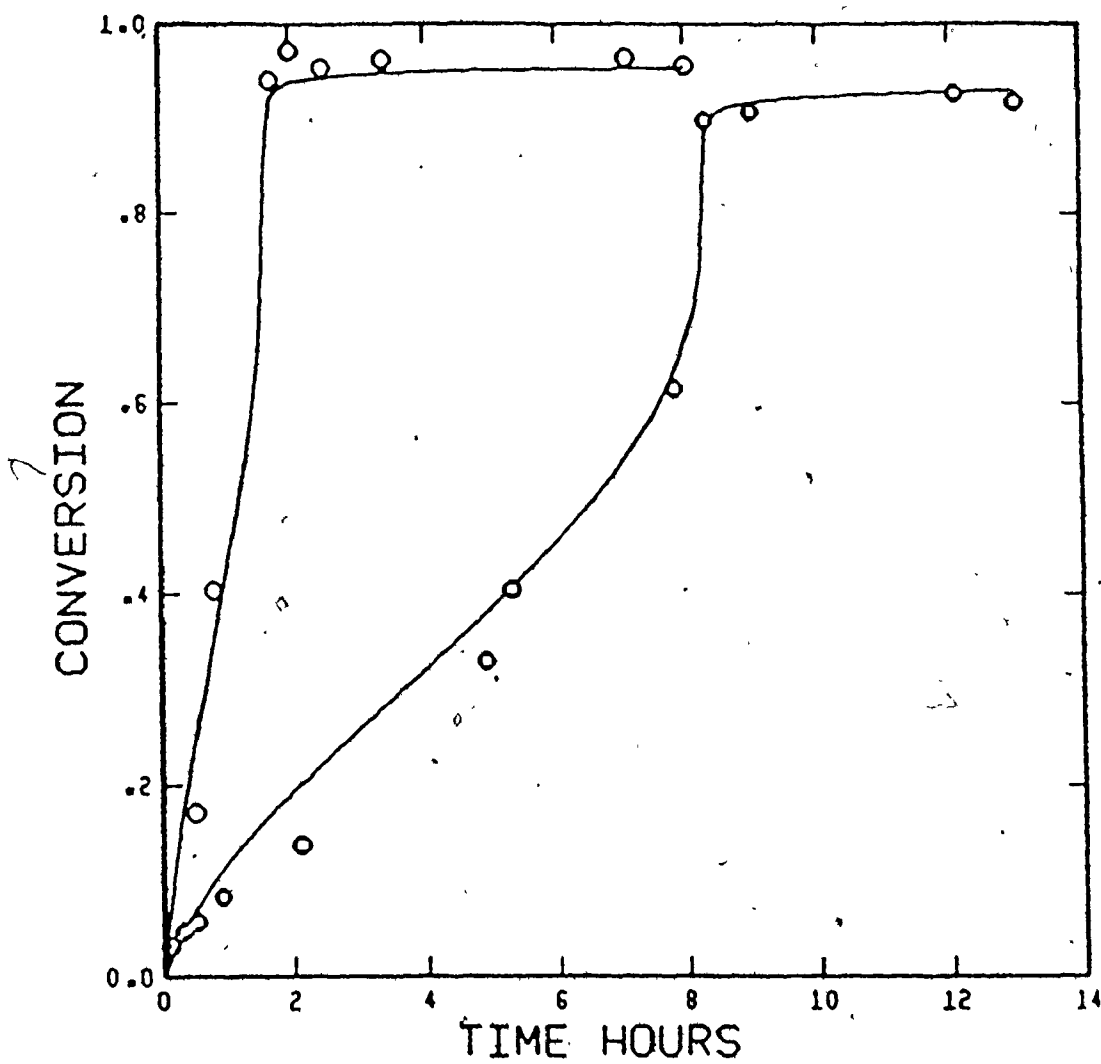


Fig.34: Measured (O:80. \circ :60°C) and predicted conversion vs. time $[I]_0 = .0157 \text{ mol/l}$, $f_{10} = 0.83$ (MMA/PMS).

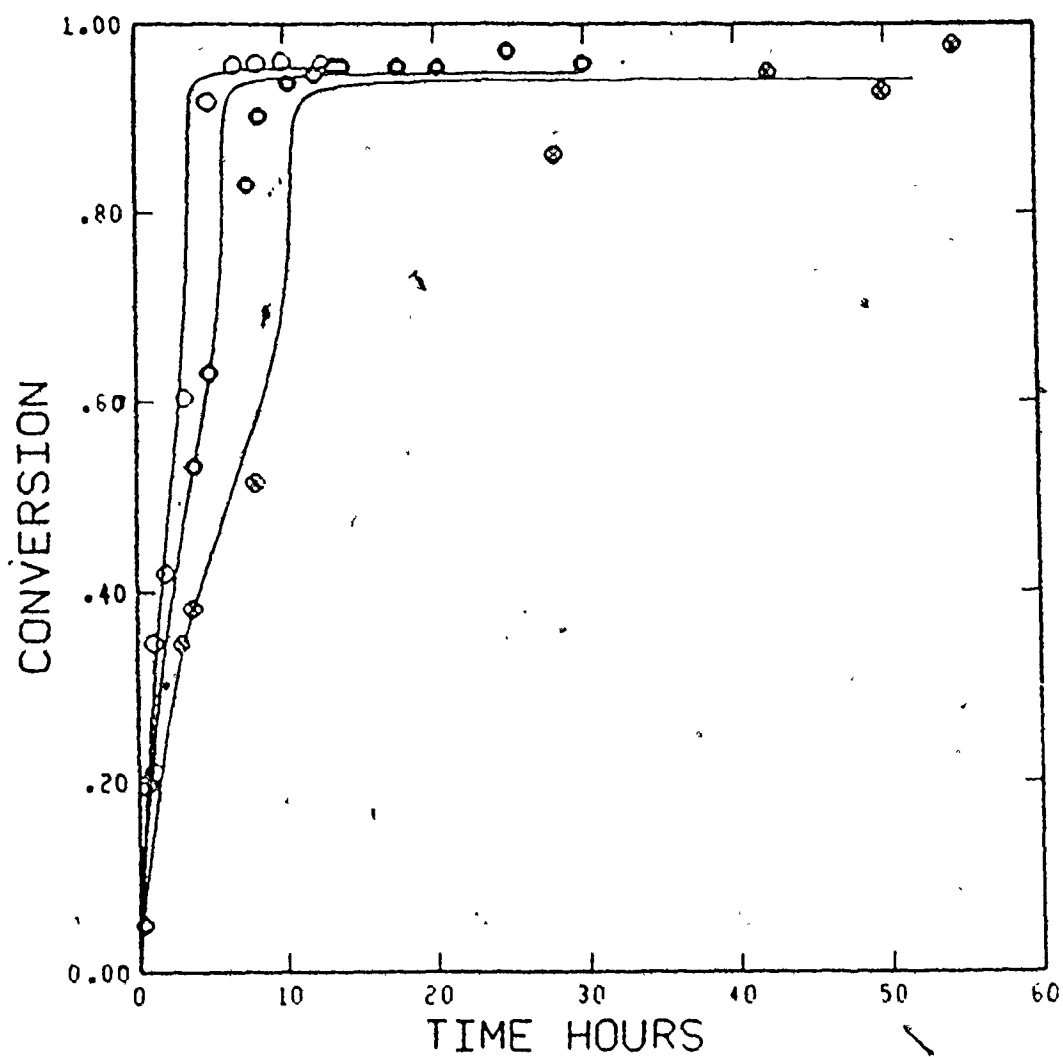


Fig. 35: Measured ($[I]_0$: 0:0.0252, \bullet :0.0157, \otimes :0.0057 mol/l) and predicted conversion vs. time, $T = 80^\circ\text{C}$, $f_{10} = 0.21$ (MMA/PMS).

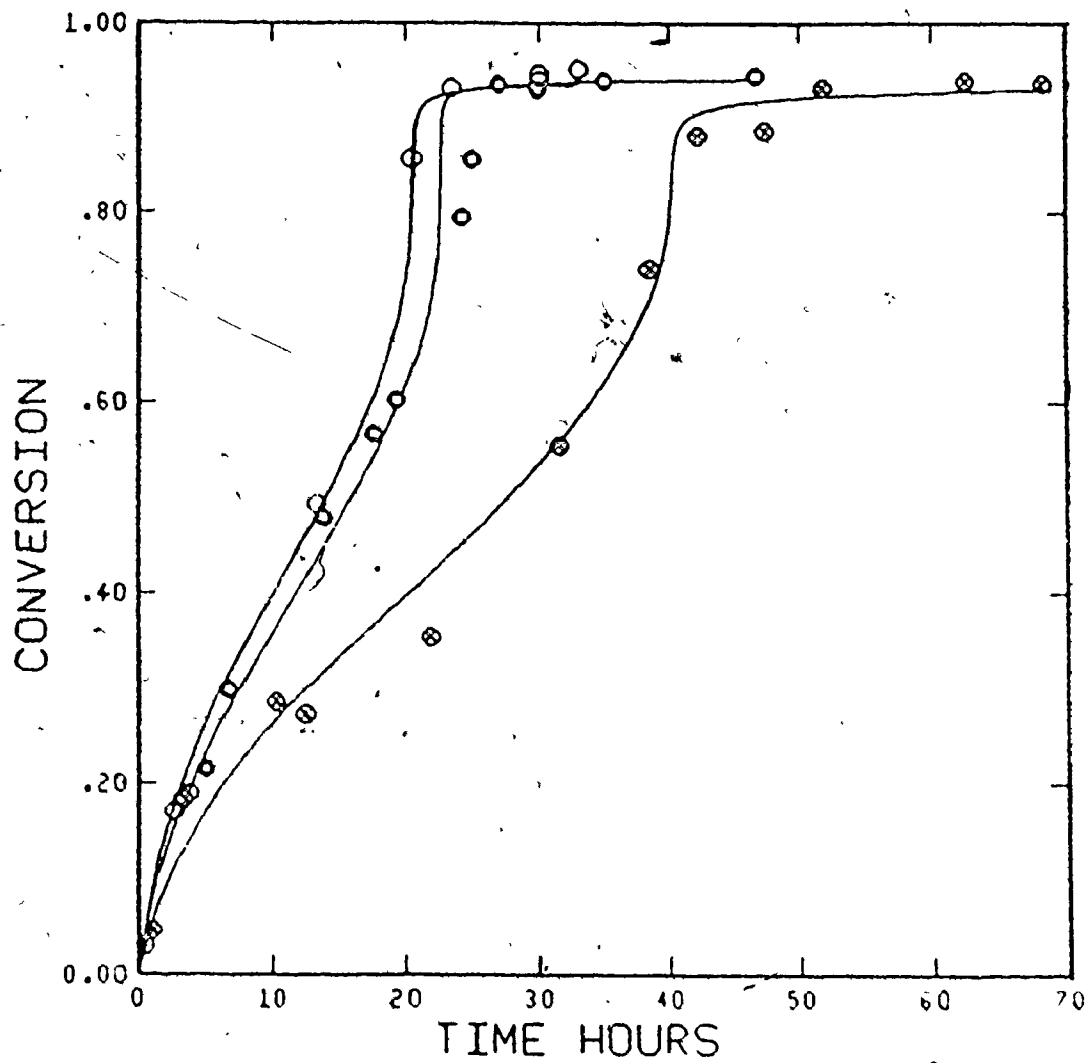


Fig.36: Measured ($[I]_0:0:0.0252$, $\bullet:0.0157$, $\blacksquare:0.0057$ mol/l) and predicted conversion vs. time, $T = 60^\circ\text{C}$, $f_{10} = 0.21$ (MMA/PMS).

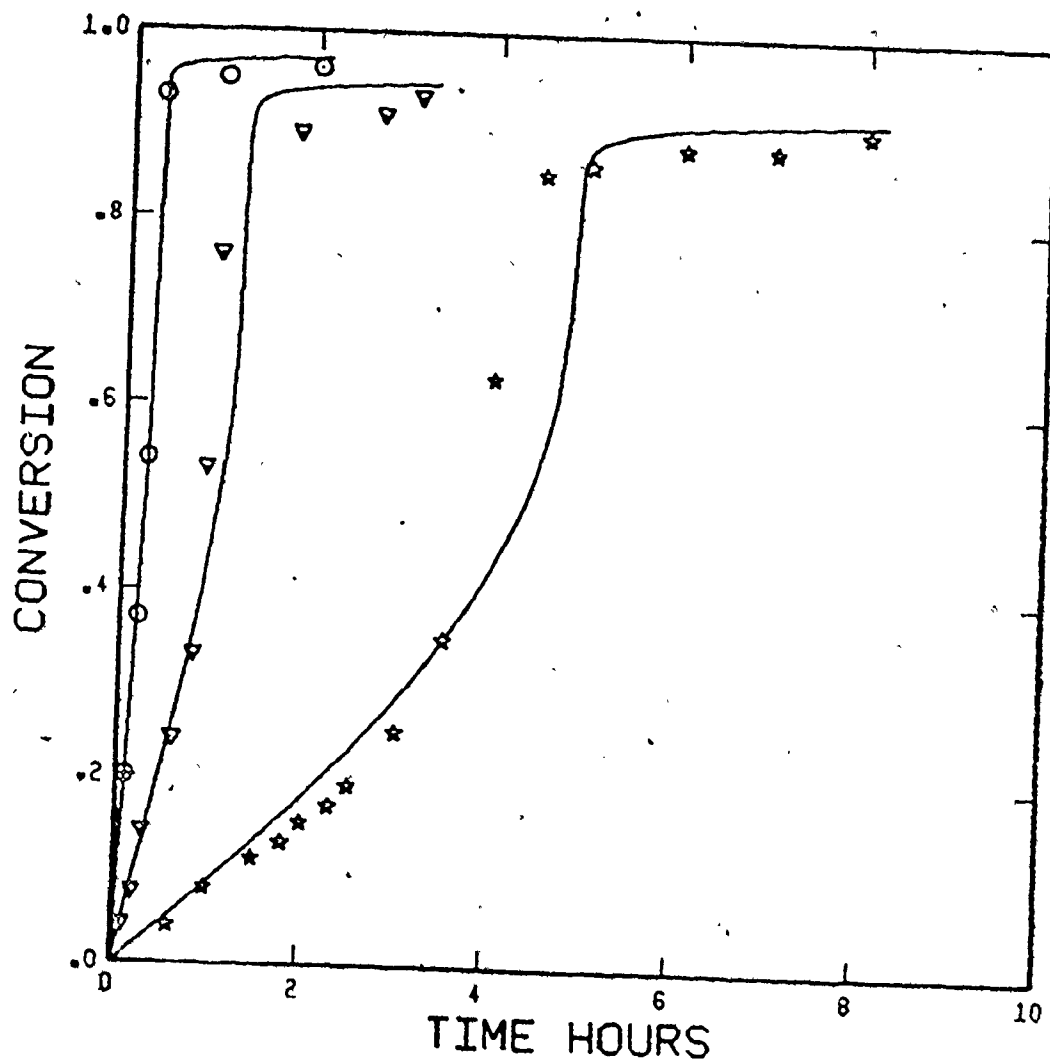


Fig.37: Measured (Δ :50, ∇ :70, \circ :90°C) and predicted conversion vs. time, $[I]_0 = 0.0252 \text{ mol/l}$, $f_{10} = 1$ (MMA/PMS).

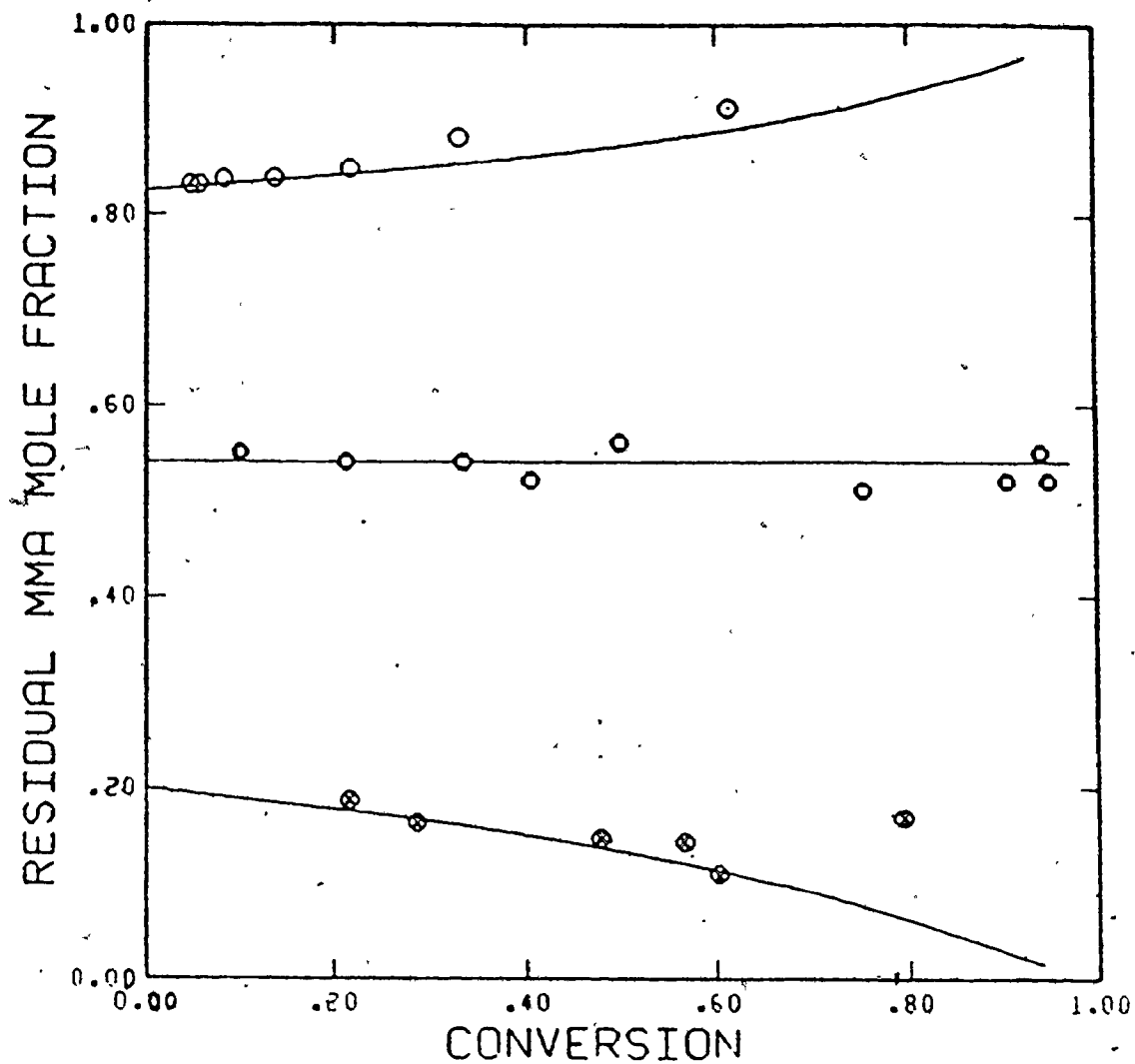


Fig.38 Measured (f_1 : ○: .83, ●: .54, ⊗: .21) and predicted f_1 vs. conversion, $T = 60^\circ\text{C}$, $[I]_0 = .0157 \text{ mol/l (MMA/PMS)}$.

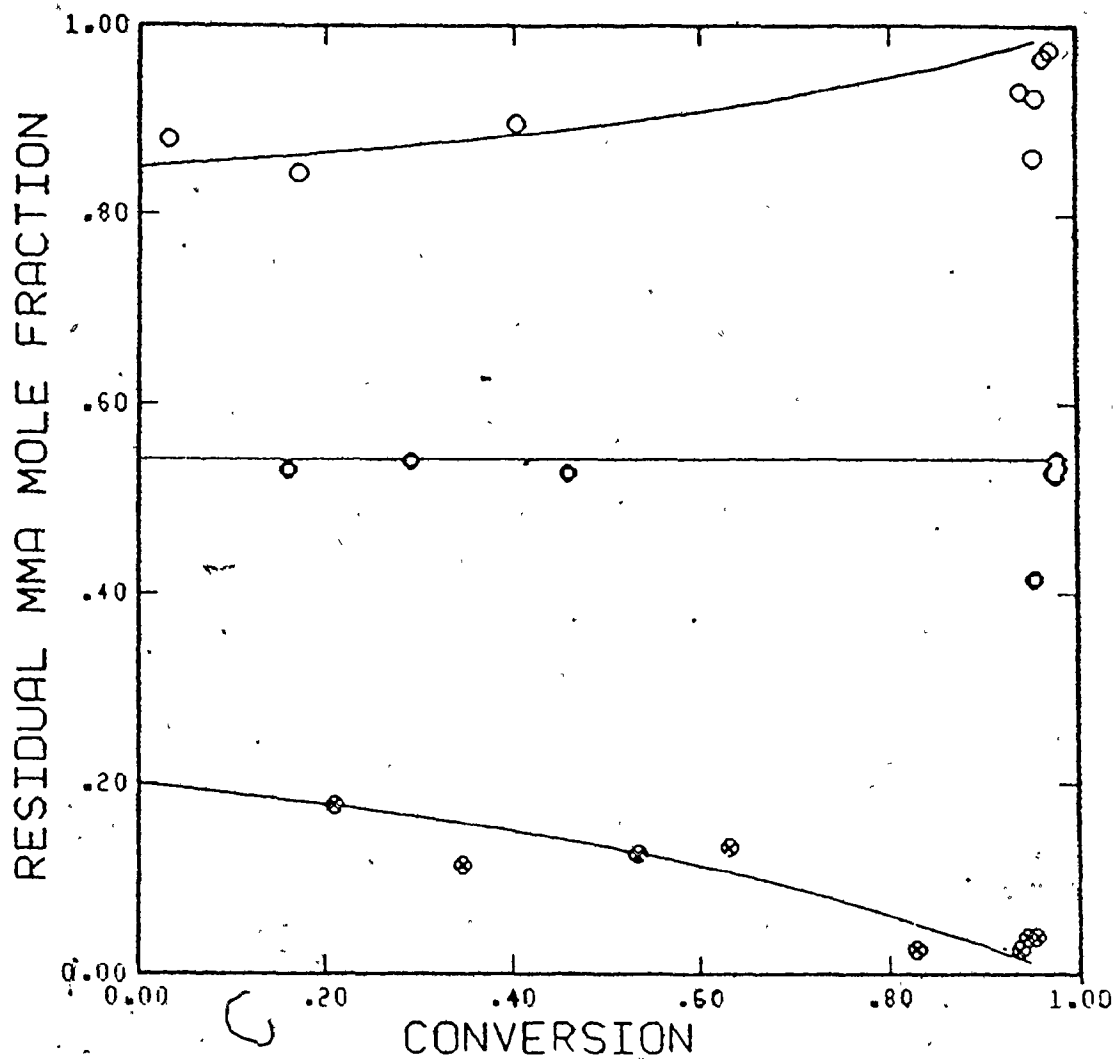


Fig.39: Measured (f_{10} : \circ :.83, \bullet :.54, \otimes :.21) and predicted f_1 vs. conversion, $T = 80^\circ\text{C}$, $[I]_0 = .0157 \text{ mol/l (MMA/PMS)}$.

diffusion rates of the two monomers, implying that, K_{ij} , K_{jj} ($i=j$) would be approximately equal, and therefore the r_1 and r_2 should change with conversion such that $r_1 r_2 = 1$ as $x \rightarrow 1$. To test this hypothesis, the differential form of the Meyer-Lowry equation was solved with r_1 and r_2 changing with conversion. As shown in the Appendix(6) and in Figure 40, the data at very high conversions are not sufficiently accurate to either prove or disprove this hypothesis. Figures 41 and 42 compare \bar{M}_W of the copolymer of the azeotropic composition obtained by LALLSP with model predictions showing reasonable fits for all the conditions. Figures 43-45 compare \bar{M}_N and \bar{M}_W data for MMA polymerizations with model predictions which are fair for \bar{M}_N but clearly inadequate for \bar{M}_W at moderate to high conversions. The poor performance of the model in simulating MMA homopolymerization data is likely due to the large value of d used to model segmental diffusion-controlled termination. This postpones the gel-effect to higher conversions than the x and \bar{M}_W data suggest. The model then requires also a higher value of A than used earlier by Marten and Hamielec(31), causing the limiting conversions to be higher than the observed data. However, the d and A together satisfied the copolymer data based on the other kinetic

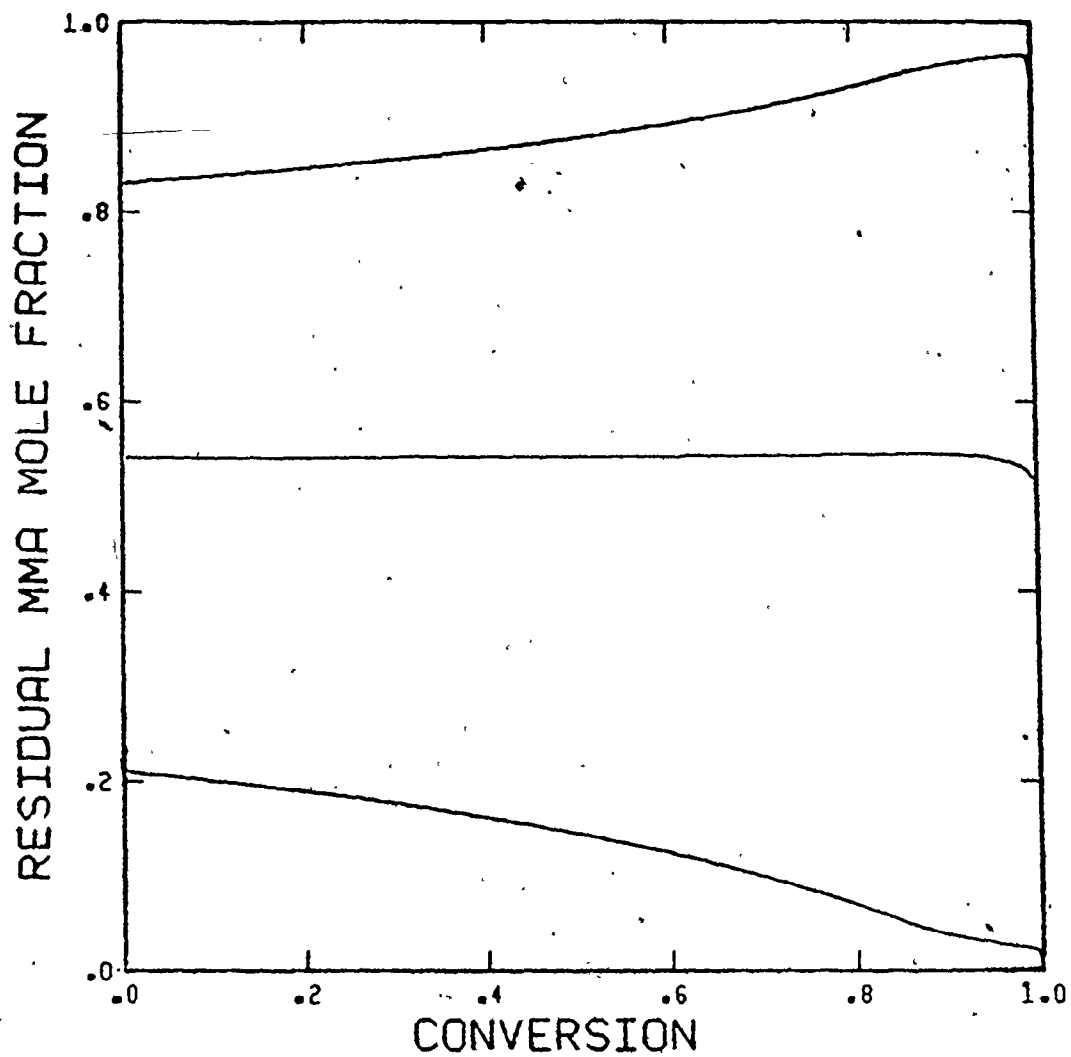


Fig.40 Predicted f_1 vs. conversion; $f_{10} = .83$, $f_{10} = .54$, $f_{10} = .2$ with r_1, r_2 dependent on conversion at high conversions (MMA/PMS).

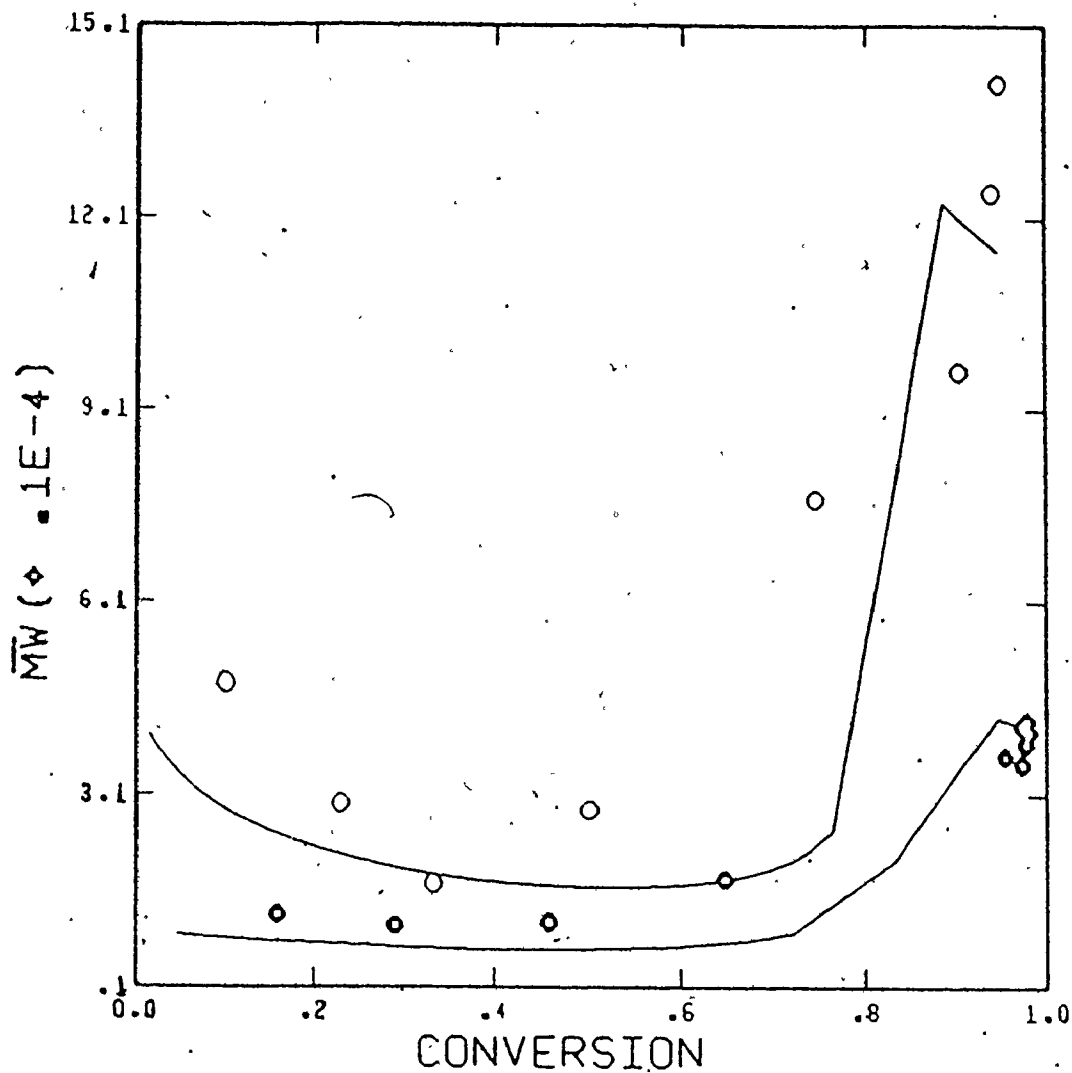


Fig.41: Measured (O:60, ●:80°C) and predicted \bar{M}_w vs. conversion, $[I]_0 = .0157 \text{ mol/l}$, $f_{10} = .54$ (MMA/PMS).

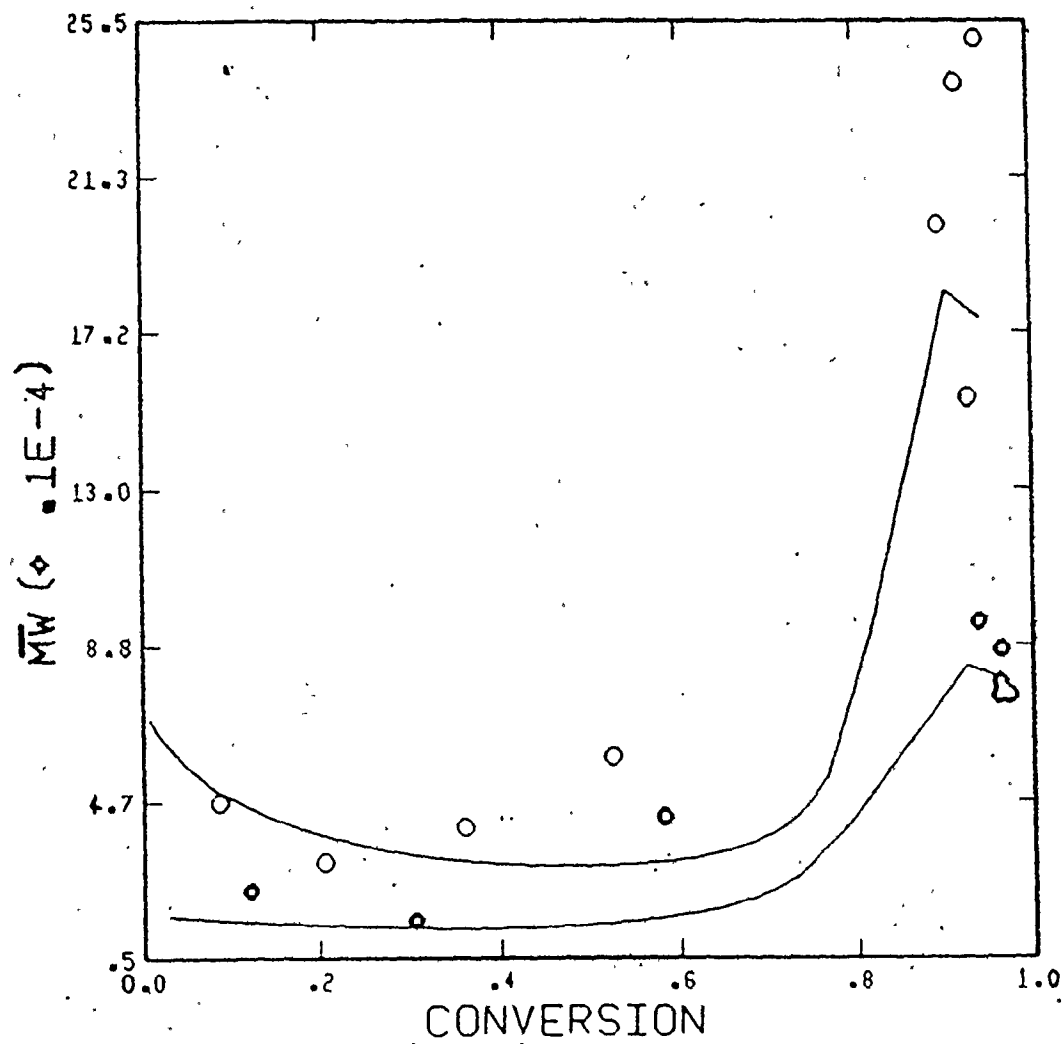


Fig.42: Measured (O:60, ●:80°C) and predicted \bar{M}_w vs. conversion, $[I]_0 = .0057 \text{ mol/l}$, $f_{10} = .54$ (MMA/PMS).

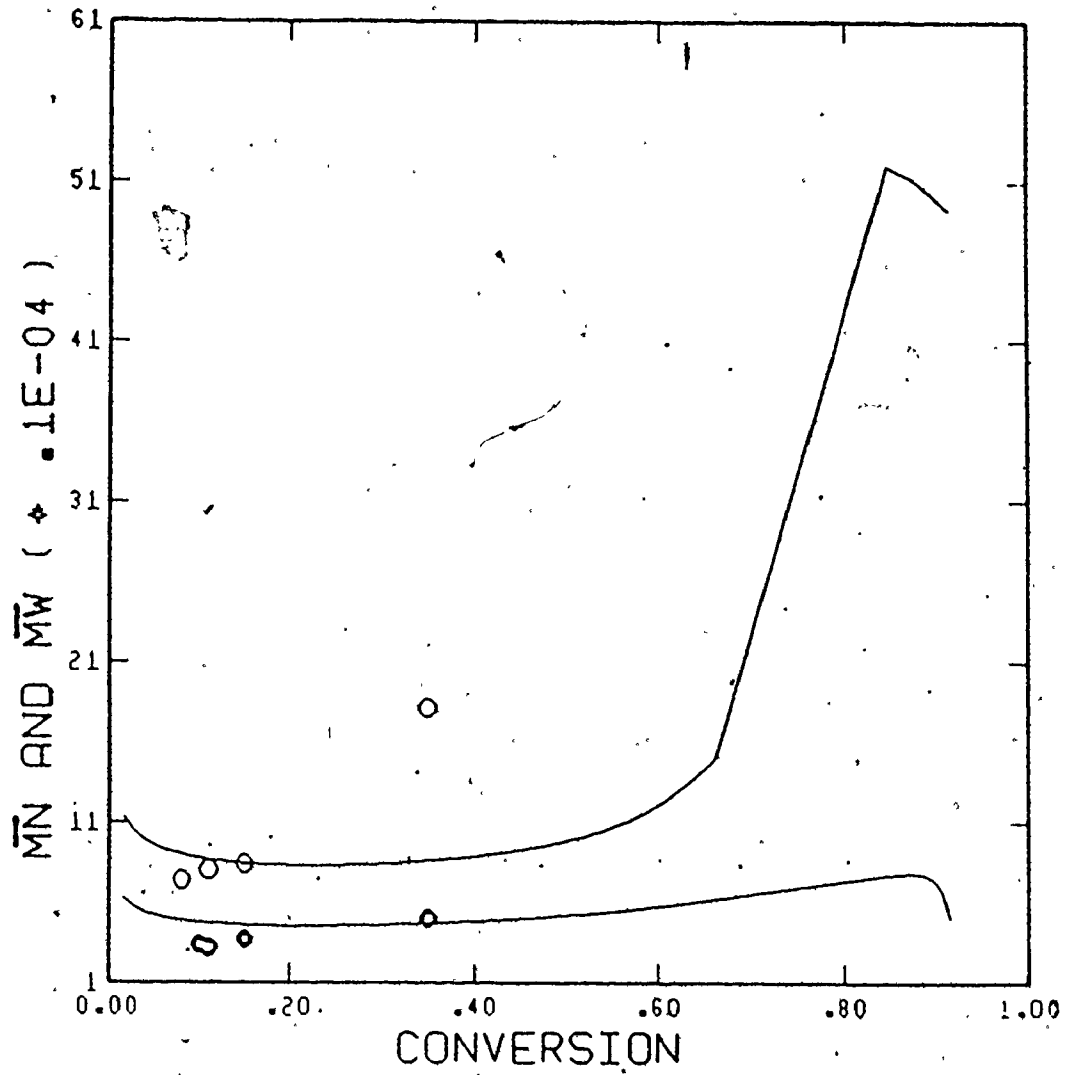


Fig.43 Measured (○: \bar{M}_w , ○: \bar{M}_n) and predicted \bar{M}_n and \bar{M}_w vs conversion, $[I]_0 = .0252 \text{ mol/l}$, $T = 50^\circ\text{C}$, $f_{10} = 1$ (MMA/PMS).

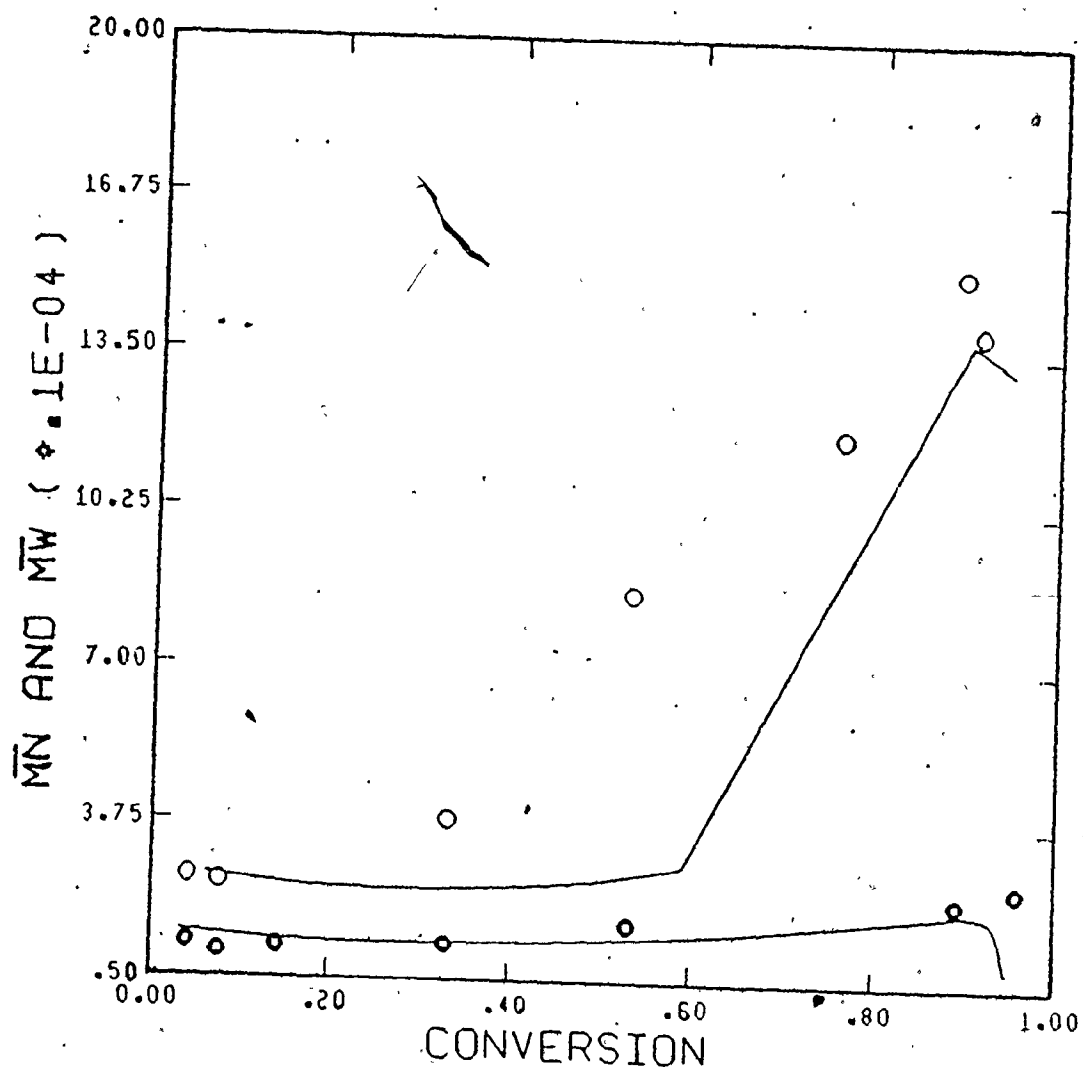


Fig.44: Measured (O: \bar{M}_w , ●: \bar{M}_n) and predicted \bar{M}_n and \bar{M}_w vs. conversion, $[I]_0 = .0252 \text{ mol/l}$, $T = 70^\circ\text{C}$, $f_{10} = 1$ (MMA/PMS).

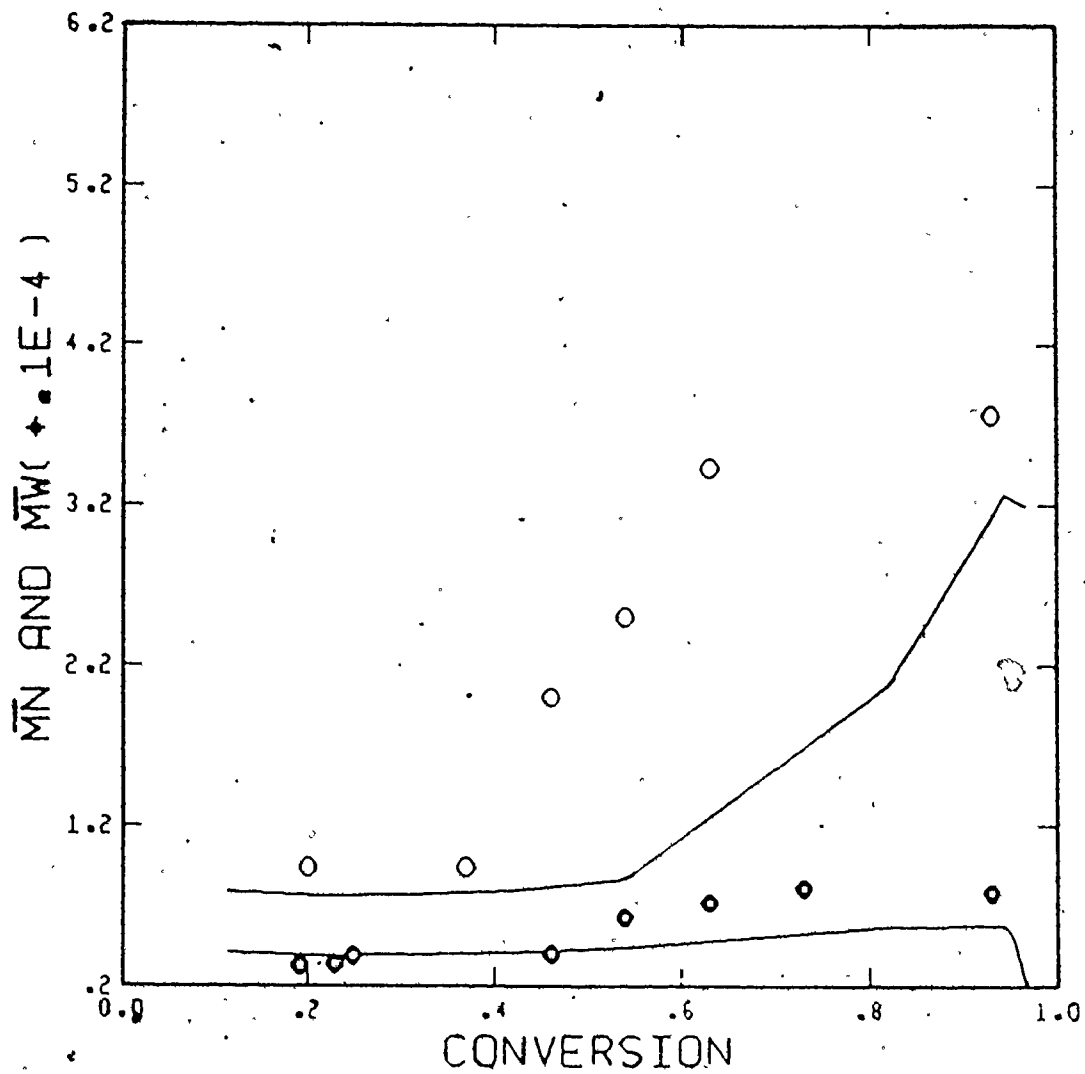


Fig.45: Measured (O: \bar{M}_w , \bullet : \bar{M}_n) and predicted \bar{M}_n and \bar{M}_w vs. conversion, $[I]_0 = 0.0252 \text{ mol/l}$, $T = 90^\circ\text{C}$, $f_{10} = 1$ (MMA/PMS).

parameters used in the model. It should be noted that the calculation of K_{t0} through initial rate measurements may not be wholly reliable and therefore may lead to erroneous values of d . Especially, with known values for K_{t22} and K_{t12} , the K_{t0} could be calculated with better accuracy and thus more reliable values of d and consequently A would then be obtained.

Both K_3 and V_{Fcr2} were found to be independent of initiator concentration with K_3 exhibiting a strong dependence on temperature. Refer to Appendix(7) for the values of these parameters. Figure 46 shows the predicted decrease in K_t with conversion showing a slight increase followed by a dramatic decrease shortly after the onset of the gel-effect and the eventual fall to approximately zero during the glassy-state transition.

Figure 47 show the predicted K_t (chemically-controlled) obtained by regressing K_t on f_{10} using equation (47), plotted as a function of f_{10} for the MMA/PMS copolymerization. K_{t22} and K_{t12} were estimated for the MMA/PMS system using the K_{t11} value reported by Meyerhoff (110) at both temperatures of 60 and 80 °C as it was felt, that the K_{t22} obtained for the

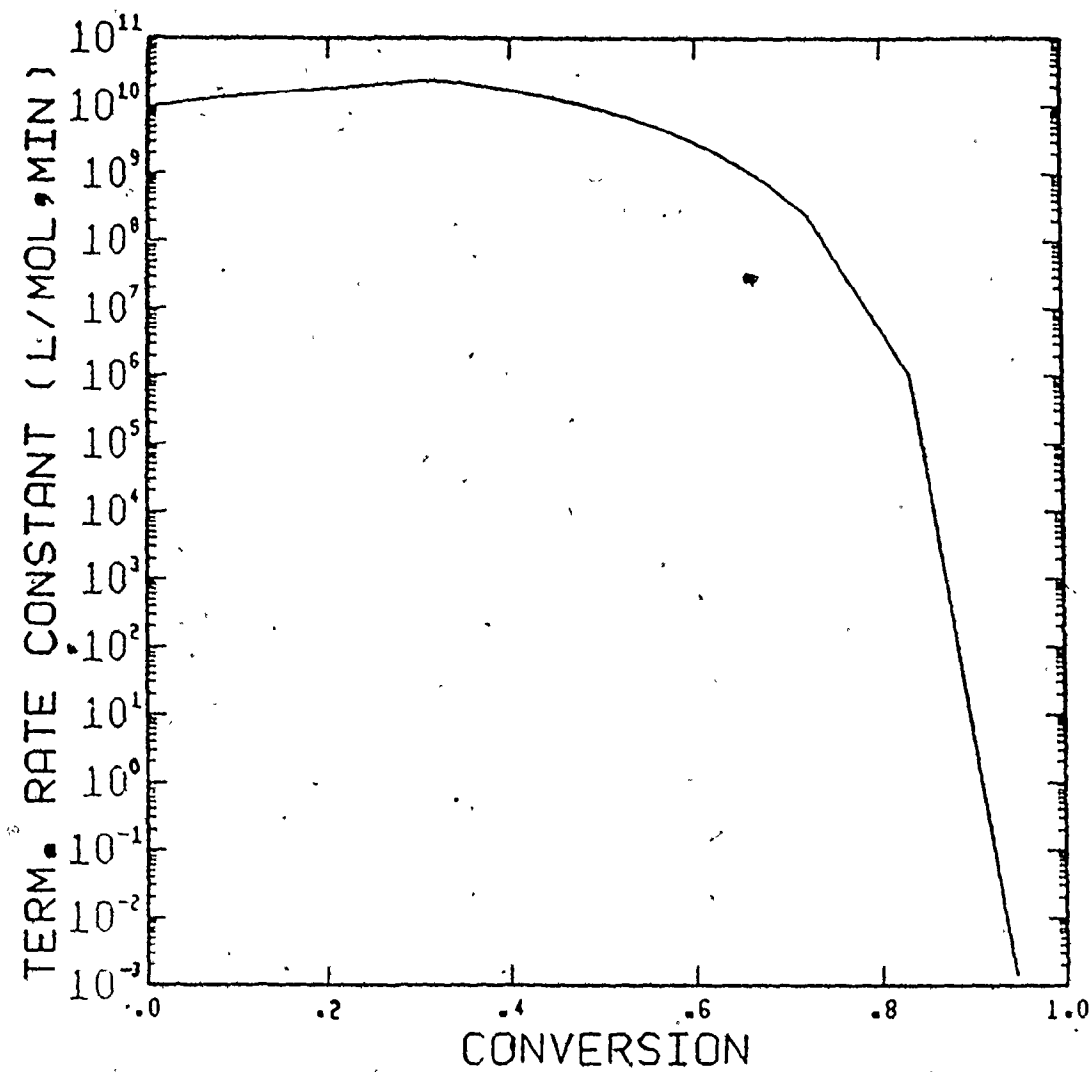


Fig.46: Predicted k_t vs. conversion, $[I]_0 = .0157$ mol/l,
 $T = 80^\circ\text{C}$, $f_{10} = .54$ (MMA/PMS).

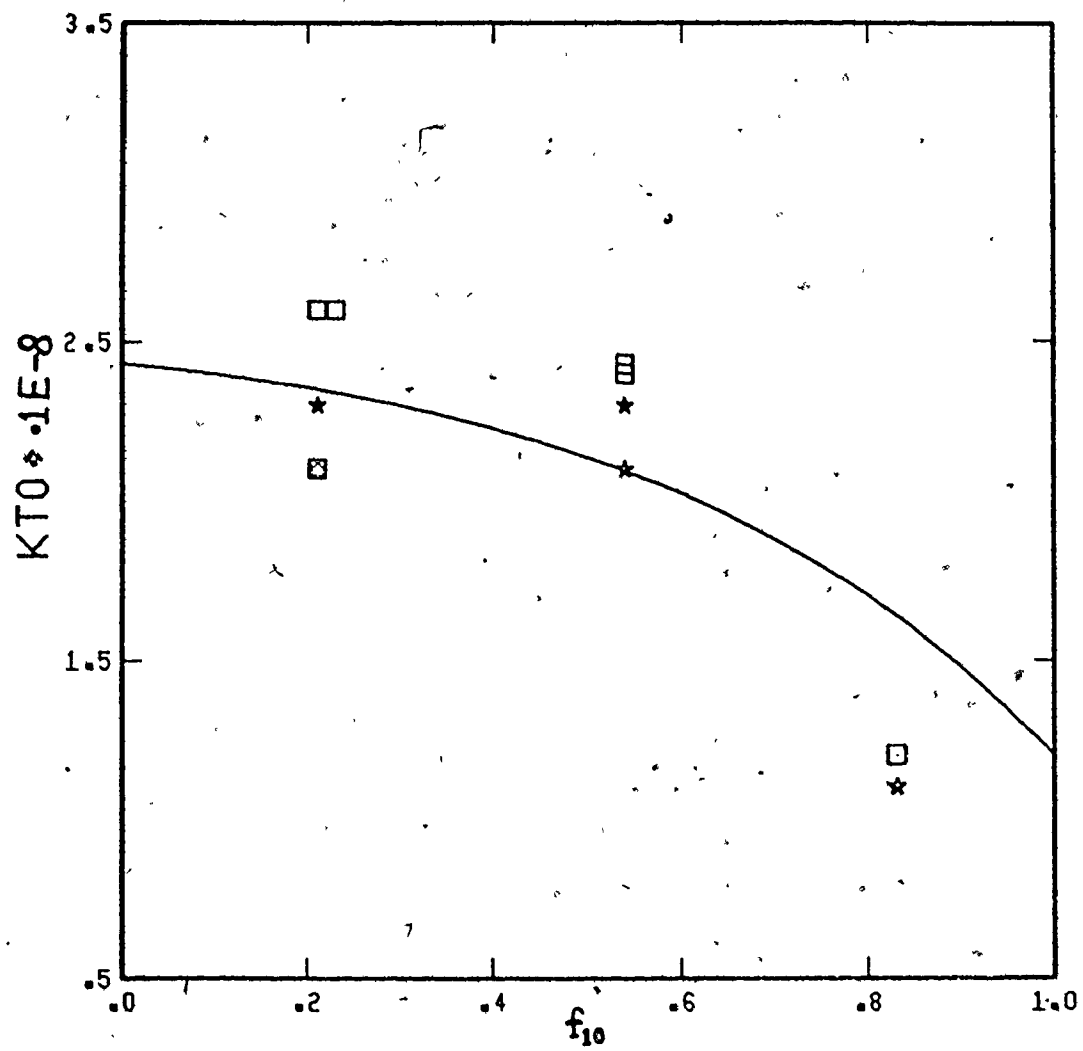


Fig.47: Chemically-controlled k_t as a function of f_{10} (MMA/PMS)

thermal copolymerization of styrene/PMS could not be reliably extrapolated to low temperatures.

It is worth mentioning that the probable reason why one value of A could be used to model each of the copolymerization systems for all compositions was, that the T_{gp} of these copolymers did not change much with composition. A more interesting and severe test of the model would be its application to a copolymerization system showing a stronger dependence of T_{gp} on copolymer composition such as MMA/butyl acrylate.

CONCLUSIONS AND RECOMMENDATIONS

A general kinetic model accounting for diffusion-controlled propagation and termination reactions was developed to model bulk copolymerizations. The model requires few adjustable parameters, and these have been correlated with temperature wherever possible and are expected to be independent of the type and level of initiator. Such a predictive model provides a quantitative description of the polymerization reaction over the entire range of conversion. It can be used to generate conversion and molecular weight versus time profiles for commercial production systems and may be employed for the optimization and control of these processes.

This model should be applicable to free-radical copolymerization systems other than the ones tested herein as it was shown to reasonably model two quite different systems; the high temperature thermally-initiated bulk copolymerization of styrene/PMS and the chemically-initiated bulk copolymerization of

MMA/PMS in batch reactors. The second system is more complex in that it exhibits composition drift and the termination reactions occur through both combination as well as disproportionation. In addition, an empirical model has been developed for the bulk copolymerization of styrene/PMS. This empirical model is valid when the molecular weight of the macroradicals depends solely upon temperature and the termination constant depends solely on temperature and polymer concentration. The usefulness of this model stems from its simplicity and ease of application.

Batch kinetic data comprising x , \bar{M}_N and \bar{M}_W versus time for the styrene/PMS system have been measured at four temperature levels and two levels of comonomer composition.

The bulk polymerization of vinyl acetate (VAC) has been modelled to illustrate the effect of diffusion-controlled termination on conversion/time and \bar{M}_W development for a polymerization where long chain branching reactions are significant. The model, though limited in its applicability to conditions not widely different from those examined in the present work, correctly predicts trends in the conversion/time,

\bar{M}_W and branching frequency histories for VAC polymerizations.

Some optimal feed policies to minimize composition drift for semi-batch copolymerization of vinyl chloride/VAC have been studied. The studies consider the effect of these policies on the molecular weight development and the rate of polymerization and include the effect of diffusion-controlled termination on the same.

Kinetic models not accounting for chain length dependence of the individual rate constants and using some average molecular weights of either the dead polymer or the live radicals are simplistic attempts to model reality, though these have obvious computational advantages. It is felt that as polymer diffusion theory advances, the mechanism of all diffusion-controlled reactions in a polymerization process will be better understood. Reptation theory has given new insight into the mechanism of polymer diffusion. Unfortunately, the scaling laws predicting the diffusivity of polymer molecules have been applicable only to monodispersed systems so far. These have to be extended to treat the general case of a

polydisperse system which are the rule for free-radical polymerizations. The scaling laws have to be refined to incorporate chain growth of the diffusing polymer radicals. Work should also be directed to model the diffusivity of macroradicals in a highly concentrated environment where polymer-polymer friction is significant. Substantial work remains to be done to model diffusion-controlled propagation reactions in free-radical copolymerizations as well as to generate reliable experimental data on copolymer compositions at high to very high conversions. It is felt that the incorporation of diffusion-controlled initiation (decreasing initiator efficiency) at elevated conversions would provide better predictions of the radical concentrations and hence improve the overall performance of the model.

The mechanism of thermal initiation after Mayo is valid, however, work has to be done to elucidate the mechanism of thermal initiation for copolymerization involving styrene. Special emphasis should be placed on the study of the effect of the by-products of thermal initiation on the rate of polymerization and molecular weight development. Detailed work on chain transfer to intermediates is

required to improve the molecular weight predictability of the kinetic model.

Modelling diffusion-controlled VAC polymerization poses a difficult problem in that the theories of polymer diffusion have not been extended to include polymers with long chain branching. It is known that branched polymers generate excess free-volume around the molecule but whether this should lead to enhanced mobility is questionable given the higher incidence of polymer-polymer contacts and therefore increased polymer-polymer friction.

These are some of the areas which need better understanding to permit the development of predictive models suitable for application in polymer production technology.

APPENDIX

1. Reactivity Ratio Estimation

The reactivity ratios r_1 and r_2 have to be estimated as the first step in the modelling of any copolymerization system. Traditional methods employed for this purpose have used the instantaneous copolymer composition equation. However, there are experimental and statistical errors associated with this scheme (77). The experimental sources of error can be removed by using the integrated form of the composition equation or the Meyer-Lowry equation.

The choice of a statistical parameter estimator is governed by the consideration of errors associated with the measurement of each of the variables of the Meyer-Lowry equation. The most desirable of these, would be one, which considers errors in the measurement of all the variables as opposed to a non-linear least squares scheme which assumes the independent variable to be free of

error. It is evident that none of the variables of the Meyer-Lowry equation can be called independent.

Patino-Leal et al (100) have applied the error-in-variable (EVM) estimation scheme to this problem wherein the model is linearized at each stage about the best estimates of the true values of the responses (variables) and the maximum a posteriori estimates of r_1 and r_2 are obtained subject to this linearization. Sutton and MacGregor (101) have suggested an approximate version of the EVM which is equivalent to an error propagation weighted least squares technique (102). This approach has been used to estimate the r_1 and r_2 for both styrene/PMS and MMA/PMS (4) copolymerization systems.

Under the assumption of model adequacy, independent experiments and normality of residuals, maximization of the likelihood function $L(\theta/Y)$ is equivalent to

$$\min_{\theta} \sum \epsilon_i^2 / \sigma_i^2 \quad (1)$$

where θ are the unknown parameters, Y represents the

vector of observations, ϵ_i are the residuals and $\sigma^2 \epsilon_i$ the corresponding variances.

$$\text{where } \epsilon_i = C_W - \tilde{C}_W \quad (2)$$

C_W being given by equation (75) and \tilde{C}_W the experimental observation of the same.

$$\begin{aligned} \sigma^2 \epsilon_i = & \left(\frac{\partial \epsilon_i}{\partial C_W} \right)^2 \sigma^2 C_W + \left(\frac{\partial \epsilon_i}{\partial f_{10}} \right)^2 \sigma^2 f_{10} + \left(\frac{\partial \epsilon_i}{\partial f_1} \cdot \frac{\partial f_1}{\partial R_S} \right)^2 \sigma^2 R_S \\ & + \left(\frac{\partial \epsilon_i}{\partial f_1} \cdot \frac{\partial f_1}{\partial R_p} \right)^2 \sigma^2 R_p \end{aligned} \quad (3)$$

$$\text{where } \frac{\partial \epsilon_i}{\partial C_W} = 1 \quad (4)$$

$$\frac{\partial \epsilon_i}{\partial f_{10}} = \left(\frac{M_r}{M_o} \right) \cdot \left(\frac{N}{N_o} \right) \cdot \left(-\frac{\alpha}{f_{10}} + \frac{\beta}{f_{20}} + \frac{\gamma}{f_{10-\delta}} - \frac{M_{m_1} - M_{m_2}}{M_o} \right) \quad (5)$$

$$\frac{\partial \epsilon_i}{\partial f_1} = \left(\frac{M_r}{M_o} \right) \cdot \left(\frac{N}{N_o} \right) \cdot \left(-\frac{\alpha}{f_1} + \frac{\beta}{f_2} + \frac{\gamma}{f_1 - \delta} - \frac{M_{m_1} - M_{m_2}}{M_r} \right) \quad (6)$$

$$\frac{\partial f_1}{\partial R_S} = K_1 K_2 R_p / (M_{m_1} M_{m_2}) \cdot \left[\frac{K_1 R_S}{M_{m_1}} + \frac{K_2 R_p}{M_{m_2}} \right]^2 \quad (7)$$

$$\frac{\partial f_1}{\partial R_p} = K_1 K_2 R_S / (M_{m_1} M_{m_2}) \cdot \left[\frac{K_1 R_S}{M_{m_1}} + \frac{K_2 R_p}{M_{m_2}} \right]^2 \quad (8)$$

R_S and R_p are the measured ratios of the areas of the monomer to the area of the internal standard for styrene and PMS, respectively, obtained from the GC. K_1 and K_2 are the GC calibration constants for styrene and PMS, respectively. The data listed in Table 7 - 1 was used in the non-linear estimation routine leading to the following converged

estimates for r_1 and r_2

$$r_1 = .971 \pm .007$$

$$r_2 = .907 \pm .0135$$

correlation coefficient = 0.35

Figure 48 shows the joint confidence region (95%) for r_1 and r_2 .

Table 7-1

f_{10}	f_1	$C_w(\text{grav.})$	RS	RP
0.19	0.18	0.205	0.95	4.70
0.27	0.26	0.32	1.44	4.44
0.18	0.17	0.47	1.05	5.51
0.21	0.21	0.845	0.41	1.74
0.25	0.22	0.91	0.30	1.20
0.24	0.24	0.06	0.98	3.36
0.45	0.43	0.10	2.75	3.42
0.66	0.67	0.23	2.05	1.04
0.77	0.77	0.25	4.75	1.53
0.78	0.74	0.88	1.06	0.41
0.81	0.81	0.32	6.09	1.62

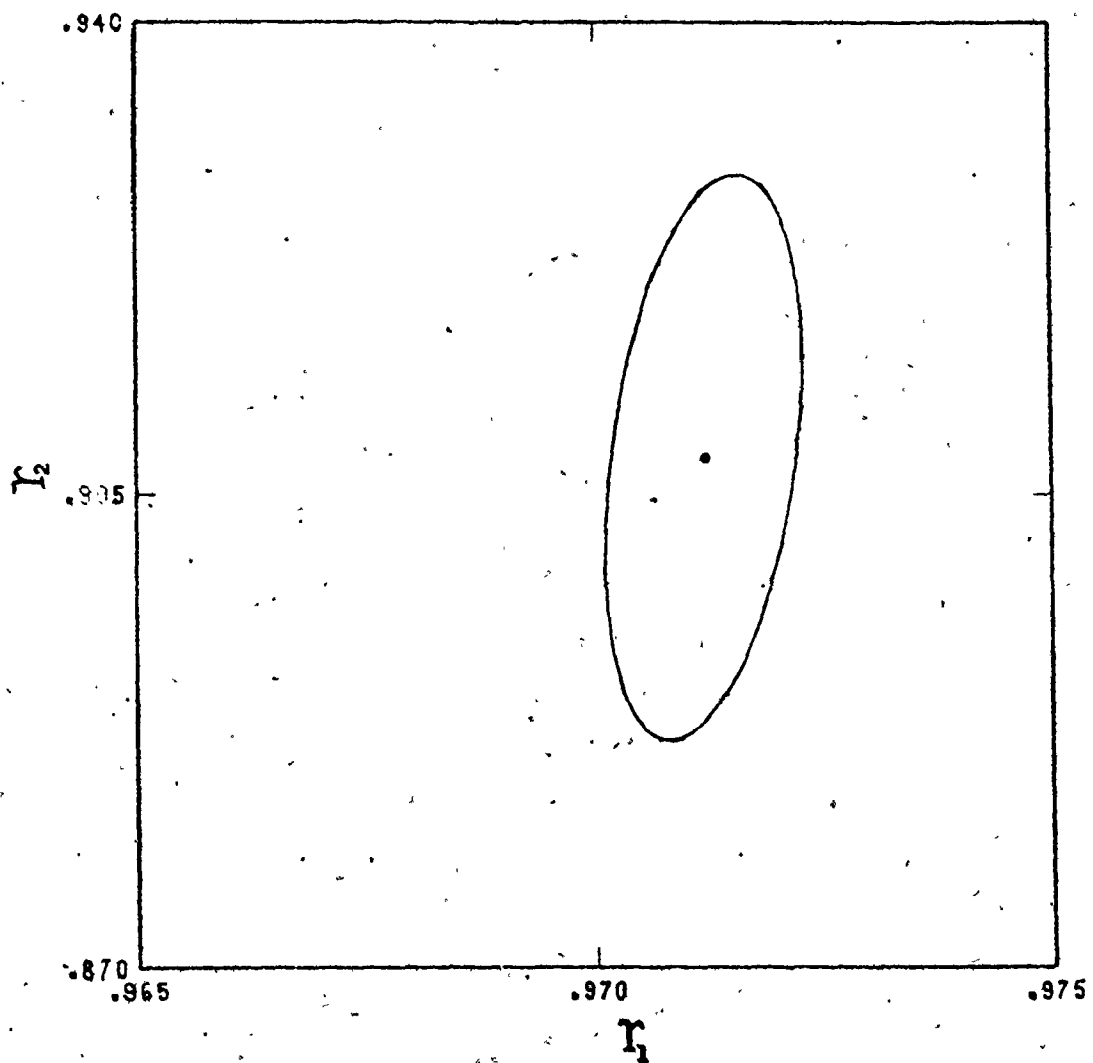


Fig.48: 95% Joint Confidence Region for r_1 , r_2 (styrene/PMS)

2. Modelling the Homopolymerization of Vinyl Acetate

2.1 Introduction

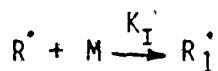
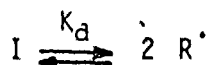
The bulk polymerization of VAC provides an interesting example of the effect of diffusion-controlled termination reactions on its rate behavior and molecular weight development. The latter has to include the effect of branching reactions via 1) transfer to polymer and 2) terminal double bond polymerization reactions.

For the present study the kinetic model of Hyun et al (99) was modified to include diffusion-controlled termination. Batch kinetics (x -time, \bar{M}_W and \bar{B}_N versus x) have been simulated upto complete conversion and compared with experimental data (103).

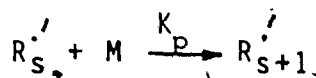
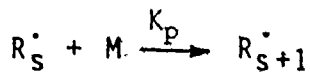
2.2 Model development

The following kinetic scheme has been used to model the bulk homopolymerization of VAC after Hyun et al (99)

INITIATION

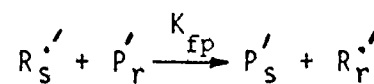
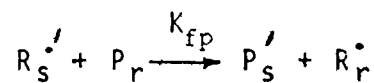
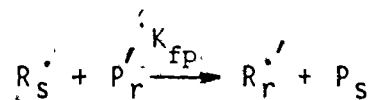


PROPAGATION

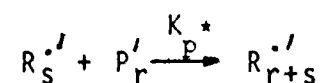
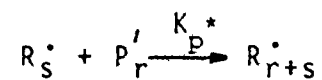


CHAIN TRANSFER

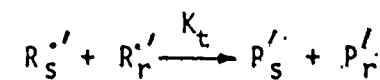
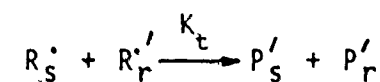
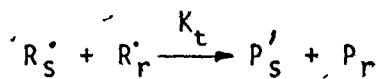




TERMINAL DOUBLE BOND POLYMERIZATION



TERMINATION (diffusion-controlled)



Termination by combination is assumed negligible (99).

In the above reaction scheme R_s^\bullet represents a polymer radical of chain length s without a double bond and $R_s^{\bullet'}$ is a radical with a double bond. P_r represents a polymer molecule of chain length r without a double bond and P_r' is a polymer molecule with a double bond.

2.2.1 Rate of monomer consumption

$$R_p = -(1/v) d(N_m)/dt = ([M]_0/(1-\epsilon x)) \cdot dx/dt = k_p [M][R] \quad (9)$$

$$[R] = (R_I/k_t)^{.5} \quad (\text{application of SSH}) \quad (10)$$

$$\text{where } R_I = 2 f k_d [I]_0 \exp(-k_d t)/(1-\epsilon x) \quad (11)$$

$$\text{and } v = v_0(1-\epsilon x)$$

From equations (9), (10) and (11) one has

$$dx/dt = \phi_x ((1-x)/(1-\epsilon x)^{.5}) \exp(-k_d t/2) \quad (12)$$

$$\text{where } \phi_x = (2k_p^2 f k_d [I]_0 / k_t)^{.5}$$

ϕ_x can be considered a measure of diffusion-

controlled termination, since both k_p and k_d are assumed to be independent of conversion at the temperatures used to model VAC polymerization.

2.2.2 Molecular weight development

The method of moments has to be used to compute \bar{M}_N , \bar{M}_W and \bar{B}_N . Writing differential balance equations for polymer radicals and polymer molecules and then summing the individual equations with respect to r to obtain the leading moments, one has

$$\frac{d(Q_n)}{dt} = \left(\frac{f}{1-x}\right)Q_n \frac{dx}{dt} + (k_{fm}[M] + k_{fp}[P] + k_t Y_t) Y_n - k_{fp} Y_t Q_{n+1} \quad (13)$$

$$\frac{d(Q'_n)}{dt} = \left(\frac{f}{1-x}\right)Q'_n \frac{dx}{dt} + (k_{fm}[M] + k_{fp}[P] + k_t Y_t) Y'_n - k_{fp} Y_t Q'_{n+1} - k_p^* Y_t Q'_n \quad (14)$$

Application of the SSH to live radical population gives for the moments of the polymer radical

molecular weight distribution

$$Y'_n(K_{fm}[M] + K_{fp}[P] + K_t Y_t + K_p^* Q_0) = nK_p[M]Y'_{n-1} + K_{fm}[M]Y'_t + K_p^* \sum_r \sum_s (r+s)^n [P'_r][R'_s] + K_{fp} Y_t Q'_{n+1} \quad (15)$$

$$Y_n(K_{fm}[M] + K_{fp}[P] + K_t Y_t + K_p^* Q_0) = nK_p[M]Y_{n-1} + K_{fp} Y_t Q_{n+1} + K_p^* \sum_r \sum_s (r+s)^n [P'_r][R'_s] + 2fK_d[I] \quad (16)$$

where [P] = conc. of polymer

$$Q_i = \sum_r r^i [P_r]$$

$$Q'_i = \sum_r r^i [P'_r]$$

$$Y_i = \sum_s s^i [R'_s]$$

$$Y'_i = \sum_s s^i [R'_s]$$

$$Y_t = \sum_s [R'_s] + [R'_s]$$

Dividing equations (13) and (14) by equation (12) to write these in a more convenient form with x as the independent variable and then substituting for Y_n and Y'_n , one has

$$d(Q_0)/dx = T/(1-x) + BQ_0 \quad (17)$$

$$d(Q'_0)/dx = C_M([M]/(1-x)) - KQ'_0/(1-x) + BQ'_0 \quad (18)$$

$$d(Q_1)/dx = ([M]/(1-x))((1+KQ'_1/[M])(C_p Q_1 + T)/A) + T/(1-x) + BQ_1 \quad (19)$$

$$d(Q_1')/dx = ([M]/(1-x))((C_p Q_1' + C_M[M] - K Q_1'(C_p Q_1' + T)/[M])/A + C_M) + B Q_1' \quad (20)$$

$$d(Q_2^T)/dx = ([M]/(1-x))(2(1 + K Q_1'/[M])([M] + K Q_1' + C_p Q_2^T + C_M[M] + T)/A + C_M + T/[M]) + B Q_2^T \quad (21)$$

$$d(Q_0^T B_N)/dx = K Q_0/(1-x) + C_p x/(1-x) + B(Q_0^T B_N) \quad (22)$$

where $A = C_M[M] + C_p[P] + T$

$B = \epsilon/(1-x)$

and $T = K_t Y_t/K_p$

2.3 Results and Discussion

2.3.1 Parameter estimation

The data used to estimate kinetic parameters for modelling the bulk polymerization of VAC were obtained from reference (103). The empirical approach

to model diffusion-controlled termination was used as free-volume theory cannot be applied to predict the diffusivity of branched molecules. ϕ_x was expressed as follows

$$\phi_x = \phi_0 \exp(-(A_1 x + A_2 x^2 + A_3 x^3))$$

giving $K_t = K_{t0} \exp(2(A_1 x + A_2 x^2 + A_3 x^3))$.

The initial slope of the x-time curves provided with the values for $K_p/K_t^{.5}$ at -50, 60, 70 and 80 °C. Equation (12) was integrated within a Gauss-Marquadt optimization procedure to estimate the diffusion-control parameters. C_M was estimated from the initial \bar{M}_W data as has been shown earlier in the modelling of MMA/PMS copolymerization. Equations (17-21) were then solved simultaneously and the model predictions were fitted to the experimental data for \bar{M}_W to best estimate K and C_p . A constant value for K was found for all the conditions. The kinetic model parameters used in this work are as follows

$$d_{VAC} = 930 \text{ gms/lit} \quad \text{reference (104)}$$

$$d_{PVAC} = 1150 \text{ gms/lit} \quad \text{reference (104)}$$

$$M_{VAC} = 86 \text{ gms/mole}$$

$$A_1 = 30.594 - .0954 T \text{ (K)}$$

$$A_2 = -53.246 + .155 T$$

$$A_3 = 11.393 - .0358 T$$

$$f = 0.5$$

$$K_d = 1.1754E16 \cdot \exp(-29500/(RT)) \text{ min}^{-1}$$

$$K_p/K_t \cdot 5 = 545.2 \exp(-1765.6/T) \text{ (non-linear least squares estimate)}$$

T(C)	C _M	C _p	K
60	.0002	.00014	.48
70	.00027	.00016	.48
80	.0003	.00018	.48

2.3.2 Comparison of model predictions with experimental data

Figures 49 and 50 compare the model predictions with the experimental x-time data at 50, 60, 70 and 80 °C. Agreement of the bulk rate data is observed to be satisfactory except at very high conversions for 60 °C, where the model underestimates the data. Figures 51-54 compare model predictions with the experimental \bar{M}_w data. The model provides satisfactory predictions for the high initiator levels at 60 °C but seriously underestimates the \bar{M}_w at the lowest initiator level. A similar trend is observed at 70 °C. The explanation is obvious in that the predictions are best where the initiator levels correspond to those used to extract the diffusion-control parameters from the x-time histories. This is borne out by the excellent agreement between the data and model predictions at 80 °C in Figure 52. When the initiator concentration is high, termination reactions play an important role in the molecular weight development and therefore the model would prove inadequate when applied to situations where the initiator level is significantly lower than

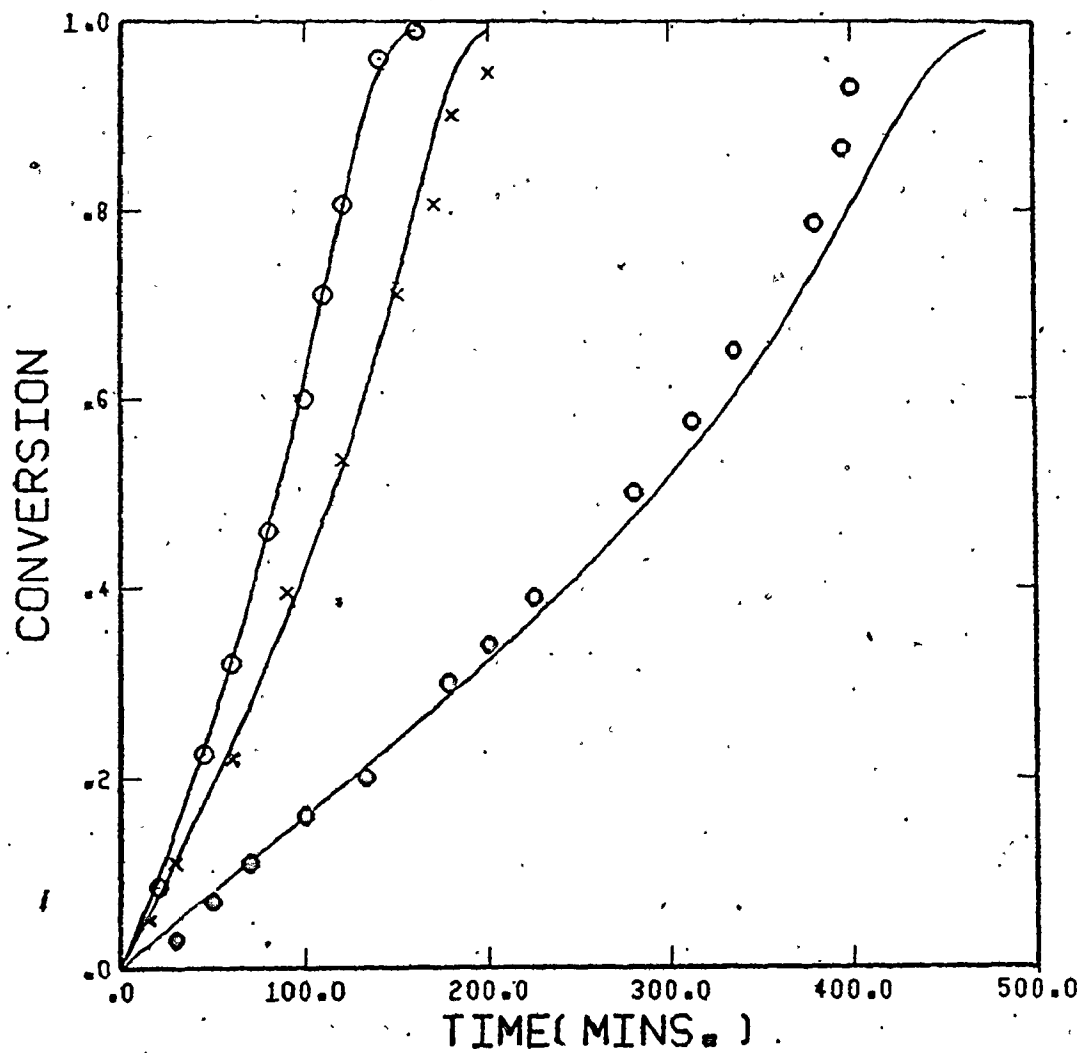


Fig.49: Measured (●:50°C, $[I]_0 = .004$, x:60°C, $[I]_0 = .004$; ○:70°C, $[I]_0 = .001$ mol/l) and predicted conversion vs: time.

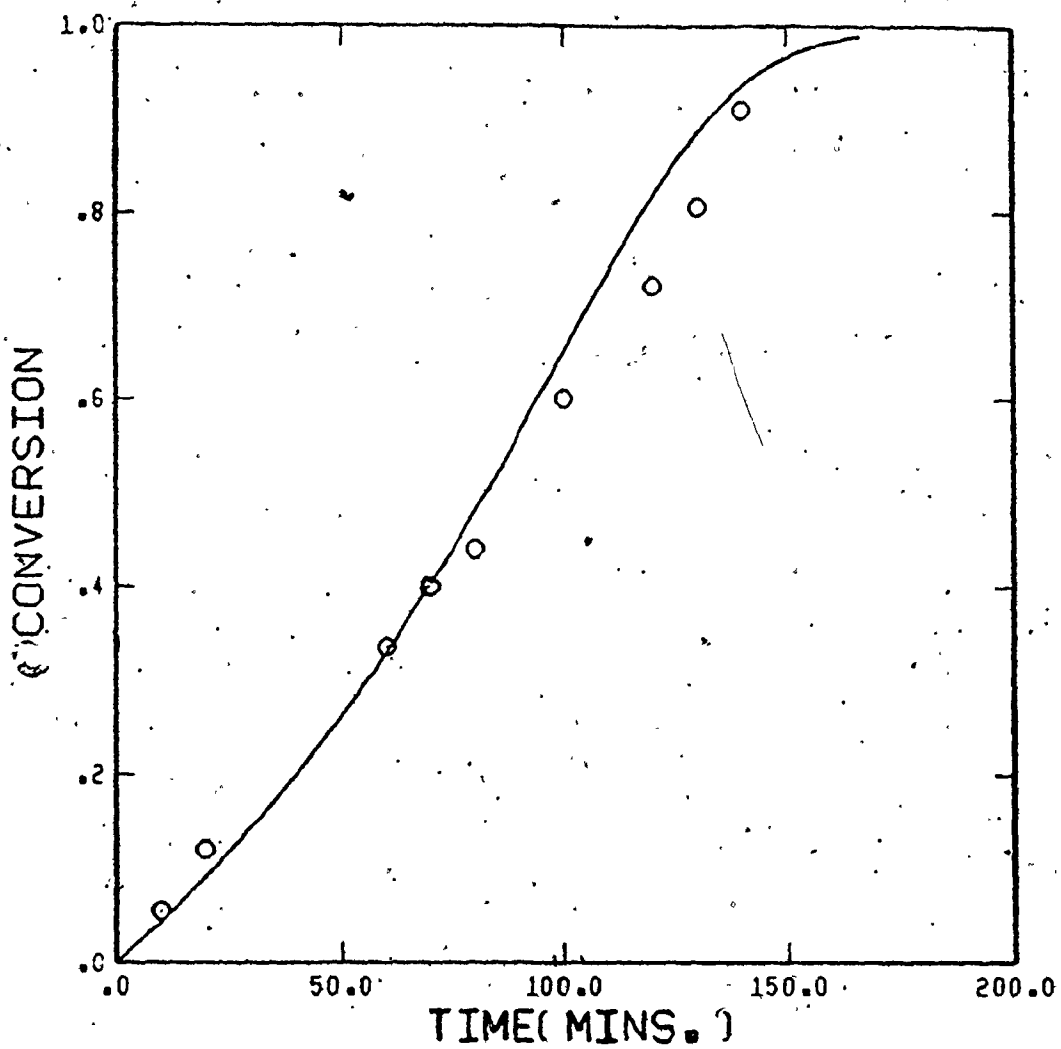


Fig. 50: Measured (O:80°C, $[I]_0 = .0002 \text{ mol/l}$) and predicted conversion vs. time.

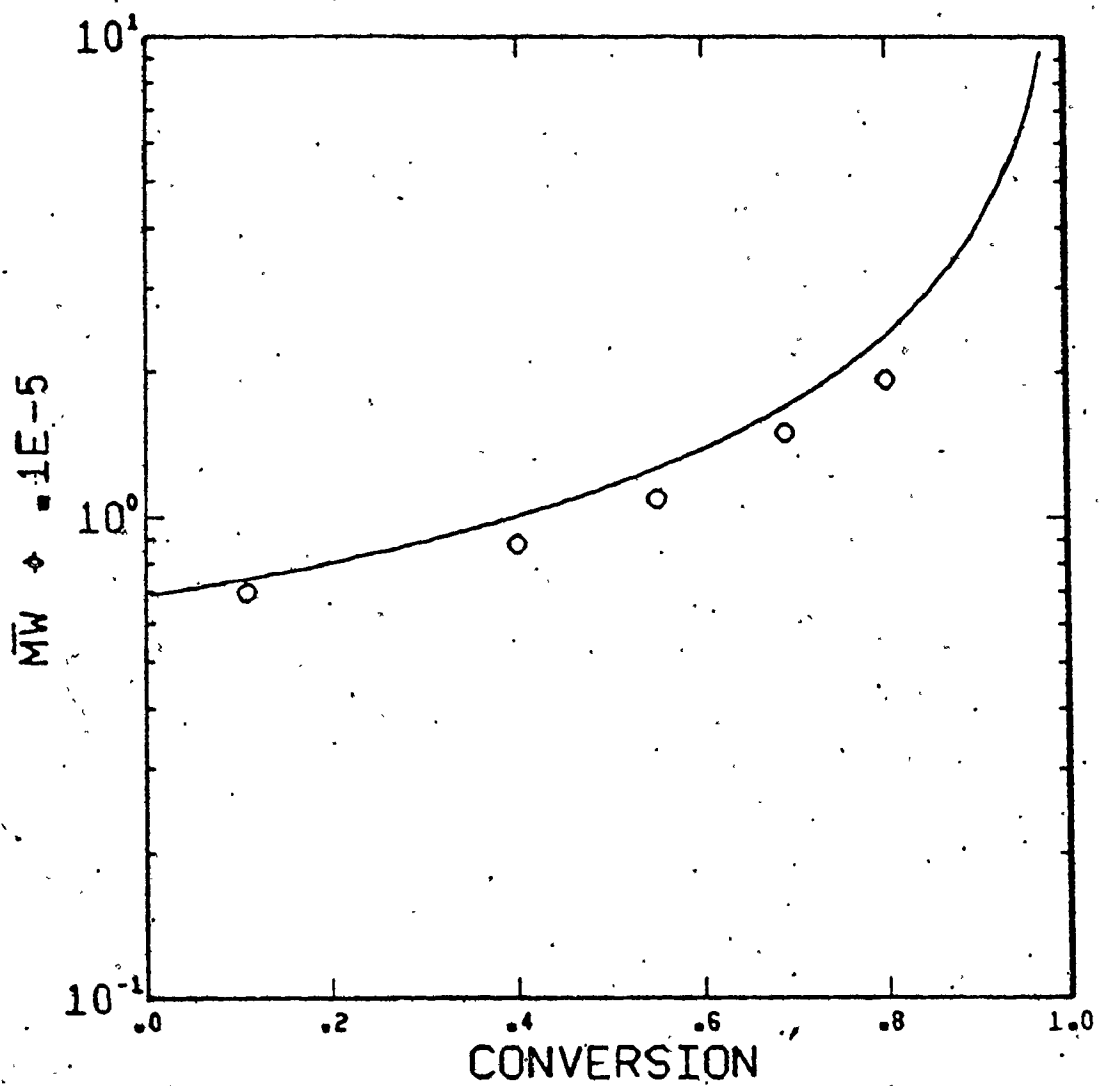


Fig. 51: Measured (O:60°C, $[I]_0 = .004 \text{ mol/l}$) and predicted \bar{M}_w vs. conversion.

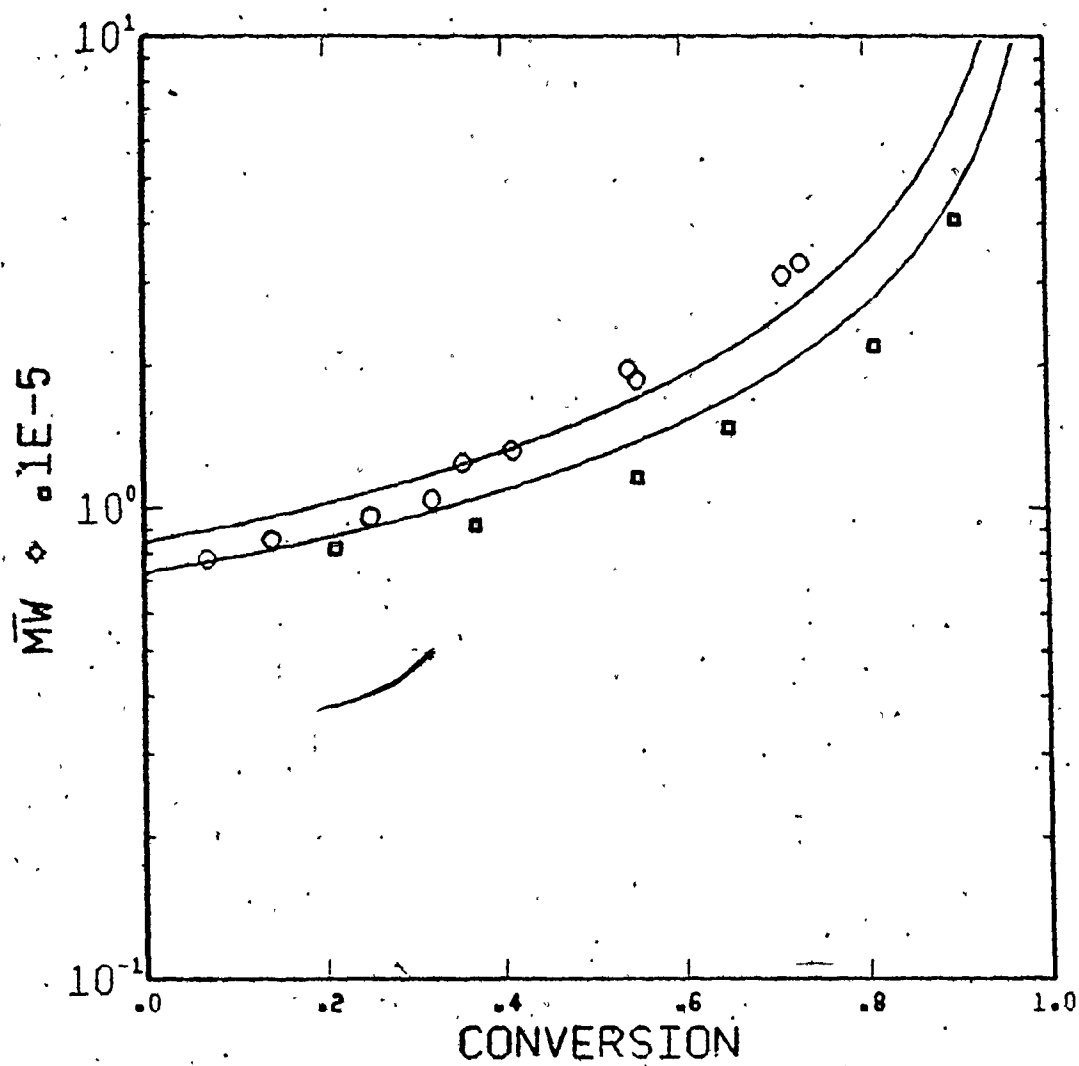


Fig.52: Measured (O: .002, □: .0002 mol/l. and predicted \bar{M}_w vs. conversion, $T = 60^\circ\text{C}$)

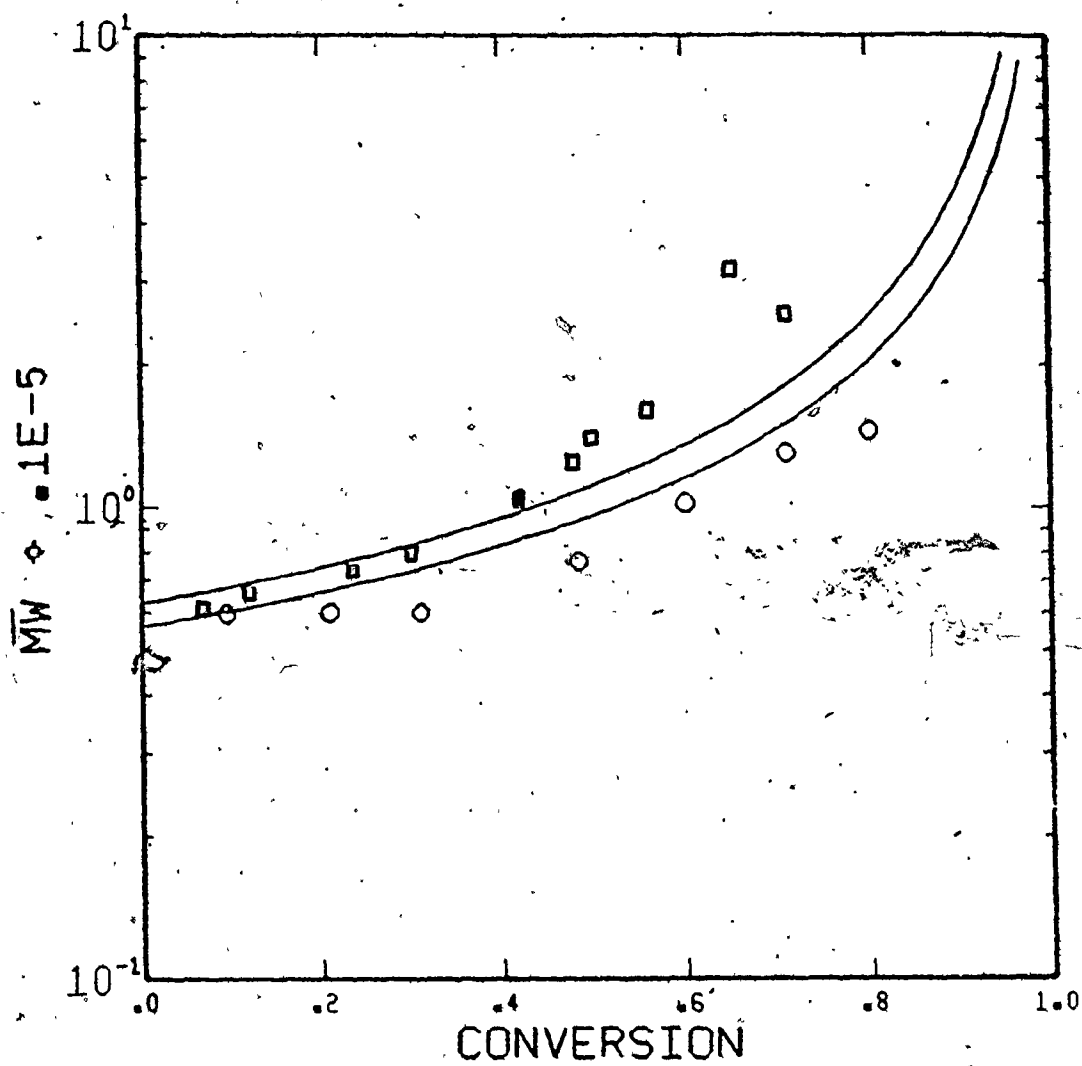


Fig.53: Measured (O: .001, ■: .00002 mol/l) and predicted \overline{M}_w vs. conversion, $T = 70^\circ\text{C}$.

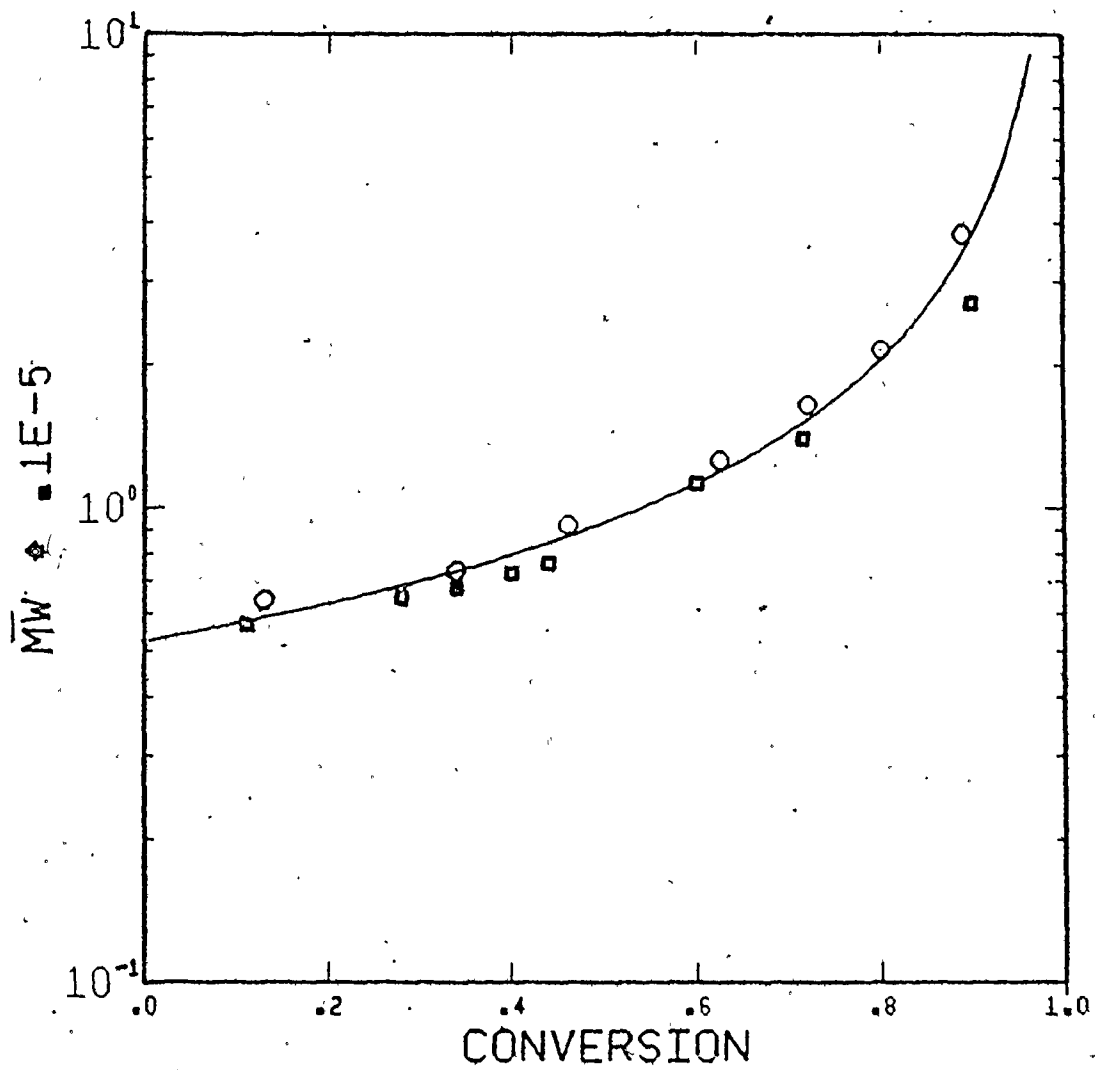


Fig. 54: Measured (O: .0001, \blacksquare : .0002 mol/l) and predicted \bar{M}_w vs. conversion, $T = -80^\circ\text{C}$.

those used to estimate the diffusion-control parameters. This shows the inadequacy of the empirical model for K_t as the polymer molecular weight is not a primary variable of the model. The molecular weights are strongly influenced by the initiator levels and temperature and in turn influence the K_t . The presence of high levels of branching makes the interpretation of diffusion-controlled K_t more difficult as it decreases the effective size of the polymer radical. Figure 55 shows the predicted \bar{B}_N as a function of x for three temperature levels with a constant $[I]$. Figure 56 shows the calculated values of r plotted as a function of $(1/T)$ along with the predicted Arrhenius plot using parameters obtained via a non-linear least squares fitting routine.

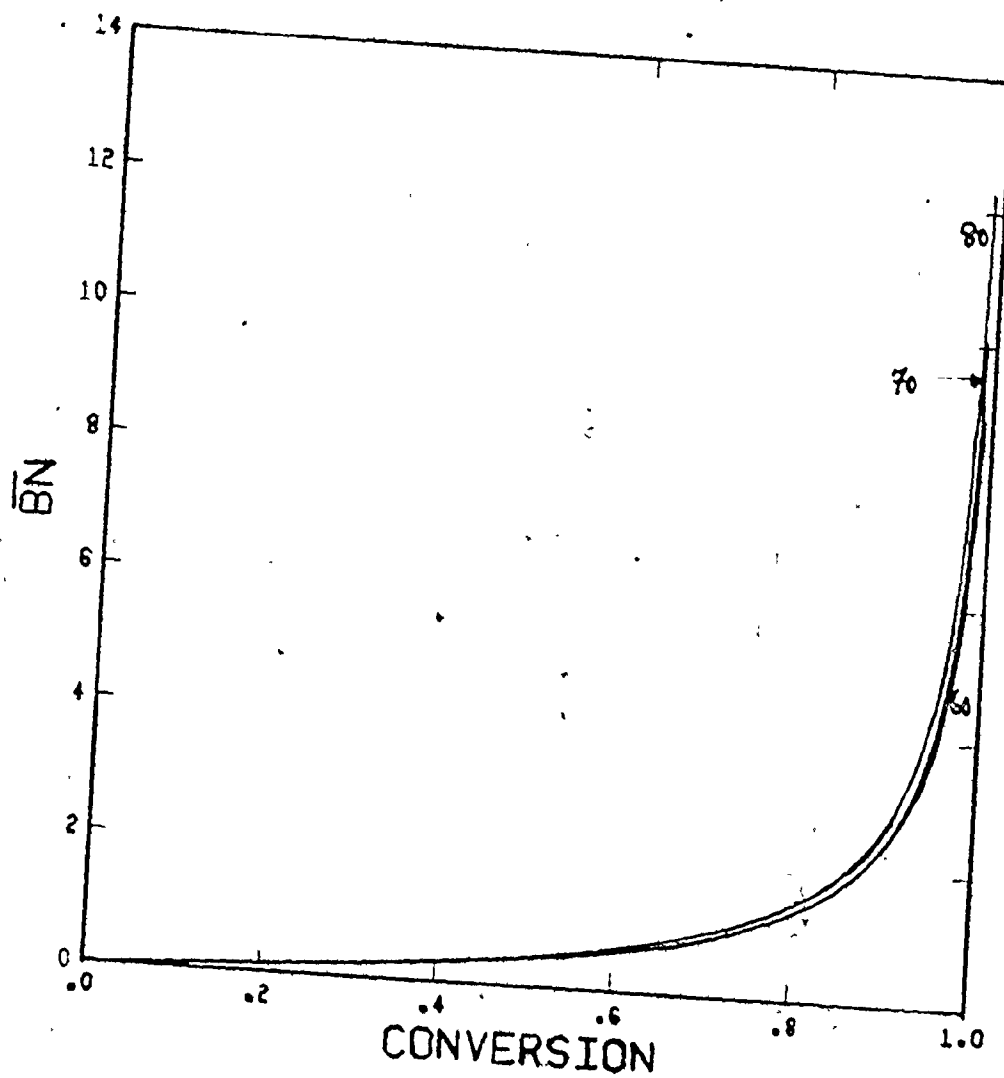


Fig. 55: Predicted \bar{P}_N vs. conversion; $T = 60, 70, 80^\circ\text{C}$, $[I]_0 = .004 \text{ mol/l}$.

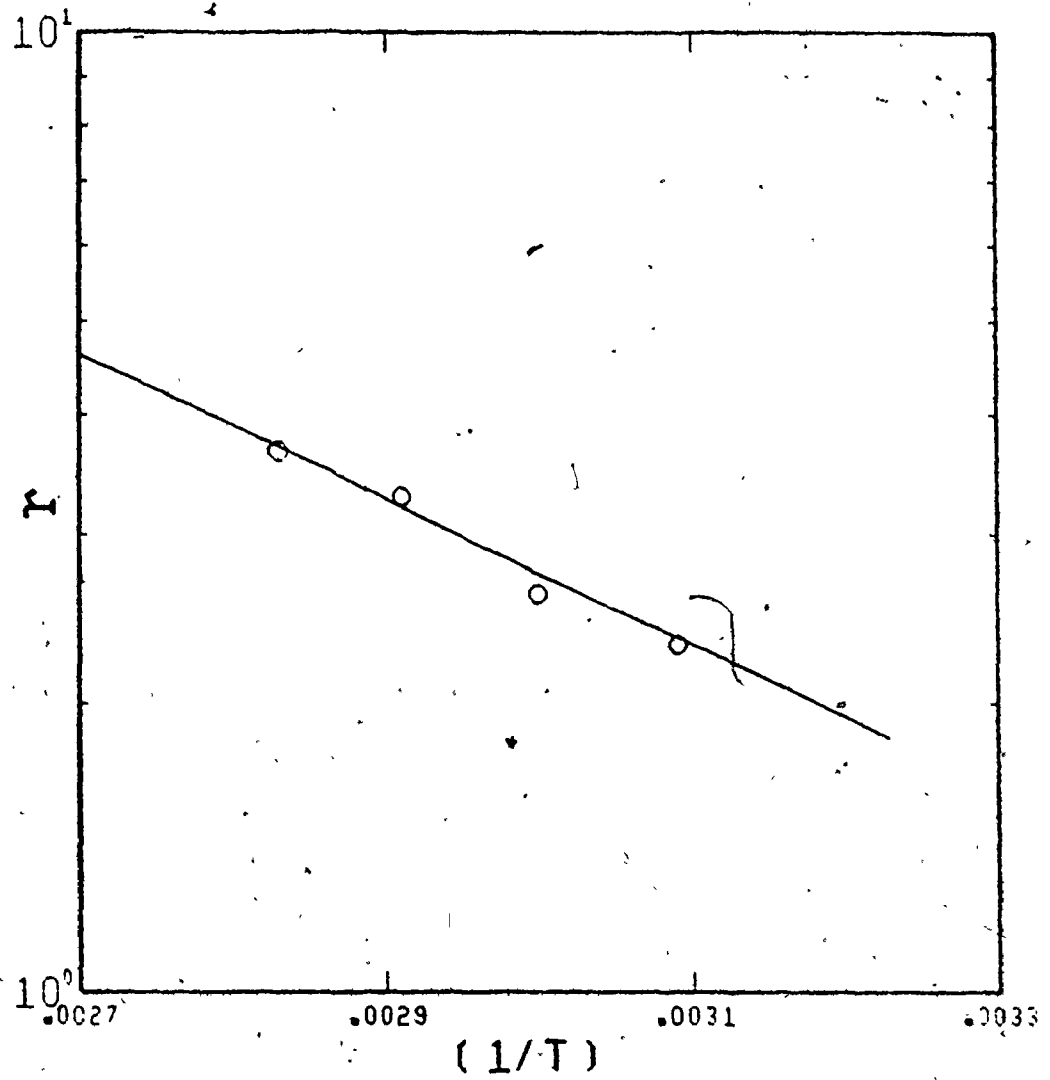


Fig.56: Arrhenius temperature dependence of $r(k_p/k_t^5)$ for vinyl acetate polymerization.

3. Semi-Batch Copolymerization of Vinyl Chloride/Vinyl Acetate : Investigation of Some Feed Policies to Control Copolymer Composition

3.1 Introduction

Controlling copolymer composition is one of the most important features of copolymer synthesis. Depending on the the individual rates of consumption of the monomers, there might arise significant drift in the overall composition of the resultant copolymer, in a batch process. Semi-batch monitoring of the monomer feed rates intuitively suggests a good control scheme.

There are many semi-batch feed policies that can be used to maintain constant copolymer composition. The optimal choice would be one which not only controls the composition but also satisfies the requirements for long chain branching and cross-linking and maximizes the rate of production of the copolymer without causing major heat removal problems.

3.2 Policy 1

This policy involves adding all of the slower monomer and some of the faster monomer at time zero to provide the desired monomer ratio and therefore, the desired copolymer composition. The faster monomer is then fed in over time at a feed rate that maintains N_1/N_2 constant. In this illustration all of the VAC (slower) and part of the vinyl chloride is added at the beginning. Within this policy various initiation rate controls are possible leading to different rates of production of the copolymer.

$$d(N_1/N_2)/dt = 0 \quad (23)$$

where N_i = number of moles of monomer i $i=1,2$

let $N_1/N_2 = c$ (constraint equation)

$$\text{or } dN_1/dt = c dN_2/dt \quad (24)$$

$$\text{and } N_{10}/N_{20} = c \text{ at } t=0 \quad (25)$$

$$\text{Now } dN_1/dt = F_1 - R_{p1} v \quad (26)$$

$$\text{and } dN_2/dt = -R_{p2} v \quad (27)$$

where F_i is the feed rate of monomer i (mols/time)

$$\text{where } R_{p1} = N_1 (K_{11}[R_1] + K_{21}[R_2])/v \quad (28)$$

$$\text{and } R_{p2} = N_2 (K_{22}[R_2] + K_{12}[R_1])/v \quad (29)$$

For long copolymer chains one has

$$K_{12} N_2 [R_1] = K_{21} N_1 [R_2] \quad (30)$$

$$[R_1] + [R_2] = [R] \quad (31)$$

From equations (26-29) one has

$$dN_1/dt = F_1 - (K_{21}K_{12} + cK_{11}K_{21})[R]N_1/D = F_1 - k_1 N_1 [R] \quad (32)$$

$$dN_2/dt = -(K_{12}K_{22} + cK_{12}K_{21})[R]N_2/D = -k_2 N_2 [R] \quad (33)$$

$$\text{where } D = K_{12} + c K_{21}$$

From equations (24) and (32) one has

$$F_1 = [R] N_1 (cK_{11}K_{21} - (c-1)K_{12}K_{21} - K_{12}K_{22})/D = K_1 [R] N_1 \quad (34)$$

Substituting for F_1 in equation (32) one has

$$dN_1/dt = -(K_{12}K_{22} + cK_{12}K_{21})[R]N_1/D = -k_2 N_1 [R] \quad (35)$$

$$\text{where } [R] = (\dot{R}_I/K_t)^{.5}$$

Neglecting volume change of the reaction mixture due to changing density of the monomer-polymer mixture,

one may write

$$F_1 = \rho_{M1} dv/dt \quad (36)$$

where ρ_{M_i} is the number of moles of monomer i /volume.

The heat generation rate \dot{Q} is given by

$$\dot{Q} = R_{p1}(-\Delta H_1)v + R_{p2}(-\Delta H_2)v \quad (37)$$

where $(-\Delta H_i)$ is the heat of polymerization of monomer i .

Case A Maintaining constant $[R^*]$

This requires changing the radical initiation rate (R_I) in a manner such that (R_I/K_t) remains constant. Equation (35) may be solved analytically to give

$$N_1 = -N_{10} \exp(-k_2[R^*]t)$$

$$\text{and } N_2 = N_{20} \exp(-k_2[R^*]t)$$

Evidently in this case the feed rate F_i would decrease exponentially with time (equation (34)). However, this case is only of academic interest since in practice K_t begins to fall sharply with increasing polymer concentration, due to diffusion-controlled termination, necessitating the removal of initiator to maintain a constant $[R^*]$.

Case B Adding all the initiator at time zero.

R_I is given by

$$R_I = 2 f K_d N_{i0} \exp(-K_d t) / v \quad (38)$$

$$v(t) = (1/\rho_{M1}) \int_0^t F_1 dt + v(0)$$

Using equation (36) and some algebra, one has

$$F_1 = (1 - k_1/k_2) dN_1/dt \quad (39)$$

$$\text{or } v(t) = v(0) + (1/\rho_{M1})(k_1/k_2 - 1)(N_{10} - N_1) \quad (40)$$

And the diffusion-controlled K_t can be empirically expressed as

$$K_t = K_{t0} \exp(A_1 W + A_2 W^2 + A_3 W^3) \quad (41)$$

where W = wt. fraction of the copolymer

$$= WN / WM \quad (43)$$

$$WN = M_{m1}(N_{10} + F_1 dt - N_1) + M_{m2}(N_{20} - N_2)$$

$$WM = M_{m1}(N_{10} + F_1 dt) + M_{m2}N_{20}$$

Using equations (38), (40-42), one can compute $[R]$ as a function of t , solving equations (35), (39) simultaneously for N_1 and F_1 .

Table 7-2 Semi-batch copolymerization of vinyl chloride/VAC producing a copolymer with $F_1 = 0.79$. $[I]_0 = 0.01$ mol/lit.

t (min)	$[M_1]$ (mol/lit)	N_1 (mol)	F_1 (mol/min)	\dot{Q} (Kcal/min)	$\bar{r}_N(10^{-4})$	$\bar{r}_W(10^{-4})$	\bar{B}_N	wt.cop. (Kg.)
0	8.2	46.4	1.57	18.4	0.112	0.23	0.	0.
2	7.3	43.0	1.78	19.3	0.115	0.23	0.02	0.72
4	6.3	39.0	2.0	20.8	0.117	0.25	0.05	1.34
6	5.3	35.0	2.3	22.8	0.12	0.26	0.1	2.08
8	4.3	29.4	2.6	24.7	0.125	0.29	0.16	2.94
10	3.3	23.7	2.9	25.6	0.135	0.35	0.29	3.90
15	1.17	9.62	2.2	16.9	0.37	2.84	2.9	6.25
16	0.9	7.55	1.8	14.0	0.642	7.89	6.0	6.60
17	0.69	5.84	1.5	11.2	1.28	29.3	13.6	6.88
18	0.52	4.46	1.2	8.8	2.65	154.0	30.0	7.11
19	0.39	3.37	0.92	6.8	4.84	1018.	58.	7.30
20	0.29	2.52	0.71	5.2	7.13	4650.	89.	7.44

3.3 Policy 2

Here both monomers are fed in over time to maintain constant $[M_1]$ and $[M_2]$ and hence copolymer composition in the reactor.

$$d[M_1]/dt = d[M_2]/dt = 0 \quad (43)$$

$$dN_1/dt = F_1 - k_1 N_1 [R] = F_1 - c_1 N_1 \quad (44)$$

$$dN_2/dt = F_2 - k_2 N_2 [R] = F_2 - c_2 N_2 \quad (45)$$

$$\text{where } c_i = k_i [R] \quad i=1,2$$

Equation (43) implies that $N_1/N_2 = \text{constant} = c$

$$dv/dt = F_1/\rho_{M1} + F_2/\rho_{M2} \quad (46)$$

$$\text{Again } dN_i/dt = [M_i] dv/dt \quad i=1,2 \quad (47)$$

$$\text{or } [M_1](F_1/\rho_{M1} + F_2/\rho_{M2}) = F_1 - c_1 N_1 \quad (48)$$

Maintaining a constant $[M_1]$ and $[M_2]$ implies a constant W . Therefore K_t is constant from equation (41). One desirable initiation rate control would be to maintain a constant R_p . This implies a constant (\dot{Q}/v) . With a cylindrical reactor, the surface area of the reactor wall in contact with the reacting mixture is proportional to its volume, hence in the absence of fouling, the heat removal system should be able to accommodate a constant (\dot{Q}/v) .

A constant (\dot{Q}/v) requires a constant $[R]$ from equation (37). Thus c_1 and c_2 are constant.

$$F_1 - c_1 N_1 = c(F_2 - c_2 N_2) \quad (49)$$

From equations (48) and (49), one has

$$F_2 = N_2 \rho_{M2} ([M_1]c_1 - [M_1]c_2 + c_2 \rho_{M1}) / (\rho_{M1} \rho_{M2} - [M_1] \rho_{M2} - \rho_{M1} [M_2]) \quad (50)$$

$$\text{and } dN_2/dt = N_2 (c_2 [M_1] \rho_{M1} / (c + \rho_{M2} [M_1] c_1)) / (\rho_{M1} \rho_{M2} - [M_1] \rho_{M2} - [M_2] \rho_{M1}) \quad (51)$$

Equations (50) and (51) can be solved to obtain $N_2(t)$ and $F_2(t)$. F_1 is then obtained from equation (49).

Since $[R]$ is a constant, R_I is also a constant

$$\text{ie } N_I/v(t) = N_{I0}/v(0)$$

$$\text{or } N_I = [I]_0 v(t) \quad (52)$$

Thus initiator has to be fed in at the rate that provides for a free initiator level given by equation (52).

From equations (48) and (49), one has

$$F_2 = N_2 \rho_{M_2} ([M_1] c_1 - [M_1] c_2 + c_2 \rho_{M_1}) / (\rho_{M_1} \rho_{M_2} - [M_1] \rho_{M_2} - \rho_{M_1} [M_2]) \quad (50)$$

$$\text{and } dN_2/dt = N_2 (c_2 [M_1] \rho_{M_1} / c + \rho_{M_2} [M_1] c_1) / (\rho_{M_1} \rho_{M_2} - [M_1] \rho_{M_2} - [M_2] \rho_{M_1}) \quad (51)$$

Equations (50) and (51) can be solved to obtain $N_2(t)$ and $F_2(t)$. F_1 is then obtained from equation (49).

Since $[R]$ is a constant, R_I is also a constant

$$\text{ie } N_I/v(t) = N_{I0}/v(0)$$

$$\text{or } N_I = [I]_0 v(t) \quad (52)$$

Thus initiator has to be fed in at the rate that provides for a free initiator level given by equation (52).

Table 7.3 Semi-batch copolymerization of vinyl chloride/VAC using policy 2 and producing a copolymer with $F_1 = 0.8$ at a constant heat generation rate ($\dot{Q}/v = 19$ Kcal/lit,min), $[M_1] = 1.66$ mol/lit, $[M_2] = 0.79$ mol/lit. and $[R] = 5.45E-7$ mol/lit.

t(min)	$\bar{r}_N(10^{-4})$	$\bar{r}_W(10^{-4})$	\bar{B}_N	wt.cop. (Kg.)	F_1 (mol/min)	F_2 (mol/min)
0	0.18	0.75	0.89	0.064	0.07	0.02
2	0.30	2.0	2.0	0.075	0.08	0.02
4	0.43	3.8	3.6	0.086	0.09	0.03
6	0.556	7.2	5.5	0.1	0.11	0.03
8	0.68	13.3	7.2	0.115	0.12	0.03
10	0.8	24.6	8.8	0.134	0.14	0.04
15	1.01	123.6	12.4	0.195	0.21	0.06
20	1.20	696.0	16.0	0.282	0.30	0.08
25	1.38	4382.0	19.8	0.407	0.43	0.12

The following table shows the effect of total monomer concentration on heat generation rate when producing the same copolymer using policy 2

Table 7-4³ Effect of $([M_1] + [M_2])$ on (\dot{Q}/V) ,
with policy II with $[M_1]/[M_2] = 2$.

(\dot{Q}/v) kcal/(lit.min)	$([M_1] + [M_2])$ moles/lit.
0	0
11	1
19	2
24	3
27	4
27	5
27	6
25	7
23	8
20	9

The $[R^*]$ decreases with increasing $([M_1] + [M_2])$ due to diffusion controlled termination causing the maximum in (\dot{Q}/v) .

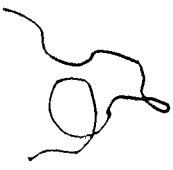
When the reactor heat removal system is being used at its full capacity, the monomer feed rate may be used to control the polymerization temperature provided the total monomer concentration is at a value less than its value at $(\dot{Q}/v)_{\max}$. Thus, operating points to the left of $(\dot{Q}/v)_{\max}$ are more productive as well as inherently stable.

3.4 Policy, 3

A variant of policy 2 and a common commercial practice is to maintain very low monomer concentrations, so that the copolymer composition produced is the same as the comonomer composition in the feed. This permits a constant pre-mixed feed rate of the monomers.

Table 7.5 Semi-batch copolymerization using policy 3 showing the instantaneous composition (F_1) and monomer concentration drift with $F_1 = 6$ mol/min, $F_2 = 2.5$ mol/min. Reactor is empty at time zero and $R_1 = 6.1E-6$ mole/lit,min

t(min)	F_1	$[M_1]$	$[M_2]$	wt.cop(Kg.)
1	0.82	8.61	3.65	0.017
2	0.82	8.30	3.58	0.069
3	0.81	7.98	3.50	0.156
4	0.81	7.65	3.43	0.281
5	0.81	7.32	3.35	0.445
6	0.81	6.97	3.26	0.649
7	0.81	6.62	3.18	0.896
8	0.80	6.26	3.08	1.189
9	0.79	5.89	2.98	1.530
10	0.79	5.50	2.87	1.925
15	0.76	3.43	2.22	4.765



The preceding calculations show that the use of this policy is accompanied by some copolymer composition drift. The total monomer concentration decreases and ultimately reaches a value where F_1 equals the monomer composition in the feed. Hereafter there is no drift in F_1 and monomer concentrations.

A comparison of policies 1 and 2 brings out the following additional points; policy 1 begins with high monomer concentrations in the reacting mixture as all the slower monomer is added at time zero. The volume of the mixture continuously increases with time, thereby the $[M_1]$ and $[M_2]$ decrease with time. This concentration behavior is similar to that in a batch reactor. Molecular weight, long chain branching and cross-linking development would also be similar with low levels of branching in the beginning and high levels developing only later. Policy 2 on the other hand has the major disadvantage of producing very high levels of branching and cross-linking especially when operating with very low monomer concentrations (to increase polymer production rates). On the other hand as can be seen from Table 7.3, the optimal feed rates F_1 and F_2 change rather modestly with time and F_1/F_2

also changes little with time suggesting that the monomers may be premixed and fed together. As discussed before, policy 2 can also be extended to policy 3 for easier operation if one can tolerate some composition drift.

3.5 Kinetic parameters used

As the preceding calculations merely serve to illustrate the effect of various feed policies on the polymer properties, no attempt was made to estimate parameters that were unavailable in the literature. The diffusion-control parameters were obtained from the bulk polymerization model for VAC at 60°C, and simplifying assumptions were made to calculate the pseudo rate constants for molecular weight development equations which have been derived in section 7.2 for VAC polymerization.

$$\begin{aligned}
 T &= 60^\circ\text{C} & d_{m1} &= 13.6 \text{ moles/lit} \\
 K_d &= .85\text{E-}6 \text{ sec}^{-1} & d_{m2} &= 10.81 \text{ moles/lit} \\
 f &= 0.6 & M_{m1} &= 62.5 \\
 K_{11} &= 1.23\text{E}4 \text{ lit/mole,sec} & M_{m2} &= 86
 \end{aligned}$$

$$K_{22} = 2.09E3 \text{ lit/mol,sec} \quad A_1 = -2.854$$

$$r_1 = 1.68 \quad A_2 = -4.5$$

$$r_2 = 0.23 \quad A_3 = 2.513$$

$$K_{f21} = K_{f11} = 12 \text{ lit/mol,sec}$$

$$K_{f12} = K_{f22} = .3724E-7 \exp(-9895/(RT)) \text{ lit/mol,sec}$$

$$K_{fp21} = K_{fp11} = .1E-3 K_{11}$$

$$K_{fp12} = K_{fp22} = .1E-3 K_{22}$$

$$K_{p1}^* = K_{p0}^* \exp(-(B_1 W + B_2 W^2 + B_3 W^3))$$

$$K_{p0}^* = .9096E-7 \exp(-5510/(RT))$$

$$B_1 = -6.878 + 0.019T$$

$$B_2 = 64.7 - 0.185T$$

$$B_3 = -149.1 + 0.43T$$

$$\Delta H_1 = -26 \text{ Kcal/mole}$$

$$\Delta H_2 = -21 \text{ Kcal/mole}$$

All kinetic constants and parameters have been taken from reference (104).

4. Experimental Techniques

4.1 Gas chromatography (GC)

Procedure

GC analysis was employed to obtain conversion on a weight basis and the residual monomer composition. After polymerization, the ampoule contents were dissolved in sufficient quantity of dioxane and an accurately measured amount of toluene (internal standard) was added to the solution. Toluene was chosen as the internal standard (I.S.) because; 1) it is structurally similar to the monomers of interest and therefore exhibits similar elution behavior 2) it shows adequate separation from the other peaks of interest viz., dioxane, styrene, PMS. 3) it provided with a linear calibration curve for both the monomers. 4) it is available readily in pure quality.

The calibration was done by injecting known mixtures of the monomers and toluene and plotting the ratio of the weights of each monomer to that

of the I.S. versus the ratio of the areas of the two. The slope of the linear part of the curve gives the calibration constants k_1 and k_2 for styrene and PMS respectively. The calibration constants were checked routinely during analysis of the polymer solution by injecting the calibration samples.

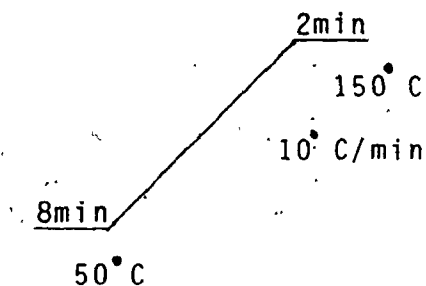
GC operating conditions

GC used : H.P. 5880 A

Column used : 10 ft. 0.125" O.D. Chromosorb T 10% Carbowax 1500 (sample and reference)

Mesh size : 40/60

carrier He	injector	detector	column programme
flow rate	temp °C	temp °C	
30(cc/min)	175	200	



Calculations

$$k_1 = (\text{wt. styrene}/\text{wt. I.S.})/(\text{area styrene}/\text{area I.S.})$$

$$k_2 = (\text{wt. PMS}/\text{wt. I.S.})/(\text{area PMS}/\text{area I.S.})$$

$$\text{residual wt. of styrene} = k_1(\text{area of styrene}/\text{area of I.S.})(\text{wt. of I.S.})$$

$$\text{residual wt. of PMS} = k_2(\text{area of PMS}/\text{area of I.S.})(\text{wt. of I.S.})$$

$$\text{conversion (wt. basis)} = (\text{wt}_0 - \text{wt}_t)/\text{wt}_0$$

where wt_0 = total weight of monomers at time zero

and wt_t = total residual weight of monomers at time t

$$f_1 = \text{res. wt. of styrene}/M_{m1} / (\text{res. wt. of styrene}/M_{m1} + \text{res. wt. of PMS}/M_{m2})$$

4.2 Light scattering (LALLSP)

Procedure

LALLSP was used to measure the \bar{M}_w of almost all the copolymer samples. The instrument used was (Chromatix, KMX-6). The light source for elastic Rayleigh scattering was of wavelength 633 nm.

Continuous measurement of the output voltage signal was done using a strip-chart recorder. The solvent used was toluene at room temperature. Polymer concentrations ranged from .1 to .5 weight %. The (dn/dc) for the copolymer of both compositions were measured in toluene using a laser differential refractometer of the same wavelength (Chromatix, KMX-16).

Calculations

Treating the copolymer as random and without composition drift, the well known equations for the determination of \bar{M}_w of homopolymers can be applied as follows.

$$Kc/R_{\theta} = 1/\bar{M}_w + A_2c \quad (53)$$

neglecting higher powers of c .

where $K = 4\pi^2 n_0^2 / (N_{AV} \lambda^4) (dn/dc)_{cop}^2$

n_0 = refractive index of toluene = 1.4921

$$R_{\theta} = R_{\theta, soln} - R_{\theta, solv}$$

$$R_{\theta} \propto G_{\theta} / G_0$$

where G_{θ} = measured intensity of the scattered beam at $\theta = 6-7^{\circ}$

and G_0 = measured int. of the incident beam at $\theta = 0^{\circ}$

λ = wavelength of the incident beam = 632.8 nm.

4.3 Size exclusion chromatography (SEC)

Procedure

SEC was done on homogeneous copolymer samples to obtain the MWD, \bar{M}_N and \bar{M}_W of the samples. Toluene at room temperature was used as the solvent for the Waters 150 C GPC. An on-line refractive index (RI) detector was used to measure the eluting polymer concentration.

Calculations

Two broad standards of known \bar{M}_W (obtained by LALLSP) were used in conjunction with the universal

calibration curve based on linear polystyrene to estimate the Mark-Houwink parameters and finally the calibration curve for the copolymer (106). The following calibration curves were used to analyse the fractionated copolymer data, one for each copolymer composition

$$F_1 = 0.2 :$$

$$\log_{10} M = 8.22636 + 0.090014 V - 0.01032 V^2 + 0.000129 V^3$$

$$F_1 = 0.75 :$$

$$\log_{10} M = 8.9877 + 0.11687 V - 0.0134 V^2 + 0.00016749 V^3$$

The two calibration curves were found to give reasonable estimates of the \bar{M}_N and \bar{M}_W of all the copolymer samples, the treatment being analogous to linear homopolymer samples.

$$\bar{M}_K = \left(\int F(V)M(V)^{K-1} dV \right) \left(\int F(V)M(V)^{K-2} dV \right)^{-1}$$

The above equation defines the K^{th} average molecular weight for the copolymer. No correction for peak broadening or imperfect resolution was made in this work.

4.4 Differential scanning calorimetry (DSC)

A differential scanning calorimeter can be used to measure the transition energy of a sample as it is heated from an initial temperature at a programmed rate to a final specified temperature. During this period the sample undergoes various thermodynamic transitions, depending on its nature. An amorphous polymer sample, as used here, shows a second order thermodynamic transition which is recorded as its glass-transition temperature by noting the point of discontinuity of the base line on its thermogram.

The principle of operation is as follows. A DSC apparatus essentially consists of a sample and a reference cell both being maintained at the same temperature throughout. An outer temperature control loop controls the total energy supplied to the system to maintain the average temperature at the desired level while an inner differential temperature control loop controls the differential energy input required to maintain the sample and the reference cells at the same temperature. Analytical data are

recorded such that the peak amplitude directly represents energy/time of transition energy and the peak area represents the total energy liberated/consumed during the transition. The abscissa provides a continuous record of the temperature of the sample. A second order thermodynamic transition in an amorphous polymer sample occurs at the point where the specific heat (C_p) of the sample undergoes a change. This causes the differential energy input to the sample/reference to increase depending on the direction of change in the C_p . A base line shift is observed at this point of transition. Generally, the quantitative performance is independent of the C_p of the sample, its geometry and the temperature scanning rate. However, it is commonly known that the T_g measurement of the polymer depends on the heating rate. For a detailed description of the theory and application of DSC techniques, the reader may refer to (113,114).

A SETARAM DSC-111 instrument was used to measure the T_g of the styrene/PMS copolymer samples.

5. Derivation of equations (45) and (46) in text.

Based on the kinetic scheme outlined for the MMA/PMS copolymerization system, the rate expression for dead copolymer is given by

$$\begin{aligned}
 (1/v)d(N_r)/dt = & K_{fm}[M][R_r^{\cdot}] + (a[R_{r,1}^{\cdot}]) \sum_1^{\infty} [R_{s,1}^{\cdot}] + \\
 & (1-a)/2 \sum_1^{r-1} [R_{s,1}^{\cdot}][R_{r-s,1}^{\cdot}] + (1-b) \sum_1^{r-1} [R_{s,1}^{\cdot}][R_{r-s,2}^{\cdot}] + \\
 & b[R_{r,1}^{\cdot}] \sum_1^{\infty} [R_{s,2}^{\cdot}] + b[R_{r,2}^{\cdot}] \sum_1^{\infty} [R_{s,1}^{\cdot}] + c[R_{r,2}^{\cdot}] \sum_1^{\infty} \\
 & [R_{s,2}^{\cdot}] + (1-c)/2 \sum_1^{r-1} [R_{s,2}^{\cdot}][R_{r-2,2}^{\cdot}] K_t \quad (56)
 \end{aligned}$$

Where N_r is the number of moles of dead polymer containing r monomer units and $[R_r^{\cdot}] = [R_{r,1}^{\cdot}] + [R_{r,2}^{\cdot}]$

$$[R^{\cdot}] = [R_1^{\cdot}] + [R_2^{\cdot}] \quad \text{and} \quad [R_j^{\cdot}] = \sum_1^{\infty} [R_{r,1}^{\cdot}]$$

Substituting for $[R_1^{\cdot}]$ and $[R_2^{\cdot}]$

$$\begin{aligned}
 (1/v)d(N_r)/dt = & K_{fm}[M][R_r^{\cdot}] + (a[\phi_2^{\cdot}]^2 [R_r^{\cdot}][R^{\cdot}]) + \\
 & (1-a)/2 [\phi_2^{\cdot}]^2 \sum_1^{r-1} [R_s^{\cdot}][R_{r-s}^{\cdot}] + (1-b)[\phi_1^{\cdot}][\phi_2^{\cdot}] \sum_1^{r-1} [R_s^{\cdot}][R_{r-s}^{\cdot}] + \\
 & b[\phi_1^{\cdot}][\phi_2^{\cdot}] [R^{\cdot}][R_r^{\cdot}] + b[\phi_1^{\cdot}][\phi_2^{\cdot}] [R_r^{\cdot}][R^{\cdot}] + c[\phi_2^{\cdot}]^2 [R_r^{\cdot}][R^{\cdot}] + \\
 & (1-c)/2 [\phi_2^{\cdot}]^2 \sum_1^{r-1} [R_s^{\cdot}][R_{r-1}^{\cdot}] K_t \quad (57)
 \end{aligned}$$

$$\text{Now } [R_r^{\cdot}] = R_p(\tau' + \beta')/K_p[M] \quad (\text{by SSH on radical population}) \quad (58)$$

where $\phi = 1/(\tau' + \beta' + 1)$

and τ' and β' represent the effective τ and β as defined in equations (59) and (60) in the text.

Substituting for R_p^* into the previous equation and defining C_M yields after some algebra

$$\begin{aligned} (1/v)d(N_p)/dt &= \phi^r R_p (\tau' + \beta') ((\tau' + \beta') [R^*] r K_t / (2K_p [M]) \\ & \left((1-a)[\phi_1^*]^2 + 2(1-b)[\phi_1^*][\phi_2^*] + (1-c)[\phi_2^*]^2 \right) + C_M + [R^*] K_t / \\ & K_p [M] \left(a[\phi_1^*]^2 + 2b[\phi_1^*][\phi_2^*] + c[\phi_2^*]^2 \right) \end{aligned} \quad (59)$$

Simplification of the above equation yields

$$(1/v)d(N_p)/dt = \phi^r R_p (\tau' + \beta') (\tau' + \beta') / 2 + r\beta' + \tau' \quad (60)$$

$$\text{where } \tau' = \frac{R_p K_t}{(K_p [M])^2} \left(a[\phi_1^*]^2 + 2b[\phi_1^*][\phi_2^*] + c[\phi_2^*]^2 \right) + C_M \quad (61)$$

$$\beta' = \frac{R_p K_t}{(K_p [M])^2} \left((1-a)[\phi_1^*]^2 + 2(1-b)[\phi_1^*][\phi_2^*] + (1-c)[\phi_2^*]^2 \right) \quad (62)$$

These equations are analogous to those used for homopolymerizations and it follows that

$$k_{tc} = \left((1-a)[\phi_1^*]^2 + 2(1-b)[\phi_1^*][\phi_2^*] + (1-c)[\phi_2^*]^2 \right) K_t$$

$$k_{td} = \left(a[\phi_1^*]^2 + 2b[\phi_1^*][\phi_2^*] + c[\phi_2^*]^2 \right) K_t$$

6. Effect of changing r_1 and r_2 on copolymer composition drift

In order to investigate the effect of imposing diffusional limitations on propagation constants at different values of V_F , an extreme case of the variation of reactivity ratios with conversion was studied for MMA/PMS copolymerization.

The differential form of the Meyer-Lowry equation is given by

$$df_1/(F_1-f_1) = d(\ln(1-x))$$

This equation along with the instantaneous copolymer composition equation was used to predict f_1 with conversion for the case where r_1 and r_2 are dependent on conversion after the onset of diffusion-controlled propagation. Taking x_{crit2} as 85%, the reactivity ratios were assumed to vary with conversion as

$$r_1 = a + bx \quad (61)$$

$$r_2 = c + bx \quad (62)$$

and the product was assumed to follow $r_1 r_2 = 1$ as $x \rightarrow 1$

The constants a, b and c were obtained by solving

equations (61) and (62).

The predicted values for f_1 are plotted versus x for three different f_{10} in Figure 45. Comparing this plot to the data at high conversions, it can be seen that the data are not sufficiently accurate to either prove or disprove the hypothesis that the reactivity ratios are dependent on conversion when propagation reactions become diffusion-controlled.

7. Parameter list for MMA/PMS Copolymerization

	Reference	
$K_d = 6.32E16 \exp(-15460/T) \text{ min}^{-1}$	31	
$f = 1.0$		
$C_{m0} = 6.E-6 (T=60^{\circ} \text{ C})$		
$= 20.9E-6 (T=80^{\circ} \text{ C})$		
$K_{11} = 9.72E8 \exp(-3500./T) \text{ l/mole, min}$	31	
$K_{22} = 6.31E8 \exp(-3560./T) \text{ l/mole, min}$		
$r_1 = .498 \pm .02$		
$r_2 = .419 \pm .03$		
$\alpha_{M1} = \alpha_{M2} = 2.2E-3^{\circ} \text{ K}^{-1}$	estimated from limiting conversion data	
$\alpha_p = .48E-3^{\circ} \text{ K}^{-1}$	31	
$T_{gp} (\text{all compositions}) = 114^{\circ} \text{ C}$		
$T_{gm1} = -114^{\circ} \text{ C}$	estimated from limiting conversion data	
$T_{gm2} = -123^{\circ} \text{ C}$		
$d_{M1} = .973 - .001164 (T-273.1) \text{ g/cc}$	31	
$d_{M2} = .9261 - .000918 (T-273.1) \text{ g/cc}$		
$d_p = 1.11 \text{ g/cc (all compositions)}$		
$n_s = 10$	$d = 3.3E-2 \text{ lit/gm}$	$A = 1.24$
$l_0 = 25 \text{ nm}$	$B = 1.0$	
$K_{t11} = 1.2E9 (\text{l/mole, min})$	$K_{t22} = 2.43E9 (\text{l/mole, min})$	
$K_{t12} = 2.23E9 (\text{l/mole, min})$		
Activation energy for all termination constants is assumed to be 0.		

T ° C	[I] ₀ mole/lit	f ₁₀	K _{t0} *.1E-8 l/mole,min	V _{Fcr2}	K ₃ *.1E-3.
60	0.0157	0.21	2.1	0.08	1.7
60	0.0252	0.21	2.1	0.09	1.8
60	0.0157	0.83	1.1	0.09	1.9
60	0.0157	0.54	2.1	0.08	2.2
60	0.0057	0.21	2.3	0.09	1.9
60	0.0057	0.54	2.3	0.08	2.3
80	0.0157	0.21	2.1	0.11	1
80	0.0157	0.83	1.2	0.1	1
80	0.0252	0.21	2.6	0.11	0.9
80	0.0057	0.23	2.6	0.11	1.2
80	0.0157	0.54	2.4	0.09	1.1
80	0.0057	0.54	2.4	0.09	1.2
50	0.0252	1.0	1.0	0.11	1.9
70	0.0252	1.0	1.2	0.11	0.9
90	0.0252	1.0	1.2	0.1	0.4

The large value of d (segmental-diffusion control) suggests that either 1) the copolymer coils contract significantly during the initial stages of polymerization due to the markedly low "goodness" of the solvent or that 2) the calculation of K_{t0} and d from the limited initial rate data is inaccurate, due to the high correlation between these parameters. Extensive low conversion rate data would be required to obtain the best value of d .

REFERENCES

1. Hamielec, A.E. and MacGregor, J.F., in Polymer Reaction Engineering, Edited by Reichert, K.H. and Geiseler, W., Hanser Publishers (1983)
2. Kaeding, W.W., Prapas, A.G. and Ragonese, F.P., Polymer Preprints, ACS Div. Pol. Chem., 23, No. 2, 93 (1982)
3. Lord, G., Garcia-Rubio, L., MacGregor, J.F. and Hamielec, A.E., Chem. Eng. Communications (in press)
4. Jones, K., Master's thesis, McMaster University (in preparation)
5. North, A.M. and Reed, G.A., Trans. Farad. Soc., 57, 859 (1961)
6. Ludwico, W.A. and Rosen, S.L., J. Poly. Sci., 14, 2121 (1976)
7. Mahabadi, H.K. and O'Driscoll, K.F., Macromolecules, 10, 55 (1977)
8. Chiantore, O. and Hamielec, A.E., Polymer,
9. Tulig, T.J. and Tirrel, M., Macromolecules, 15, 459 (1982)
10. Graessley, W.W., Adv. Poly. Sci., 16, 1 (1974)
11. Mahabadi, H.K. and Rudin, A., J. Poly. Sci., Poly. Chem. Ed., 17, 1801 (1978)
12. Matthews, C.Y. and Rosen, S.L., J. Poly. Sci., Poly. Phys. Ed., 22, 139 (1984)
13. Turner, D.T., Macromolecules, 10, 221 (1977)
14. O'Driscoll, K.F., Wertz, W. and Husar, A., J. Poly. Sci., A-1, 5, 2159 (1967)

15. Smoluchowski, M.Z., *Phys. Chem.*, 92, 129 (1918)
16. deGennes, P.G., *J. Chem. Phys.*, 56, 572 (1971)
17. Klein, J., *Nature*, 271, 12 (1978)
18. Tulig, T.J. and Tirrel, M., *Macromolecules*, 14, 1501 (1981)
19. Ito, K., *Polymer J.*, 12, 499 (1980)
20. Klein, J., *Macromolecules*, 11, 852 (1978)
21. Boots, H.M.J., *J. Poly. Sci., Poly. Phys. Ed.*, 20, 1695 (1982)
22. Ross, R.L. and Laurence, R.L., *A.I.Ch.E. Symp. Ser.*, 72, 74 (1980)
23. Hui, A.W.T. and Hamielec, A.E., *J. Appd. Poly. Sci.*, 16, 749 (1972)
24. Husain, A. and Hamielec, A.E., *J. Appd. Poly. Sci.*, 22, 1207 (1978)
25. Duerksen, J.H. and Hamielec, A.E., *J. Poly. Sci., Pt. C*, 155 (1968)
26. Wu, G.Z.A., Denton, L.A. and Laurence, R.L., *Poly. Eng. Sci.*, 22, 1 (1982)
27. Horie, K., Mita, I. and Kambe, H., *J. Poly. Sci., A-1*, 6, 2663 (1968)
28. Arai, K. and Saito, S., *J. Chem. Eng. Japan*, 9, 302 (1976)
29. Chiu, W.Y., Carratt, G.M. and Soong, D.S., *Macromolecules*, 16, 348 (1983)
30. Cardenas, J.N. and O'Driscoll, K.F., *J. Poly. Sci., Poly. Chem. Ed.*, 14, 883 (1976)

31. Marten, F.L. and Hamielec, A.E., ACS Symp. Ser. 104, 43 (1979)
32. Bueche, F., Physical Properties of Polymers, Wiley Interscience, New York (1962)
33. Cardenas, J.N. and O'Driscoll, K.F., J. Poly. Sci., Poly. Chem. Ed., 15, 2097 (1977)
34. Marten, F.L. and Hamielec, A.E., J. Appd. Poly. Sci., 27, 489 (1982)
35. Soh, S.K. and Sundberg, D.C., J. Poly. Sci., Poly. Chem. Ed., 20, 1299 (1982)
36. Soh, S.K. and Sundberg, D.C., J. Poly. Sci., Poly. Chem. Ed., 20, 1345 (1982)
37. Ferry, J.D., Viscoelastic Properties of Polymers, Wiley, New York (1970)
38. Schulz, G.V., Z. Phys. Chem. (Frankfurt am Main), 8, 290 (1956)
39. Hayden, P. and Melville, H., J. Poly. Sci., XLIII, 201 (1960)
40. Soh, S.K. and Sundberg, D.C., J. Poly. Sci., Poly. Chem. Ed., 20 (1982)
41. Stickler, M., Makromol. Chem., 184, 2563 (1983)
42. Kelley, F.N., and Bueche, F., J. Poly. Sci., 50, 549 (1961)
43. Fujita, H., Kishimoto, A. and Matsumoto, K., Trans. Farad. Soc., 56, 424 (1960)
44. Chalykh, A.E. and Vasenin, R.M., Vysokomol. Soedin, 8, 1908 (1966)
45. Friis, N. and Hamielec, A.E., ACS Symp. Ser., 24, 82 (1976)

46. Berens, A.R., ACS Symp. Ser., 39, 236 (1978)
47. Harris, B., Hamielec, A.E. and Marten, F.L., ACS Symp. Ser., 165, 315 (1981)
48. Stickler, M., Panke, D. and Hamielec, A.E., J. Poly. Sci., Poly. Chem. Ed., 22, 2243 (1984)
49. Sundberg, D.C., Hsieh, J.Y., Soh, S.K. and Baldus, R.F., ACS Symp. Ser., 165, 327 (1981)
50. Soh, S.K. and Sundberg, D.C., J. Poly. Sci., Poly. Chem. Ed., 20, 1330 (1982)
51. Schulz, G.V. and Husemann, E., Z. Phys. Chem., B, 34, 184 (1936)
52. Breitenbach, J.W. and Rudorffer, H., Mh. Chem., 70, 37 (1937)
53. Flory, P.J., J. Amer. Chem. Soc., 59, 241 (1937)
54. Suess, H., Pilch, K. and Rudorffer, H., Z. Phys. Chem., A 179, 361 (1937)
55. Schulz, G.V., Dinglinger, A. and Husemann, E., Z. Phys. Chem., B43, 385 (1939)
56. Mayo, F.R., J. Amer. Chem. Soc., 75, 6136 (1953)
57. Zimm, B.H. and Bragg, J.K., J. Poly. Sci., 9, 476 (1952)
58. Russell, K.E. and Tobolsky, A.V., J. Amer. Chem. Soc., 75, 5052, (1953)
59. Overberger, C.G. and Lapkin, M., J. Amer. Chem. Soc., 77, 4651 (1965)
60. Kopecky, K.R. and Evan, S., Can. J. Chem., 47, 4041 (1969)
61. Hiatt, R.R. and Bartlett, P.D., J. Amer. Chem. Soc., 81, 1149, (1959)

62. Aso, C., Kunitake, T., Shinsenji, M. and Miyazaki, H., J. Poly. Sci., A-1, 7, 1497 (1969)
63. Mayo, F. R., J. Amer. Chem. Soc., 90, 1289 (1968)
64. Muller, V. K. F., Die Makromol. Chem., 79, 128 (1964)
65. Brown, W. G., Die Makromol. Chem., 128, 130 (1969)
66. Buchholz, K. and Kirchner, K., Die Makromol. Chem., 177, 935, (1976)
67. Kaufmann, H. F., Olaj, O. F. and Breitenbach, J. W., Die Makromol. Chem., 177, 939 (1976)
68. Olaj, O. F., Kaufmann, H. F. and Breitenbach, J. W., Makromol. Chem., 178, 2707 (1977)
69. Kirchner, K. and Riederle, K., Die Angewandte Makromol. Chem., 111, 1 (1983)
70. Kirchner, K. and Schlapkohl, H., Makromol. Chem., 177, 2031 (1976)
71. Pryor, W. A. and Coco, J. H., Macromolecules, 3, 500 (1970)
72. Matheson, M. S., Auer, E. E., Bevilacqua, E. B. and Hart, E. J., J. Amer. Chem. Soc., 73, 1700 (1951)
73. Pryor, W. A. and Lasswell, L. D., Adv. in Free Radical Chem., 5, G. H. Williams, Ed., Elek Science, London (1975)
74. Wall, F. T., J. Amer. Chem. Soc., 63, 1862 (1941)
75. Mayo, F. R. and Lewis, F. M., J. Amer. Chem. Soc., 66, 1591 (1944)
76. Alfrey, T. and Goldfinger, G., J. Chem. Phys., 12, 205 (1944)
77. Garcia-Rubio, L., Ph.D. Thesis, McMaster Univ. (1980)
78. deButts, E. H., J. Amer. Chem. Soc., 72, 411 (1950)

79. Walling, C., *J. Amer. Chem. Soc.*, 71, 1930 (1949)
80. O'Driscoll, K.F. and Knorr, P., *Macromolecules*, 1, 367 (1968)
81. Johnson, M., Karmo, T.S. and Smith, R.R., *Europ. Poly. J.*, 14, 409 (1978)
82. Dionisio, J.M. and O'Driscoll, K.F., *J. Poly. Sci., Poly. Lett. Ed.*, 17, 701 (1979)
83. Terramachi, S., Hasegawa, A. and Uchiyama, N., *J. Poly. Sci., Poly. Lett. Ed.*, 22, 71 (1984)
84. Kale, L.T., O'Driscoll, K.F. and Garcia-Rubio, L.H., accepted for publication in *J. Poly. Sci.*
85. Melville, H.W., Noble, R. and Watson, W.F., *J. Poly. Sci.*, 2, 229 (1947)
86. Atherton, J.N. and North, A.M., *Trans. Farad. Soc.*, 58, 2409 (1962)
87. Allen, P.E.M. and Patrick, C.R., *Makromol. Chem.*, 47, 154 (1961)
88. Benson, S.W. and North, A.M., *J. Amer. Chem. Soc.*, 84, 935 (1962)
89. Russo, S., and Munari, S., *J. Macromol. Sci.-Chem.*, A2, 1321 (1968)
90. Chiang, S.S.M. and Rudin, A., *J. Macromol. Sci.-Chem.*, A9(2), 237 (1975)
91. Prochazka, O. and Kratochvil, P., *J. Poly. Sci., Poly. Chem. Ed.*, 21, 3269 (1983)
92. Lee, H.B. and Turner, D.T., *Macromolecules*, 10, 226 (1977)
93. High, K.A., Lee, H.B. and Turner, D.T., *Macromolecules*, 12, 332 (1979)

94. Lee, H.B. and Turner, D.T., Poly. Prepr., Amer. Chem. Soc., Div. Poly. Chem., 18, 539 (1977)
95. Lee, H.B. and Turner, D.T., Poly. Prepr., Amer. Chem. Soc., Div. Poly. Chem., 19, 603 (1978)
96. Meyer, V.E. and Lowry, C.G., J. Poly. Sci., A-3, 2843 (1965)
97. Mayo, F.R., Gregg, R.A. and Matheson, M.S., J. Amer. Chem. Soc., 73, 1691 (1951)
98. Olaj, O.F., Monatsch. Chem., 97, 1437 (1966)
99. Hyun, J.C., Graessley, W.W. and Bankoff, S.G., Chem. Eng. Sci., 31, 945 (1976)
100. Hugo Patino-Leal, Reilly, P.M. and O'Driscoll, K.F., J. Poly. Sci., Poly. Lett. Ed., 18, 219 (1980)
101. Sutton, T. and MacGregor, J.F., Can. J. Chem. Eng., 55, 602 (1977)
102. Box, M.J., Technometrics, 12, 219 (1970)
103. Idahie, M.Y., unpublished data (1977)
104. Course Notes, An Int. Short Course on Poly. Prod. Tech., McMaster University, May (1984)
105. Fedors, R.F., J. Poly. Sci., Poly. Lett. Ed., 17, 719 (1979)
106. Omorodion, S.N.E. and Hamielec, A.E., ACS Symp. Ser., 138, 183 (1980)
107. Wiley, R.H. and Davis, B., J. Appd. Poly. Sci., 46, 423 (1960)
108. Dionisio, J., Mahabadi, H.K., O'Driscoll, K.F., Abuin, E. and Lissi, E.A., J. Poly. Sci., Poly. Chem. Ed., 17, 1891 (1979)

109. Polymer Handbook, Brandrup, J. and Immergut, E.H., Ed., 2nd Edition, John Wiley Int. (1975)
110. Meyerhoff, G., Sack, R. and Kouloumbri, M., paper presented at the 189th ACS national meeting, Poly.Chem.Div., Miami Beach, April 28-May 3 (1985)
111. Balke, S.T. and Hamielec, A.E., J. Appd. Poly. Sci., 17, 905 (1973)
112. Chong, Y.K., Rizzardo, E. and Solomon, D.H., J. Amer. Chem. Soc., 105, 7761 (1983)
113. Slade, P.E. and Jenkins, L.T., Thermal Characterization Techniques, Marcel Dekker, Inc., New York (1970)
114. O'Neill, M.J., Anal. Chem., 36, 1238 (1964)
115. Hui, A.W.T., Ph.D. Thesis, McMaster University (197)
116. Kaeding, W.W., Young, L.B. and Prapas, A.G., Chemtech, 12, 556 (1982)